RADIO RESOURCE VIRTUALIZATION IN CELLULAR NETWORKS

by

Xin Wang

Bachelor of Science in Electrical Engineering, Shanghai Normal University, China, 2006

Master of Science in Electrical Engineering, Shanghai University, China, 2010

Submitted to the Graduate Faculty of

the School of Information Sciences in partial fulfillment

of the requirements for the degree of

Doctor of Philosophy

University of Pittsburgh

2014

UNIVERSITY OF PITTSBURGH

THE TELECOMMUNICATIONS AND NETWORKING PROGRAM

This dissertation was presented

by

Xin Wang

It was defended on

December 4th 2014

and approved by

Prashant Krishnamurthy, Associate Professor, Telecommunications and Networking

David Tipper, Associate Professor, Telecommunications and Networking

Martin Weiss, Associate Dean and Professor, School of Information Sciences

Ioannis Broustis, Senior Inventive Scientist, AT&T Labs

Dissertation Director: Prashant Krishnamurthy, Associate Professor, Telecommunications and Networking

RADIO RESOURCE VIRTUALIZATION IN CELLULAR NETWORKS

Xin Wang, PhD

University of Pittsburgh, 2014

Virtualization of wireless networks holds the promise of major gains in resource usage efficiency through spectrum/radio resources sharing between multiple service providers (SPs). Radio resources however are not like a simple orthogonal resource such as time slots on a wire and its shared quantity is a function of geography and signal strength, rather than orthogonal slices. To better exploit the radio resource usage, we propose a novel scheme – radio resource virtualization (RRV) that allows SPs to access overlapping spectrum slices both in time and in space considering the transmit power, the interference, and the usage scenario (capabilities/needs of devices). We first investigate the system capacity of a simple two-cell network and show that RRV often leads to better efficiency than the well-known separate spectrum virtualization (SSV) scheme. However, the use of RRV requires careful air-interface configuration due to interference in the overlapping slices of spectrum. Therefore we next examine scenarios of a multi-cell network with fractional frequency reuse (FFR) implementing five radio resources configuration cases. From the evaluation of capacity data obtained from simulations, a variety of tradeoffs exist between SPs if RRV is applied. One example shows that capacity of the SP that operates smaller cells almost doubles while capacity of the SP deployed in larger cells may drop by 20% per subscriber. Based on these tradeoffs, we suggest configuration maps in which a network resource manager can locate specific configurations according to the demand and capabilities of SPs and their subscribers. Finally, we consider a case study on top of LTE. A system-level simulator is developed following 3GPP standards and extensive simulations are conducted. We propose and test 3 schemes that integrate RRV into the LTE radio resource management (RRM) – unconditional RRV,

time domain (TD) muting RRV and major-interferer time domain (MI-TD) muting RRV. Along the same line as the capacity analysis, we compare those schemes with the traditional SSV and suggest configuration maps based on the produced tradeoffs. Our investigation of RRV provides a framework that evaluates the resource efficiency, and potentially the ability of customization and isolation of spectrum sharing in virtualized cellular networks.

Keywords: wireless virtualization, radio resource virtualization, radio resource manager, cellular networks, LTE/LTE-A, multiple-input multiple-output, fractional frequency reuse.

TABLE OF CONTENTS

1.0 INTRODUCTION 1

1.1 What is Wireless Virtualization? 1

1.2 Scope of Our Research 4

1.3 Contribution of Our Research 9

2.0 BACKGROUND AND RELATED WORK 11

2.1 Wired Network Virtualization 11

2.2 Related Incarnations 13

2.2.1 Cognitive Radio 13

2.2.2 Mobile Virtual Network Operator 14

2.3 Work in Wireless Virtualization 15

2.4 Technologies in Our Analysis Model 17

2.5 Wireless Network Virtualization Paradigms 19

2.5.1 Universal virtualization 19

2.5.2 Cross-infrastructure virtualization 20

2.5.3 Limited intra-infrastructure virtualization 21

3.0 SYSTEM MODEL OF VIRTUALIZATION 23

3.1 Radio Resource Virtualization 23

3.2 General RRV Model 24

3.3 Evaluation Metric 30

3.3.1 Shannon capacity of MIMO channel with interference 30

3.3.2 X percentile MU throughput 32

4.0 RADIO RESOURCES VIRTUALIZATION IN A SIMPLE CELLULAR NETWORK . . . 33
4.1 Motivation . . . 33
4.2 Hierarchical Sharing . . . 34
4.3 Numerical Results . . . 36
4.3.1 RRV and Capacity . . . 37
4.3.1.1 Aggregate Spectral Efficiency . . . 40
4.3.1.2 Individual Cells . . . 46
4.3.2 Analyzing the Combined SINR Matrix . . . 50
4.3.3 Customization in RRV . . . 55
4.4 Discussion and Conclusions . . . 60
5.0 ON CONFIGURING A FFR VIRTUAL NETWORK . . . 62
5.1 Motivation . . . 62
5.1.1 Fractional Frequency Reuse and Radio Resource Virtualization Cases 64
5.2 Simulation Results and Analysis . . . 68
5.2.1 General Trends . . . 71
5.2.2 Comparison of Cases . . . 75
5.2.3 Configuration Map . . . 78
5.2.4 Impact of Number of Antennas . . . 81
5.3 Discussion . . . 82
5.3.1 Isolation . . . 83
5.3.2 Impact on cell-edge users due to FFR in SP_A's layout . . . 84
5.3.3 Other Issues . . . 86
5.4 conclusions . . . 87
6.0 A CASE STUDY: LTE NETWORK VIRTUALIZATION . . . 88
6.1 Motivation . . . 88
6.2 Radio Resource Management with Virtualization . . . 89
6.2.1 LTE Downlink Radio Resource Management . . . 90
6.2.2 Scheduling in LTE RRV System . . . 91
6.3 System model . . . 92

6.3.1 RRV configuration in the LTE Network 94
6.3.2 Throughput Evaluation 95
6.3.3 Scheduling 99
6.4 Simulation Results and Analysis 100
6.4.1 Performance of SP_A 102
6.4.2 Performance of SP_B 107
6.4.3 Configuration Maps 107
6.5 Limitations and Discussion 115
7.0 CONCLUSION AND FUTURE DIRECTIONS 117
APPENDIX. COMPARISON OF THE LTE SIMULATOR WITH OTHER'S WORK 120
BIBLIOGRAPHY 122

LIST OF TABLES

1 Parameter Settings for Various Scenarios 38
2 Achievable data rate (in bps) per MU 61
3 Available frequency bandwidth per MU 69
4 Parameter Settings for Various Scenarios 70
5 Percentages of cell edge MUs 85
6 System parameters 101

LIST OF FIGURES

2.1 Cross-infrastructure wireless network virtualization 21
2.2 Cross-infrastructure wireless network virtualization 22
3.1 Two-SP SSV Vs. RRV 25
3.2 Limited intra-infrastructure wireless network virtualization 26
3.3 Three-SP SSV Vs. RRV 27
3.4 A three-SP virtual system 29
4.1 A two-cell system 35
4.2 Aggregate capacity of two cells with water-filling 38
4.3 Aggregate capacity of two cells with equal power allocation 39
4.4 Capacity Vs. Distance & Radius ($\alpha = 4$) 41
4.5 Capacity Vs. Distance & Radius (conditional $\alpha = 2$) 42
4.6 Capacity Vs. Distance & Power ($\alpha = 4$) 43
4.7 Capacity Vs. Distance & Power (conditional $\alpha = 2$) 44
4.8 Capacity Vs. Power & Radius – top ($\alpha = 4$) and bottom (conditional $\alpha = 2$) 45
4.9 Achievable data rate at large cell (per MU) 47
4.10 Achievable data rate at small cell (per MU) 48
4.11 Average achievable data rate (per MU) at large cell with RRV employed in only one sector 49
4.12 CDF of singular values at different separation distance (for MUs in the large cell) 51
4.13 CDF of singular values at different separation distance (for MUs in the small cell) 52

4.14 CDF of singular values at different radii of small cell (for MUs in the large cell) 53
4.15 CDF of singular values at different radii of small cell (for MUs in the small cell) . . . 54
4.16 CDF of singular values (as seen by MUs in the large cell) with 2 MU antennas in the small cell, but varying numbers of BS antennas in the small cell . . . 56
4.17 CDF of singular values (as seen by MUs in the small cell) with 2 MU antennas in the small cell, but varying numbers of BS antennas in the small cell . . . 57
4.18 CDF of singular values (as seen by MUs in the large cell) with varying numbers of MU and BS antennas in small cell . . . 58
4.19 CDF of singular values (as seen by MUs in the small cell) with varying numbers of MU and BS antennas in small cell . . . 59
5.1 2D-Schematic of multicell virtual system with FFR . . . 64
5.2 Radio Resource Allocation Cases . . . 67
5.3 Aggregate spectral efficiency of the multi-cell system . . . 72
5.4 Achievable data rate (per MU) – top (SP_A's layout) and bottom (SP_B's layout) 74
5.5 Comparison of achievable data rate per MU in SP_A and SP_B's layouts for a power ratio of 3 dB . . . 76
5.6 Comparison of achievable data rate per MU in SP_A and SP_B's layouts for a power ratio of 15 dB . . . 77
5.7 Capacity in SP_A v.s. capacity in SP_B layouts – top (3dB) and bottom (15dB) 79
5.8 Using configuration map by resource manager . . . 80
5.9 Capacity in SP_A layout v.s. capacity in SP_B layout for various MIMO settings 81
5.10 Variation in Capacity . . . 83
5.11 Achievable data rate per MU for cell center MUs and cell edge MUs . . . 85
6.1 System model of LTE simulator . . . 93
6.2 TD muting RRV at SP_B . . . 96
6.3 MI-TD muting RRV at SP_B . . . 97
6.4 SP_A performance for Scenario 1 – top (5%-ile) and bottom (50%-ile) . . . 104
6.5 SP_A performance for Scenario 2 – top (5%-ile) and bottom (50%-ile) . . . 105
6.6 SP_A performance for Scenario 3 – top (5%-ile) and bottom (50%-ile) . . . 106

6.7 SP_B performance for Scenario 1 – top (5%-ile) and bottom (50%-ile) 108
6.8 SP_B performance for Scenario 3 – top (5%-ile) and bottom (50%-ile) 109
6.9 5%-ile throughput based configuration map 111
6.10 50%-ile throughput based configuration map 112
6.11 5%-ile throughput of MI-TD muting RRV 113
6.12 50%-ile throughput of MI-TD muting RRV 114
6.13 SP_A performance for Network Layout 1 116
A.1 Comparison with the work in [56] 121

1.0 INTRODUCTION

1.1 WHAT IS WIRELESS VIRTUALIZATION?

In the past decades, the evolution of wireless communication technologies has triggered a significant growing need for resources in wireless networks. Due to natural limitations and cost, important physical resources in wireless network – infrastructure and spectrum are scarce. The current static network architecture cannot relieve the conflict between the scarce resources and the desire from various wireless services for more resources. On the other hand, the explosive capacity demand in cellular networks has required mobile network operators (MNOs) to increase capital (CAPEX) and operational expenses (OPEX) in order to improve their networks accordingly. However, MNOs have to limit the cost due to the predicted decreasing profit margin [1].

In traditional wireless networks, such MNOs play two roles. They invest to form networks, including building up infrastructures and bidding for spectrum. They also provide wireless services to end users accessing their networks. Usually, only large companies with huge amounts of capital can own large-scale wireless networks. This is the reason why a few big companies monopolize the current wireless market. However, the resources owned by most MNOs are usually underutilized [2]. Focusing on spectrum, it is regulated by the government (e.g. Federal Communications Commissions (FCC) in the USA) in most countries. The government assigns certain range of frequency bandwidth to MNOs on a long-term basis for large geographical regions. Since the bandwidth demands of those license holders vary highly along the time or space dimensions, the spectrum is often underutilized.

To address those problems, *wireless network virtualization* has been proposed recently, with the benefits of increasing resource efficiency, enabling customized applications, and

yet providing isolation between services [3]. To facilitate virtualization, functionalities of the traditional MNOs may be decoupled into infrastructure providers (InPs) and service providers (SPs). InPs manage the physical resources, including infrastructure and spectrum. They are responsible for installation and maintenance of physical architecture (e.g. base stations (BSs), mobility management entities (MMEs), S-Gateways, access points (APs), spectrum, etc.). SPs form wireless virtual networks (VNs) and provide end-to-end wireless services by aggregating resources from multiple InPs. In the virtual wireless environment, multiple wireless VNs coexist on the same physical substrate. Such wireless VNs are managed by different SPs. Each VN creates an illusion that it is an entire system by itself and the corresponding SP need not necessarily know the underlying physical substrate [3].

The economic advantages of wireless virtualization appear to be clear. Currently, the MNOs need to pay for both maintaining the physical network architecture and coordinating the network operation. With wireless virtualization, an InP is only required to concentrate on the maintenance of the physical equipment so that the energy and cost can be saved for the InP. Second, wireless virtualization brings more competition and more service differentiation into the wireless market. Wireless virtualization enables many SPs to enter the market. They can lease resources from InPs instead of setting up their own infrastructure. Third, the advent of more SPs gives end users more options [3].

In our work, *we are conceived with the major benefit of virtualization for wireless system performance that is similar in nature to what virtualization has brought to wired networks – high resource utilization efficiency.* In a wireless virtual environment, InPs allow multiple SPs to operate on shared nodes simultaneously. Resources on nodes are allocated dynamically. Using spectrum as an example, the frequency bandwidth allocated to a SP can now depend on its time-varying traffic. Spectrum sharing between VNs can at the very least bring multiplexing gain and improve resource utilization efficiency. For SPs, it may enhance the QoS of their VNs, e.g., higher throughput or shorter service time. For the entire system, it approaches better resource utilization efficiency.

We assume that wireless network virtualization consists of two parts – infrastructure virtualization (e.g. base station (BS) virtualization) and spectrum virtualization. Wireless networks naturally are access networks connecting end users to the wired core network. They

are comprised of many components similar to those in wired networks, that could be targets of virtualization. Virtualization has been widespread in wired networks [4]. Hence, many research issues regarding the implementation of wireless virtualization can be mapped from the wired network virtualization. For example, in wired networks, InPs partition physical resources like physical routers/switches/cross-connects, physical links, and bandwidth on each link. Such slices of resources then are assigned to SPs based on the agreements they have made with InPs. Multiple SPs may form their VNs using slices of resources but actually on top of the same physical substrate. Infrastructure virtualization are quite similar to wired network virtualization, like virtualization for servers, routers and wired links. A number of solutions exist in the literature [5, 6, 7]. However, an important type of resource in wireless networks, *spectrum or radio resources*[1], is not like any other resource in wired networks (e.g., CPU resources, time slot on a wire or wired bandwidth). Transmit powers, interference, mobility, channel conditions, the use of MIMO (device capability), and distances between transceivers, all impact the available capacity that could be obtained in slices of spectrum. If we partition spectrum orthogonally and assign the slices to SPs like other wired resources, the resource utilization efficiency improves only due to multiplexing gain. In fact, the complicated characteristic of spectrum has potential of reuse in time and space, that could perhaps lead to even higher resource utilization efficiency. In the mean time, more issues arise such as isolation between SPs and customization of applications. This makes spectrum a special resource and worth studying. Therefore, *the focus of our work is on spectrum/radio resources virtualization.*

Wireless networks have various types of networks, e.g., WLAN, mesh network, cellular network, that have different ranges of coverage, different protocols, and many other different factors. Virtualizing each of them faces different challenges depending on the system features. Deploying wireless virtualization may become a case-by-case task, and it is nearly impossible to generalize easily. Therefore, *we choose cellular networks as our model for studying virtualization.* Interest in spectrum sharing has been increasing in cellular networks because of the evolving cellular architecture [8, 9]. Highly overlapping urban cells or subur-

[1]Please note that, from now unless otherwise specified, the word "spectrum" and "radio resources" have equal meaning, unless otherwise mentioned.

ban femtocells embedded in macrocells are examples of opportunities that can be exploited to pool up the spectrum owned by several InPs in the same geographic area. SPs that have agreements with any of these InPs are then able to access the entire frequency band instead of a (typical) limited licensed band. A certain number of spectrum slices may be allocated to a SP on a short-term basis and allow it to perform its air-interface through them. Once cellular infrastructure ownership is decoupled from providing services, spectrum sharing could happen between multiple radio access technologies (RATs) served by one SP, or between SPs that co-exist on the same piece of infrastructure, or between InPs that possess large amount of "hard metal", or ultimately it could be viewed as an "unbundled cloud" links end users to Internet. Chapter 2 illustrates three types of virtualization according to spectrum sharing at different degrees - universal, cross-infrastructure and limited intra-infrastructure.

1.2 SCOPE OF OUR RESEARCH

Wireless virtualization is a broad and vague concept, and essence of it depends on how people define it and what physical form exists underneath. Here we specify the virtualization model studied in this dissertation and narrow the problem down to practical spectrum/radio resources virtualization in cellular networks. Our focus is a single-InP network that owns multiple cells with different sizes, each of which is operated by some SP/SPs. Every SP accesses part of the InP's spectrum in its cell/cells. More details of our virtualization model are discussed in Chapter 3. The essential problem we formalize and study is *how to efficiently virtualize radio resources among geographically overlapped SPs.*

We first look at the traditional way of spectrum virtualization – multiplexing. Due to the fluctuating nature of the traffic demands of users supported by a given SP, the utilization of spectrum varies. Thus it is possible to increase the overall utilization of several slices of spectrum with well-designed schedulers. In most work related to wireless network virtualization, the sharing of spectrum is considered at the level of orthogonal slices of frequency bandwidth. As a simple example, let us suppose that an InP has two slices of spectrum S_A and S_B, and two SPs A and B who are allocated these slices respectively by this InP. Spectrum sharing,

where user A can use *both the slices* S_A and S_B when B does not need the slice S_B, results in multiplexing gains improving the resource usage (see for example, [10, 11]). As mentioned previously, spectrum however is not like a simple resource such as time slots on a wire and it is possible to exploit further gain through spectrum sharing. The reality is that we should consider *radio resources* that are a function of geography and signal strength as the shared quantity, rather than orthogonal slices of spectrum to facilitate reuse of spectrum temporally and spatially. This reuse is more likely in diverse applications (e.g., high-speed broadband and low-speed local applications). When we consider it, transmit powers, interference, and usage scenario (capabilities/needs of devices) become important in determining how much of sharing is possible. However, this type of potential gain in utilizing spectrum has been neglected so far in the research literature. To differentiate from the separate/orthogonal spectrum virtualization (SSV) that brings multiplexing gain, we call this "radio resource virtualization" or RRV (illustrations of SSV and RRV are in Chapter 3) in this dissertation.

To virtualize radio resources in cellular networks, we place two prerequisites in all virtual networks. First, a *resource manager* is responsible for providing spectrum slices assignment and *correct configuration* of those slices for various SPs in each time unit. Details of the resource manager is described in Chapter 3. Second, spectrum aggregation [12] is considered as an available feature (pooling together each SP's assigned slices of spectrum) for configuration by the resource manager.

We therefore investigate the virtualizing radio resources problem through answering two questions as follows:

- Is the proposed virtualization scheme RRV going to benefit SPs in resource utilization efficiency?
- How should we manage cellular networks considering RRV to exploit this benefit (if any)? Or how can we configure the network to enable RRV to achieve suitable resource utilization?

To understand/quantify the potential benefits of RRV, in Chapter 4, we use a two-cell system as a simple example, where the coverage of one cell is a subset of another, and implement RRV that allows a certain overlapping allocation of the spectrum slices to

multiple SPs in the same time interval in overlapping or neighboring geographical areas. The aggregate spectrum efficiency and achievable data rate for each cell are obtained under various scenarios. Efficiencies and capacities of RRV and SSV are compared and the results illustrate (albeit in a simple scenario) that RRV often leads to better resource efficiency compared to SSV.

The next question therefore turns into how we should manage cellular networks considering RRV. The configuration problem becomes quite intricate as the network architecture becomes more complicated, such as when frequency reuse is adopted. For example, the resource manager has to decide what power level (in a given slice of spectrum) should be assigned to a given SP in a given cell. It has to determine how many antennas a given SP (or mobile units (MUs)) can use in a given cell. It has to decide how these may change depending on the distances between infrastructure entities like base stations (BSs).). In Chapter 5, we try to start answering the configuration question by examining fairly involved scenarios that include a range of configuration cases.

Instead of a simple two-cell system, we consider an InP's network with radio resources being shared between two SPs, one SP is deployed in 3 large cells with fractional frequency reuse (FFR) in these cells, and the other SP operates in a smaller cell which is a subset of one of the 3 large cells. In practice, it is likely that many SPs may operate in many different sized cells (A generalized sharing problem is discussed in Chapter 3.) In such scenarios, simultaneous usage of spectrum across SPs can be possibly limited in many spectrum slices or in small areas near BSs. Most SPs would be configured to use dedicated/orthogonal slices of spectrum for the rest of their coverage. Our focus is on the more complicated problem of SPs that may be configured to use RRV/"overlapping" slices of spectrum. One example of the results shows that SPs that are deployed in smaller cells can benefit significantly by using the spectrum of SPs that are deployed over larger cells. However, if such configurations are enabled, the capacity of SPs deployed in larger cells may drop by 20% per subscriber. If the demand in larger cells can tolerate this drop (example during lean periods), this may be a preferred option for the resource manager. If not, more antennas may be used in larger cells to counteract the drop in capacity if the BS and subscriber devices are thus capable.

In both simple two-cell system and multi-cell system with FFR, we consider Multiple-

input Multiple-output (MIMO) to understand how system capacity may change with capabilities of SPs and their subscribers. Capacity of spatial multiplexing MIMO [2] channel is evaluated using the Shannon-capacity formula (described in Chapter 3). Simulation results show the advantage of RRV and how the benefit changes as configuration of the RRV-enabled network. These analysis and simulation results can be viewed as ideal upper bounds of physical layer performances and are valuable for operators when they consider virtualization. However, Shannon capacity-based analysis neglects everything that is above the physical channel and it only provides an upper bound of the physical channel capacity. There are some important procedures in cellular downlink transmissions having great influence in system capacities, like scheduling, buffering, coding and modulation. Further, in the previous analysis, spectrum assigned to a SP is assumed to be equally divided and randomly distributed to the given SP's MUs. In reality, the bandwidth allocation to individual MU is way more complicated and depends on the air-interface of a given RAT. It is worth studying RRV on top of a realistic standard-based cellular system.

In this dissertation, LTE is chosen to be the platform for an RRV case study. LTE makes massive use of radio resource management (RRM) procedures such as link adaptation, hybrid automatic repeat request (HARQ), power control and channel quality indicator (CQI) reporting. Theses functions are placed at physical and MAC layers, and strongly interact with each other to improve the usage of available radio resources. In Chapter 6, a LTE system-level simulator is developed following 3GPP standards. It has two main RRM functions – CQI computation (considering adaptive modulation and coding (AMC)) and proportional fair (PF) PF scheduler. The whole scheduling process can be described in a sequence of operations: In every transmission time interval (TTI), each MU measures its channel condition, computes its CQI and reports to the resource manager. Then the resource manager uses the CQI information within PF scheduler to allocate resource blocks (RBs). Here CQI information includes measured channel signal to interference plus noise ratio (SINR) and is used to compute MU throughput. The PF scheduler chooses the MU with high throughput relative to the average MU thought until this TTI. When a MU estimates throughput, the

[2]There are several ways to deploy MIMO serving different purpose, e.g. transmit/receive diversity that leads to power gain and lower bit error rate (BER), multi-user MIMO that generates multiple information streams aiming at multiple MUs, etc. In our model, we only consider spatial multiplexing MIMO.

simulator assumes the AMC selects the best modulation and coding scheme according to MU's SINR. An adjusted Shannon capacity formula [13] is used to simply benchmark the LTE capacity considering AMC and MIMO. It takes into account the system bandwidth efficiency and SINR efficiency, the former is determined based on system parameters, and the latter is extracted from detailed link level studies [13].

A two-SP virtualization model is built up and tested on top of this simulator. Along the same line of study as in Chapter 4 and 5, our focus is on the SPs that have potential to use "overlapping" spectrum in the same area. We still try to answer those two important questions: Is RRV beneficial? and How can we configure a RRV network? Therefore we assume that one SP covers several large cells and the other SP operates 4 small cells, all of the 4 being subsets of one of the large cells. For simplicity, no frequency reuse scheme is deployed in cells. Inherent from conventional LTE RRM, every eNB has its own resource manager module that operates scheduling, while resource managers exchange information extensively over X2 interface. They can also been seen as one "virtual" resource manager. The purpose of this design is to facilitate virtualization but to keep minimum modifications to an existing LTE system. To enable virtualization between SPs, we integrate RRV into the resource manager, allowing SPs to use each other's radio resources under certain conditions. We propose and test three schemes over our simulator – unconditional RRV, time domain (TD) muting RRV and major-interferer time domain (MI-TD) muting RRV. In unconditional RRV, both SPs' scheduled MUs can access the entire system bandwidth within any subframe. TD muting RRV regulates the SP that operates small cells to be muted in some portion of time-domain subframes. Similar to TD muting RRV, MI-TD muting RRV mutes the SP that is deployed in small cells in some subframes. However, it distinguishes the small cell that generates the strongest interference to a given MU associated to the larger cell then mutes only that specific small cell when the MU is scheduled. Simulation results show that unconditional RRV only increase the system capacity of the SP that is operating in the small cells. Most configurations of TD muting RRV improves one SP's system performance at the sacrifice of the other SP's. MI-TD muting RRV provides some alternatives to improve both SPs' system performances.

1.3 CONTRIBUTION OF OUR RESEARCH

The contribution of our work can be concluded as follows.

First, we propose RRV and hierarchical spectrum sharing scheme which exploits both multiplexing gain and RRV gain in virtualization. We analyze the RRV gain as a function of transmit power, separation distance between interfering BSs, cell radius and the degrees of freedom in a MIMO channel. A combined SINR matrix is used to observe the change of capacity in MIMO channels. The effect of degrees of freedom in MIMO channel is illustrated. With the customized MIMO settings for SPs, they can isolate their own networks and provide various services to MUs.

Second, our investigation of the RRV scheme in a relatively complicated cellular environment provides a framework that evaluates the resource efficiency, and potentially the ability of customization and isolation in a virtual wireless network. The results of this evaluation can be seen as a manual or guideline showing possible network configurations of SPs' for a resource manager. On the other hand, pricing of radio resources that may be dynamically leased by a SP from an InP, the cost of reconfiguration and management of the network, and service agreements between SPs and InPs, hinge on the ability to manage the radio resources appropriately. Hence, our technical evaluation of scenarios can assist in such economics and policy decisions.

Third, a case study of LTE virtual system is initiated. We develop a LTE system-level simulator following 3GPP standards and integrate RRV into LTE radio resource management. We proposed and tested 3 different ways of RRV implementation – unconditional RRV, TD muting RRV and MI-TD muting RRV. Extensive system-level simulations are conducted, through which we claim that RRV is worth applying in LTE networks however tradeoffs between SPs exist and strategies concerning isolation and customization of virtual networks are necessary.

The rest of this dissertation is organized as follows. In Chapter 2 we go over the background and related work of wireless virtualization. In Chapter 3, the scope of our research problem is described in terms of a general spectrum-sharing model and evaluation metrics. Analysis of a two-cell virtualization is presented in Chapter 4 where the value of our study

is showed. Chapter 5 extends the analysis of virtualization to a multi-cell FFR model to exploit possible proper configurations. In Chapter 6, we introduce our LTE system-level simulator and proposed RRV implementations. Finally, we discuss limitations and future research directions, and conclude this dissertation in Chapter 7.

2.0 BACKGROUND AND RELATED WORK

In this chapter, we walk through the evolving path of virtualization and briefly introduce some related incarnations and existing work. As the focus of this dissertation is cellular virtualization, new cellular technologies that are considered to pave the "virtualization" road are also discussed. However, we only introduce technologies used in our analysis models. Chapter 6 covers functions/algorithms used in LTE RRM following 3GPP standards. At the end of this chapter, we propose three paradigms of wireless network virtualization, one of which is the foundation of the system model we consider throughout this dissertation.

2.1 WIRED NETWORK VIRTUALIZATION

Wired virtualization is not a new topic among the research communities. The impetus to conquer the "development ossification" of the Internet that set-in due to its multi-provider nature inspired the idea of virtualization. The Internet's stunning success has infiltrated every aspect of our lives. Its architecture supports multitude of distributed applications and a vast array of network technologies. Unfortunately, its popularity has led to its own growing ossification. Due to the multi-provider nature of Internet, the chance that multiple providers jointly agree on any major architecture change is slim. Even if an agreement is achieved, the cost of the replacements of routers and host software might be significant. Simple incremental updates have occurred to adapt to the increasing requirements of applications, but they may just serve a short-term purpose. Sometimes they might make the deployment of new network technologies more difficult [14, 15].

Wired network virtualization requires no fundamental change to the existing network.

SPs are dissociated from InPs. InPs focus on managing and upgrading the physical infrastructure. SPs offer end-to-end networks through their VNs. Each wired VN is a collection of virtual nodes and virtual links. The virtual nodes and links are usually part of the real nodes and links. Wired network virtualization enables multiple SPs to dynamically compose the wired VNs based on one underlying network. Coexisting VNs provides services to their own customers while maintaining isolation from each other. Such a dynamic environment eliminates the inherent limitations of the Internet without huge amounts of investment. It is a convincing proposal to fend off the ossification and a candidate for future networks.

Two views on the concept of wired network virtualization exist in recent articles. The architecture "purist" considers network virtualization as a means to evaluate new architectures. It is nothing more than a high-level abstraction that hides the underlying physical details [14]. The other comes from the "pluralist". It thinks that the network virtualization is an architecture attribute of Internet itself by enabling a plurality of diverse network to coexist [15]. However, either the pure overlay network or new network architecture refers to the barrier-free design and resource sharing. There is no essential difference between those two views.

Some virtual techniques and incarnations have been developed in the wired field. For instance, Virtual Local Area Networks (VLAN) [16], Virtual Private Networks (VPN) [17], active and programmable networks [18], and overlay networks [19]. They are developed at different protocol layers, but all have the architecture of multiple coexisting networks. Some techniques virtualize the nodes and links, like servers and routers [6, 20]. Some want to build up a virtual framework on the fly to fulfill specific objectives [21, 19].

Viewed as an extension of wired network virtualization, wireless network virtualization approaches can be developed along similar paths. Wired network virtualization has been playing a significant role in shaping the way we could improve the network. Some mature methods and strategies to virtualize wired networks can be adopted directly by wireless networks, especially some hardware virtualizing techniques. Besides, due to the same nature of resource sharing, wireless networks and wired networks may have the same challenges in terms of instantiation, operation, and management.

2.2 RELATED INCARNATIONS

Although wired network virtualization has received immense attention all over the world, wireless virtualization is an important but missing piece that has not received appropriate attention it is entitled to. However, economists have noticed the development of wireless networks. They argue that market mechanisms are necessary for resource management. Some incarnations related to virtualization have been well known in wireless networks.

2.2.1 Cognitive Radio

Cognitive radio (CR) is a promising approach to access the unutilized portion of spectrum. It can be viewed as a type of spectrum virtualization. In a CR environment, unlicensed users may sense and access the licensed bands on a negotiated or an opportunistic basis. However, it is very difficult to address a technical problem – "hidden nodes" in the practice of this user-centric paradigm. Even if a CR user A detects a certain portion of the spectrum available and then starts sending signals, A still may interfere with some other radio transmissions. As a future-working mode to coordinate a large number of CRs, some research papers integrated brokers into the telecommunication business model [22, 23]. Those dynamic frequency brokers (DFBs) are responsible for assigning frequency bands to radio nodes within their geographic area. Such radio nodes submit their reports (channel conditions, QoS requirements etc.) to DFBs every given time interval. DFBs work in a hierarchical manner, with national level DFBs on top of the regional level DFBs. The allocation is enforced from top to bottom [24]. In this model, no barriers or obstacles are placed for the utilization of spectrum across the entire bandwidth. The spectrum pool is drained based on users' demand. In other words, the wireless network evolves into a virtual environment with the presence of DFBs. Spectrum users run their operations on a high level of the network without knowing the underlying architecture. However, spectrum virtualization of wireless networks described in this dissertation is an even broader concept than the DFB system. Spectrum virtualization need not be applied in a user-centric network or be associated with CRs.

The idea of DFBs was proposed from the economists' perspective. The bidding pro-

cedures (between users and SPs, or between SPs and spectrum brokers) have been widely modeled based on game theory in literature [25, 26, 24, 27, 28, 29]. Work in [30] discussed the potential in spatio-temporal operating a dynamic spectrum access (DSA) environment, the perspective of which is similar to our work. But what we concentrate on is system-performance issues of wireless virtualization, which is more technical and practical and has lacked attention so far. Furthermore, our analysis of wireless virtualization could be a reflection of the economic models and create counter-effect to the implementation of those models.

2.2.2 Mobile Virtual Network Operator

Mobile Virtual Network Operator (MVNO) is a special network operator who leases radio access from its host MNO. It can be seen as a special implementation of wireless virtualization. As we all know, a cellular network is a radio access network (RAN) distributed over a geographic area. It connects mobile users to the core network. The strict definition of MVNO differs from country to country. A RAN of MVNO that is leased from MNOs connects MVNOs subscribers to its own switching center. The network operated by MVNO can be connected to the MNOs networks that have agreements with the MVNO. The huge shift in traffic from voice to data in cellular networks has driven new MVNO models. In the case of the Amazon Kindle, when a customer purchases a Kindle, he also gets a network contract. Customers need not worry about the monthly wireless charges since Amazon have already paid the wireless fees. Customers can buy Amazon books over a cellular network any place, any time. Although the MVNO concept has brought much service differentiation to cellular networks, it is still not a complete model of virtualization. MVNOs lease a fixed amount of spectrum from MNOs. The radio resources in the access network cannot be shared among multiple MVNOs or MNOs in a finer granularity in time. A MVNO does not enable a sharing of the RANs among MNOs. The common situation is that a MVNO uses a single MNO. Once the agreement is built out, resources in the RAN and in the backhaul are leased exclusively to a certain MVNO on a long term. Unlike MVNOs, wireless virtualization allows sharing to occur in fine-grained manner. The partition of either spectrum or other

physical resources is fluid according to the spatial and temporal demands of different SPs. A complete sharing in wireless networks can fully exploit the available resources, but also induces challenges and issues. Since transmissions in wireless networks go through air interfaces, virtualization may cause fierce interference among the transmissions of SPs without a coordinated configuration.

2.3 WORK IN WIRELESS VIRTUALIZATION

In previous work, analysis and experimental models have been proposed to depict wireless virtualization and evaluate the virtual architecture [31, 32, 25, 33, 26, 10, 34, 35]. On one hand, people interested in market profit prefer seeing the virtual wireless network as a whole spectrum pool with hierarchical DFB management. Two categories of marketing interactions are studied – users and SPs and SPs and InPs, both of which are usually modeled as stochastic games. Solving the Nash equilibrium [25, 33] leads to the optimum price. On the other hand, work that focuses on implementation of wireless virtualization experiment on a particular platform, like LTE. Case studies and simulations have been conducted on straightforward sharing platforms, and they have shown advantages of wireless virtualization. But compared to the former one, work in the latter one is limited. Also, a little work aiming at BS virtualization presented optimizing techniques like weighted slice allocation that are integrated in physical BSs. With these techniques, MVNOs can customize their own virtual BSs [31, 36, 37].

Even in understanding of what wireless virtualization means, the picture is diffrent from researcher to researcher. Ideas can be interpreted in two ways. Some researchers consider wireless virtualization as a composition of infrastructure and spectrum virtualization. Others view the whole radio access process as cloud. Each network entity chooses a package of network components that it wants and configures them in the way it desires. For instance, a network operator manages a virtual network consisting of a group of femtocells (small scale cellular BSs designed for home or small business, is discussed later) and one large microcell. Femtocells with high capacity cover densely populated area. Microcells cover a large but

sparsely populated area. At the core network site, this virtual wireless network is a cloud inside which components are unnecessary to be known to the end-user [26].

Work that shares similar interests as ours focuses on potential improvement in resources utility efficiency. A key to achieve high efficiency is to allocate resources wisely, especially spectrum. Recently research has investigated wireless virtualization over different air-interfacing technologies (e.g. cellular and Wi-Fi networks). Virtualization in LTE inherits the idea of physical entities (servers/routers) from wired networks. A "hypervisor" is placed in base stations (BSs, eNodeBs or eNBs). This hypervisor divides an eNB into a number of virtual eNBs then assigns them to SPs [10, 38, 39]. The air interface resources (physical resource blocks (PRBs) in LTE) and other physical resources in eNBs are allocated by the hypervisor among multiple SPs, using different configuration methods to complete scheduling. Work in [40] used control theory to manipulate the contention window in the CSMA/CA IEEE 802.11 based medium control protocol, virtualizing a wireless local area network (WLAN) access point (AP) in an optimal fair way. Also, a "SplitAP" architecture was designed to emulate a single AP as multiple virtual APs and provide air-time fairness for group of WLAN users [41]. In [42], necessary additions and modifications to virtualize a WiMAX BS were addressed and an isolation mechanism that significantly improves user throughput was proposed. An interesting framework that virtualizes WiMAX networks with an optimal slice scheduler was proposed in [36]. The authors claimed such work aimed at three crucial issues in wireless virtualization - efficient resource utilization, isolation and customization. Although isolation and customization could only be achieved on a long-term basis, which hardly ensured a targeted data rate for users in every time unit, this is an original framework that has blended those three issues into the resource allocation. A weighted fairness algorithm combined with concave utility functions achieved isolation and customization while scheduling chunks/slices of spectrum [36].

Advanced scheduling schemes have been well studied in resources allocation for wired networks [43, 44, 45]. Hence, almost all existing work of spectrum slices scheduling in wireless network virtualization followed the same line and developed spectrum schedulers which partition and allocate spectrum as other resources in wired networks (i.e., bandwidth on a link, time slots on a wire, etc.). However, the quality of a frequency band varies with

interference, channel condition, and capabilities of transmitter and receiver. Those factors were barely considered in the previous work. Frequency bands can be used by multiple VNs in the same geographic area when interference is acceptable at the same time. This simultaneous usage in a geographical area happens more likely in diverse applications (e.g., high-speed wide coverage broadband by a virtual network and local applications with small coverage by another virtual network or even low-speed SCADA networks by a third one). The complex spectrum sharing problem provides opportunities in getting more benefits from sharing, but also induces challenges in isolation among SPs and customizing applications. In [46], the authors also noticed spectrum waste but the scale of wireless experiments they considered is very small. A time-space combined resources allocation scheme was developed by fitting in as many experiments as possible in one time slot. Different from this time division multiplexing (TDM) plus space division multiplexing (SDM) scheduler in a limit indoor grid, our work digs deeper in the shared spectrum quantity taking multiple scenarios into account.

2.4 TECHNOLOGIES IN OUR ANALYSIS MODEL

The multi-SP network structure considered in this dissertation is somehow similar to a typical heterogeneous network (HetNet) where small cells are distributed in the macrocell/microcell to enhance coverage and offer users larger bandwidth. HetNet deployment aims at achieving "offloading gain" that alleviates the load on a macrocell's crowded spectrum. The objective of a virtualized network is not to offload users from one SP to another, but to make wireless networks a flexible environment that accommodates diverse SPs and provides reliable services for each SP. Note that HetNets are operated by the same MNO that owns the network infrastructure and spectrum. In HetNet deployment, the cross-tier signal-to-interference plus noise ratio (SINR) is evaluated to guarantee reliable coverage in each tier [47, 48]. Indoor femtocells naturally provide interference separation (due to building walls, etc.) ensuring the quality of indoor transmissions without interfering with the users in the outdoor cells. Outdoor HetNets either coordinate concurrent transmissions of macrocell and small cells

to avoid severe interference or operate them in separate bandwidths. Such coordination is possible because one operator controls both macrocells and small cells. However, our work not only focuses on the overall system capacity improvement but also the balance of capacity tradeoffs between SPs sharing the same radio resources. Also, unlike a single-operator HetNet, layouts in the virtual network in this paper are used by different SPs. Coordinated transmissions, if any, have to be facilitated by a resource manager making it more complicated. Though the idea of virtualization is completely different from HetNet, some insights from this work might be applied in HetNets also.

In our analysis models, FFR and MIMO are considered as interference mitigation strategies (in Chapters 4 and 6, no frequency planning is considered). FFR was originally proposed by Halpern [49] to manage inter-cell interference. FFR schemes partition the total frequency band into multiple parts. Some parts are used in the center area of every cell while the others are reserved for use at cell edges. Users with good reception conditions may access bands with low reuse factor (i.e., reuse factor= 1). Users with bad reception conditions (at the edges) access bands with high reuse factor (e.g., reuse factor= 3). FFR increases system-wide spectral efficiency without loss in cell edge performance. Based on the same idea of cell wise usage restrictions, Gerlach and et al. invented an "inverted" FFR that further improved spectral efficiency and optimized frequency planning in a self-organized way [50]. The work in [51] implemented heterogeneous elements on top of the macrocell FFR layout and demonstrated gains in throughput and reliable coverage. In this dissertation, in addition to deploying spectrum sharing, we also test the ability of FFR to increase spectral efficiency in Chapter 5. Further, we include the benefits of MIMO with the virtual settings and use MIMO channel capacity as the capacity evaluation metric. This information theoretic metric was proposed in [52] to evaluate the capacity of a MIMO channel with interference using a combined SINR matrix. Multiuser detection methods for combating inter-cell interference have been developed and evaluated using this matrix [53]. The outage capacity of MIMO channels under different types of interference has also been calculated [54].

2.5 WIRELESS NETWORK VIRTUALIZATION PARADIGMS

Generally, network virtualization, irrespective of whether it is in wired or wireless environments, can be viewed as splitting the entire system. It is possible to view the network as being composed of InPs that create and manage only the infrastructure and SPs, which actually provide various services to subscribers. The resources that belong to one or more InPs are virtualized and split into slices. A SP requires a minimum of one slice of the resources from an InPs and provides end-to-end services to end-users, without knowing the underlying physical architecture of the InP. After splitting the resources into slices, each slice creates an illusion that it is an entire system by itself. This "slice" system consists of its own (virtualized) core network and (virtualized) access network corresponding to the wired slice and the wireless slice, respectively. We focus only on the wireless slice and assume the physical infrastructure that forms this slice is cellular network.

Inspired by the different degrees of virtualization, we propose three paradigms for wireless network virtualization employing the idea of InPs and SPs, namely: (1) universal, (2) cross-infrastructure, and (3) limited intra-infrastructure [3].

2.5.1 Universal virtualization

A grand vision view of wireless network virtualization is to make no assumptions whatsoever about InPs or SPs. This view of wireless network virtualization looks at the whole path of radio access as an "unbundled cloud" where virtualization is pervasive. The cloud is comprised of heterogeneous BSs (macrocells, picocells, and femto-cells, relays, and other kinds of points of access and wired backbones) that are transparent to the user [26]. It is the responsibility of a SP of a specific service to choose a package of network components, links, and spectrum and the SP configures them in the way it desires. Ideally, this could happen dynamically in an on-demand type fashion. For example, to support a specific application such as one that involves extremely low power transmissions at low rates with not very stringent delay constraints, the network components to be used may be femtocells using a small slice of spectrum or even sensor relays that use multiple hops to a destination.

This "cloud" like virtualization has complicated management, control and economic issues that have not been considered in the literature. For example, how much and what type of management capabilities are given to a SP on InP system or how can mandated/regulated services like E-911 localization be ensured, are not clear.

2.5.2 Cross-infrastructure virtualization

In this paradigm we assume that wireless virtualization is possible across InPs (inter-InP) and within InPs. This enables all of the InPs in a geographical area to allow their network resources to be shared across SPs. A simplified example is shown in Figure 2.1, assume that BS 1 and 2 belong to InP 1 while BSs 3 and 4 belong to InP 2. Two SPs are in the system SP A and SP B and they are allowed to use all resources of BS 1-4. A centralized management has to be implemented to ensure the co-operation and isolation between SPs (for this purpose, an entity named resource manager is added on top of the SPs). Notice that an InP might have bandwidth slices that support multiple radio access technologies (RATs) such as, GSM, UMTS and LTE. Inter-InP virtualization allows spectrum sharing between different SPs, different RATs and different InPs. InPs that cover the same region provide their physical resources to SPs. SPs are allocated specific resources based on their requirements, every specific time unit. There are no clear boundaries between multiple network infrastructures belonging to different InPs. It is as if all the resources are in the same pool for SPs to employ. SPs might choose the resource with the best quality or with the lowest price. However, inter-InP wireless virtualization has strict coverage/interference requirements. The coverage of InPs should either completely overlap or there has to be a way of determining what BSs from which InP covers what part of a geographical area. Otherwise there may be "service holes" when users enter an area which is not covered by a set of InPs used by a SP. Due to the limited wireless coverage of each cell, this virtualization design might be more suitable for certain areas (e.g., urban) that have highly overlapping multiple cells. Not only are the radio resources shared among different SPs, but also the nodes and links, which connect the access network to the core network. Such nodes and links should be shared in a virtualized fashion.

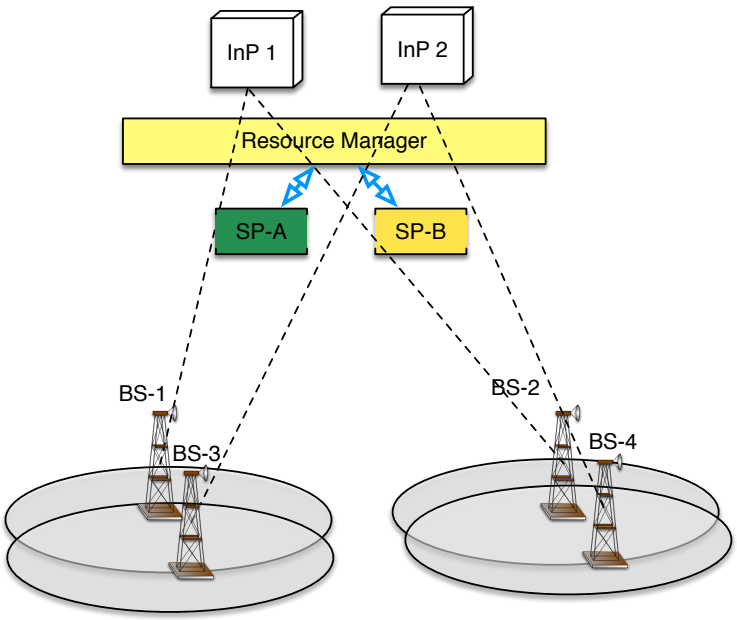

Figure 2.1: Cross-infrastructure wireless network virtualization

To design an appropriate cross-infrastructure virtualization strategy, several factors have to be taken into account, such as the entire network architecture, the QoS promised by each SP, and the fluctuation of traffic. DFB management can help with the interference mitigation and allocation of spectrum resources. For cross-infrastructure wireless virtualization, a completely centralized management may be preferable. A well-designed centralized strategy will have a higher probability of bringing significant improvement to the network utilization, reliability, and quality of service. But a bad strategy might encroach upon some SPs deserved resource, and such a SPs may not be able to ensure a level of QoS for its users, especially the ones at the edges of coverage.

2.5.3 Limited intra-infrastructure virtualization

Limited intra-infrastructure wireless virtualization in our view considers only virtualization within a single InP, which may have spectrum that is used by different RATs. Spectrum sharing occurs between SPs and across RATs. For a given cell, we can think of a single

InP that can manage its resources and make decisions to allocate them to various SPs. The multiplexing gains are likely to be lower than those possible with a cross-infrastructure strategy as there may be InPs with demand from SPs that is greater than they can meet while other InPs have resources that are not being completely utilized. Limited virtualization can be described by the example shown in Figure 2.2. In cell 1 of a cellular system, two SPs A and B lease a certain amount of resource from BS 1 in each time interval. BS 1 is virtualized and resource manager is in charge of the spectrum allocated to SPs. Every SP can be viewed as a virtual operator (VO) with time-varying resources based on factors such as its own requirement, the amount of money it is willing to pay for resources, fairness, and other InP policies. This is similar to the single-level DFB structure where we can consider the InP as a DFB that assigns spectrum to nodes in its region and SPs as those nodes.

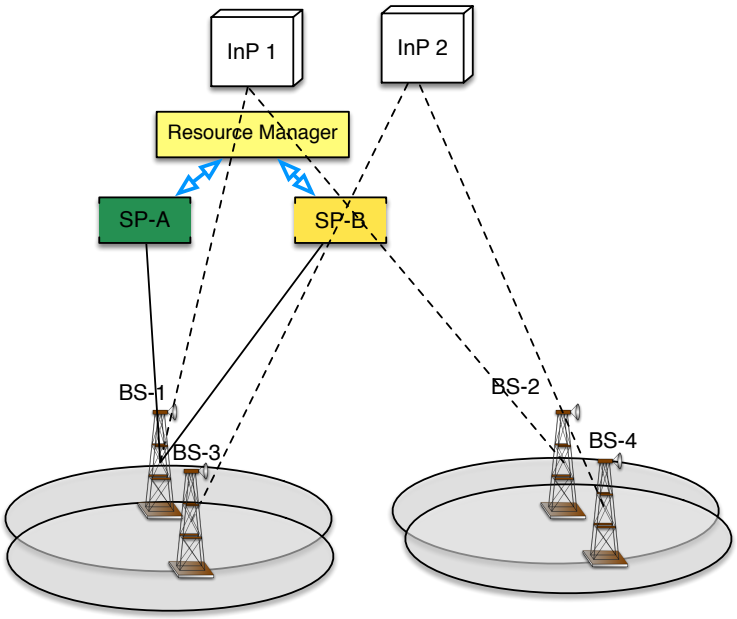

Figure 2.2: Cross-infrastructure wireless network virtualization

3.0 SYSTEM MODEL OF VIRTUALIZATION

In this chapter, we describe the scope of the problem addressed in this dissertation, illustrate the specific radio resource sharing scheme and our virtual system structure. Also, we introduce the evaluation metrics.

As mentioned before, wireless virtualization consists of infrastructure sharing and spectrum sharing, latter of which is our concern. Wireless virtualization is classified as universal virtualization, cross-infrastructure virtualization, and limited intra-infrastructure virtualization (see Chapter 2). As to how InPs pools up their licensed frequency bandwidth or how they inter-connect backhaul networks is beyond the scope of our research problem. We build up our system models based on limited intra-infrastructure virtualization. Therefore, we focus on how a resource manager can configure radio resources to enable SPs to simultaneously use them on top of the infrastructure owned by one InP.

3.1 RADIO RESOURCE VIRTUALIZATION

The problem we examine is how to better exploit resource utilization efficiency through spectrum virtualization? Here we introduce our spectrum virtualization scheme – RRV through comparison with SSV.

To illustrate our proposed RRV, we use a simple two-SP example: assume that two SPs – SP_A and SP_B are on top of one InP's infrastructure and serve in the same area. A traditional network distributes distinct spectrum bands for each MNO (no decoupling of SPs and InPs) over a long term. In contrast, a virtualized network does not separate the bandwidth. SP_A and SP_B can get varying amounts of spectrum units in every time unit based on

their requirements, agreements with the InP, and the corresponding policies. In SSV, the spectrum slices allocated to the two SPs in the same time interval do not overlap (this is the case considered in the virtualization research literature). The multiplexing gain with SSV can be simply explained as follows. If x denotes the fraction of total available bandwidth B assigned to SP_A in the first time unit, then $1-x$ is assigned to SP_B. SSV in Figure 3.1 shows that in the second time unit, SP_A takes a proportion $a(t)$ of SP_B's bandwidth for its use as determined by the fluctuating traffic load, policies, etc. The multiplexing gain for SP_A can be defined as $B_{A'}/B_A$, where $B_{A'}$ is the available bandwidth for SP_A after multiplexing and B_A is the original bandwidth assigned to SP_A (which is xB). The gain for SP_A is $1+\frac{a(t)(1-x)}{x}$. Similarly, SP_B, could get an extra bandwidth $1+\frac{b(t)x}{1-x}$. Since the total available bandwidth is unchanged, $a(t)$ and $b(t)$ could be positive or negative and $a(t)(1-x)+b(t)x=0$ in every time unit. This multiplexing gain has been considered in the literature as mentioned previously [11, 10].

We argue that *radio resources* should be considered as a function of geography and signal strength potentially allowing some spatial-temporally overlapping allocation of spectrum slices to SPs in the same time interval (RRV in Figure 3.1). RRV sharing can be implemented in conjunction with SSV. The combination of RRV and SSV can improve the usage of spectrum due to an extra RRV gain in addition to multiplexing gain. The RRV gain depends on the amount of overlapping spectrum slices simultaneously used by SPs. Obviously, there will be interference within those overlapping spectrum slices, which will impact the RRV gain. Also, whether or not interference in the simultaneously used spectrum slices is tolerable depends on the requirements of both of the SPs.

We study two-SP RRV in a simple two-cell network and a multi-cell FFR network in Chapter 4 and Chapter 5 respectively. The RRV gain is quantified if there is any.

3.2 GENERAL RRV MODEL

Based on understanding the idea of RRV in the two-SP example, we extend RRV to a three-SP limited intra-virtualization scenario shown as Figure 3.2, and generalize the problem

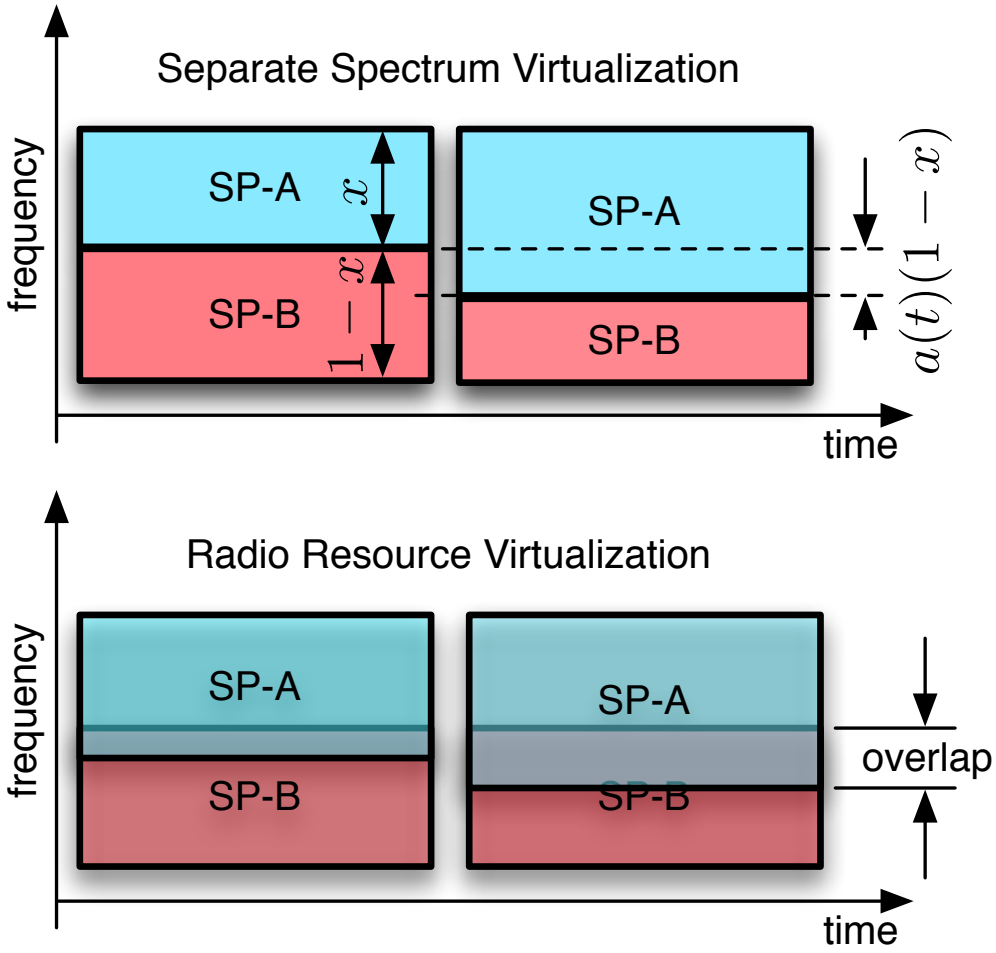

Figure 3.1: Two-SP SSV Vs. RRV

addressed in our work. In Figure 3.2, an InP owns cellular infrastructure that covers an area (BS 1, 2, 3, and 4). It has agreement with 3 SPs (SP_A,SP_B and SP_C) that SPs can form their individual virtual networks over this infrastructure. A resource manager is placed and in charge of allocation of spectrum to SPs in every time unit based on each SP's traffic and the agreement with the InP. An example of deployment is shown in Figure 3.2, on top of BS 1, 2 and 3, SP_A and SP_C use some spectrum to form virtual networks with 3 large cells. SP_B makes use of some of BS 4's spectrum to operate a small cell.

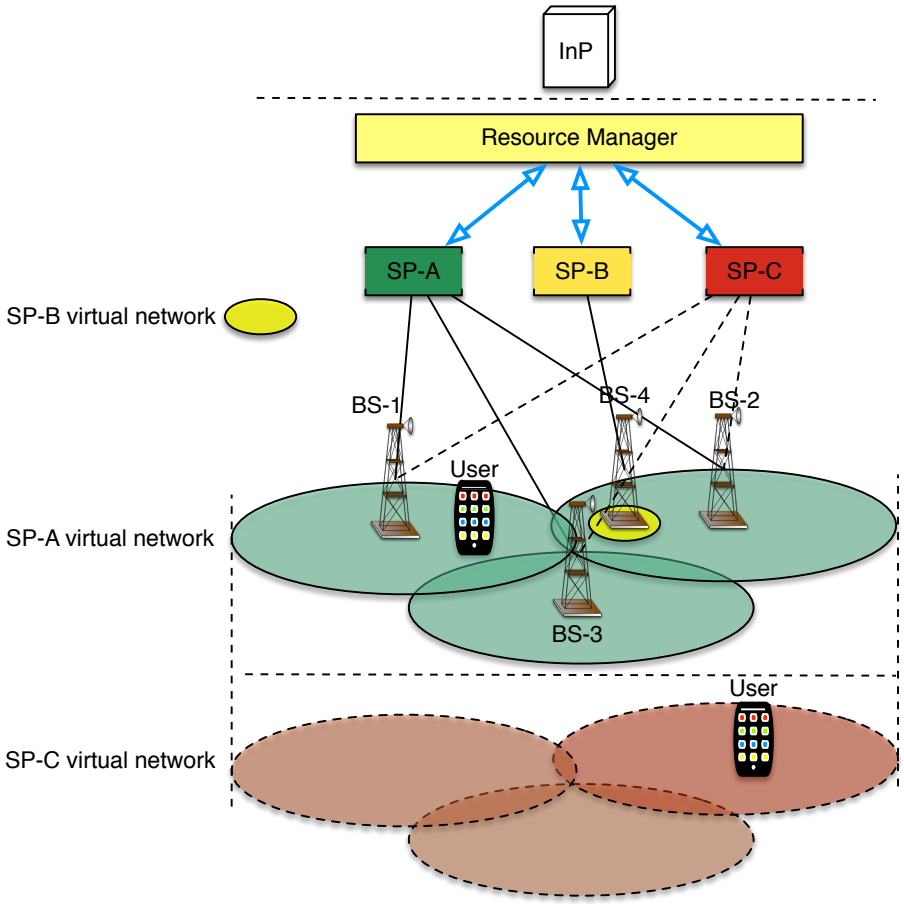

Figure 3.2: Limited intra-infrastructure wireless network virtualization

A RRV scheme of a three-SP virtualization is depicted in Figure 3.3. The top half shows the corresponding three-SP SSV. Spectrum slices allocated to SP_A, SP_B, and SP_C in the same time interval do not overlap, but may change dynamically in time. RRV that allows a certain overlapping allocation of the spectrum slices to multiple SPs in the same time interval

in overlapping or neighboring geographical areas is shown in the low half of Figure 3.3.

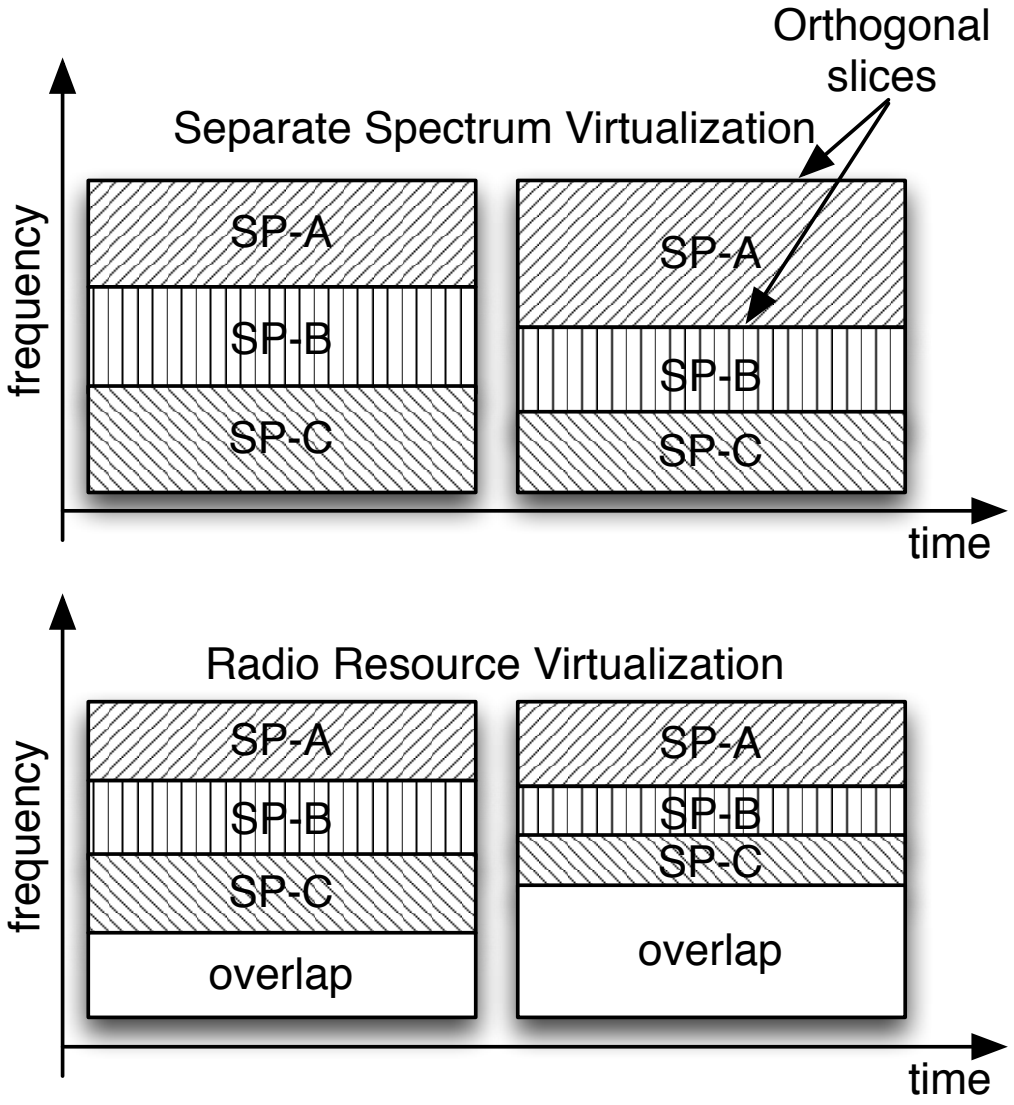

Figure 3.3: Three-SP SSV Vs. RRV

We implement RRV (shown in Figure 3.3) in the three-SP system (shown in Figure 3.2), then use Figure 3.4 to illustrate the general problem addressed in our work. The problem is described as follow. There is an infrastructure in place with multiple BSs, of which four are shown in the figure (BS 1 to BS 4). The BSs can be configured for use by multiple SPs (they are "hard metal" infrastructure being shared by virtual networks). The usage may vary - in Figure 3.4, we show two SPs SP_A and SP_C making use of BS 1, BS 2, and BS 3 at the same time, each having the same approximate coverage. The spectrum used by SP_A

and SP_C are orthogonal (in a manner similar to SSV). We can assume that the slicing of resources between them is completely orthogonal with minimal interaction between them. In contrast, SP_A and SP_B are configured such that they are sharing spectrum (described below in more detail). The difference is that the configuration is used only with SP_B's use of BS 4. In other words, we can view SP_B as operating a hotspot that is configured to use SP_A's spectrum in addition to its own. If SP_B is also using BS 1 to BS 3, it is configured to use orthogonal spectrum. The case we are considering here is one where SP_A and SP_B are configured such that the *spectrum that is shared, is used over the three macro-cells served by BS 1 to BS 3 for subscribers of SP_A, and one micro-cell served by BS 4 for subscribers of SP_B*. If spectrum is shared between the macrocells simultaneously in space and time, it is likely that the interference will be too high. Our objective is to examine the ramifications of this sharing that is limited in space.

Note that Figure 3.4 is a generalized example we use here to emphasize our research problem. Actually only two SPs, SP_A and SP_B, are considered in this dissertation. The number of cells and the network structure vary in our study as well. The three-cell model in Figure 3.4 is only considered in Chapter 5 where we look into various configuration cases including the effects of frequency reuse schemes (e.g., FFR) and analyze the impact to develop a configuration framework for the resource manager. In Chapter 5, we consider a simple two-cell model to see if RRV leads to higher resource efficiency than SSV. In Chapter 6, a virtualization model in which each SP leases spectrum from multiple cells (one InP) is built on top of a LTE network.

Also all assumptions we have in Chapter 4 and 5 are not absolutely necessary. The analysis is based on only snapshots of networks. In a completely virtualized system, the resource manager often makes configuration decisions every given unit of time and the configurations will change dynamically to meet the needs of the SPs. We make the assumptions to simplify the problem and obtain some preliminary insights as relaxing these assumptions would make the problem intricate, and the results hard to easily generalize. To give a more comprehensive study on virtualization, we relax some of our assumptions and approach a practical virtualized system by a LTE case study in Chapter 6)).

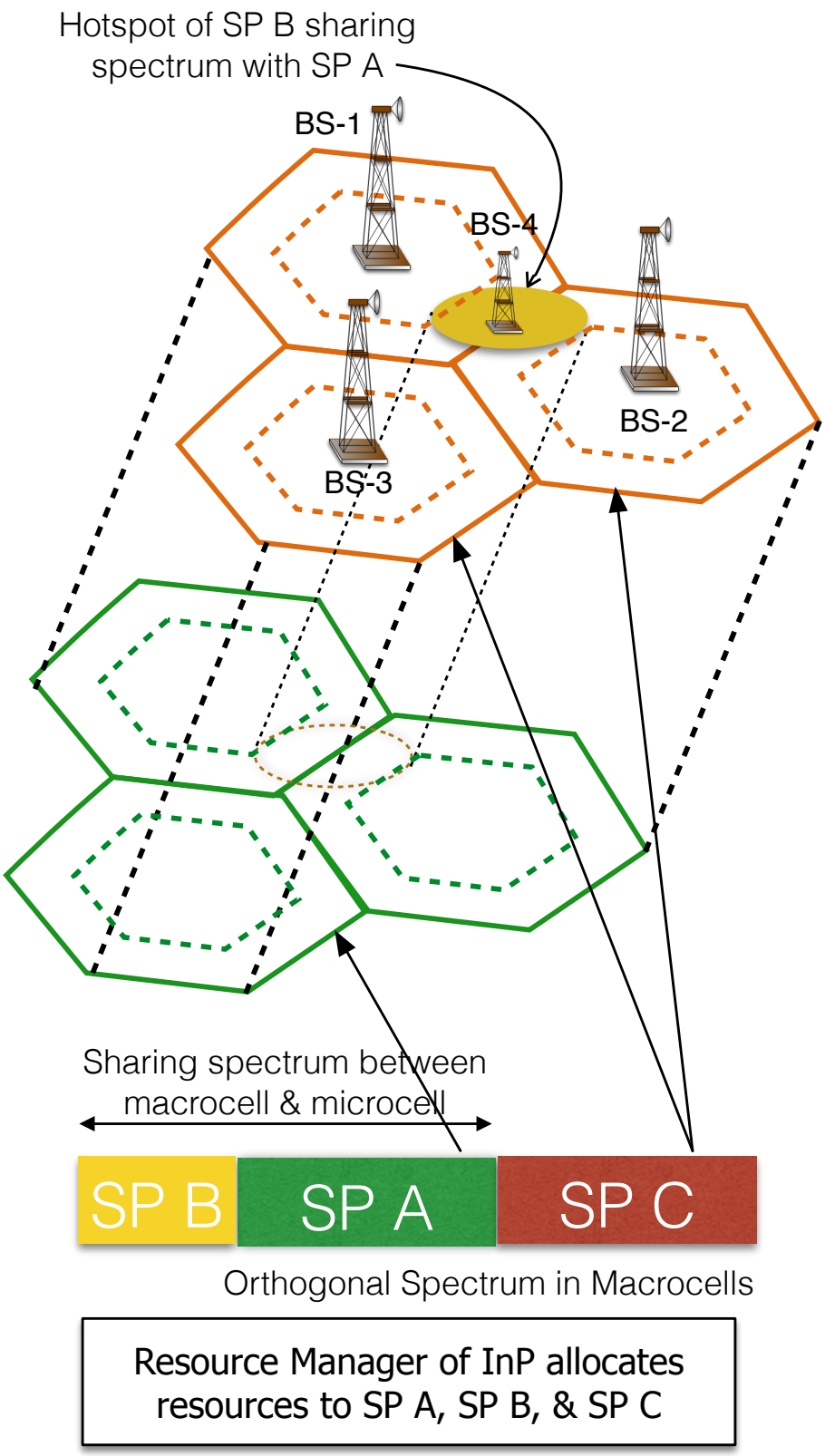

Figure 3.4: A three-SP virtual system

3.3 EVALUATION METRIC

In our analysis, a common evaluation metric is Shannon capacity while in our case study, the 5-percentile and 50-percentile MU throughput are computed as evaluation metrics.

3.3.1 Shannon capacity of MIMO channel with interference

From an information-theoretical perspective, capacities are calculated within system models and viewed as a upper-bound of system performance in terms of physical channel capacities. In Chapter 4 and Chapter 5, Shannon Capacities provide obvious trends of RRV and valuable insights of configuration.

Generally, SPs may be using very different radio access technologies and devices. In order to get some insight into the potential of system capacity gains, we utilize capacity calculations rather than specific modulation, coding, and application requirements in this paper. Our objective is to consider these specific aspects in future work to the extent possible. Here, we assume that all the downlink transmissions (by all BSs forall SPs) employ MIMO[1] for exploring spatial degrees of freedom and for combatting any interference. We assume the commonly employed frequency-flat quasi-static MIMO fading environment, where the transmission between the ith transmit antenna and the jth receiving antenna can be modeled by

$$y = \sqrt{D^{-\alpha} 10^{\zeta_j/10}} h_{ij} \times x + N \tag{3.1}$$

where x, y are transmit and receive signals respectively, D is the distance from a transmitter to a receiver (the transmitters are the BSs, but transmissions may end up at receivers that do not belong to them as interference), α is the path loss exponent, $\zeta = N(0, \sigma)$ is the shadow fading component, h_{ij} is the Rayleigh fading channel gain of the channel between the ith transmit antenna and the jth receiving antenna, and N is the thermal noise with variance $N_0/2$. This model applies to all BSs and all SPs.

Assume that the transmission operates in a $n_T \times n_R$ downlink MIMO channel, where n_T is the number of transmit antennas at BS and n_R is the number of receiving antennas at the

[1]It is possible that the applications and devices may be very different, some using SISO and others MIMO. We assume MIMO with all SPs for simplicity.

MU. The achievable data rate of a single MU can be estimated by the (Shannon) capacity formula [52, 53],

$$C = w \log_2 \det[(\mathbf{I}_{n_R} + (\mathbf{R}^{-1/2}\mathbf{H})P_T(\mathbf{R}^{-1/2}\mathbf{H})^H] \tag{3.2}$$

where w is the available bandwidth for one particular mobile user (MU), and the transmit power is P_T. $\mathbf{H}$ is the complex channel gain matrix, consisting of $\sqrt{D^{-\alpha}10^{\zeta/10}}h_{ij}$ where ζ varies independently for each user (but it is kept fixed over time once the sample has been drawn from the distribution for a given user). $\mathbf{R}$ is the interference and thermal noise combined matrix, which is given as:

$$\mathbf{R} = \sum_k \mathbf{H}_{Ik}\mathbf{H}_{Ik}^H P_{Ik} + wN_0\mathbf{I}_{n_R} \tag{3.3}$$

where $\mathbf{H}_{Ik}$ is the interfering channel matrix from interfering Cell k. For example, MUs in SP_A's layout face interference from BS-4 in the small cell but MUs in SP_B's layout receive interference from BSs 1, 2 and 3. P_{Ik} is the interferer's transmit power and $\mathbf{I}_{n_R}$ is an identity matrix of dimensions. From an information theoretic point of view, the capacity in Eq. 3.2 is equivalent to the capacity of the combined SINR channel $\mathbf{R}^{-1/2}\mathbf{H}$ under Gaussian white noise. With this interpretation, the capacity can be calculated as a Gaussian white noise channel [55]. We assume that the orthogonal sub-channels created through MIMO are dedicated to the same user, and so, the achievable data rate is

$$C = \sum_{i=1}^{min(n_T,n_R)} w \log_2(1 + \lambda_i P_i) \tag{3.4}$$

where P_i is power allocated in ith orthogonal sub-channel, $\sum P_i = P_T$ (P_T is the total transmit power.) and λ_i is the ith orthogonal sub-channel gain, which is obtained through a singular value decomposition (SVD) process as follows.

$$\mathbf{H}^H\mathbf{R}^{-1}\mathbf{H} = \mathbf{U}\Lambda\mathbf{U}^H \tag{3.5}$$

Here, $\Lambda = diag(\lambda_1, ...\lambda_{n_R})$ are the singular values of $\mathbf{H}^H\mathbf{R}^{-1}\mathbf{H}$ and $\mathbf{U}$ is a unitary matrix consisting of the eigenvectors of $\mathbf{H}^H\mathbf{R}^{-1}\mathbf{H}$. Note that, when we compute the singular values, large-scale fading (distance, path-loss, ζ) scales them in *both the interfering MIMO channel matrix and the desired MIMO channel matrix for a given SP's receiver.*

The transmit power allocation for each antenna can be determined in different fashions. The optimal strategy that maximizes capacity [52, 53] is the classic water-filling algorithm. However, it requires comprehensive channel information to be known by both the transmitter and the receiver.

$$C = \sum_{i=1}^{min(n_T, n_R)} w \log_2(1 + p_i \lambda_i) \tag{3.6}$$

where p_i is the power allocated to the ith orthogonal sub-channel and $\sum p_i = P_T$ [2].

We use as one of our metrics, the area aggregate spectral efficiency [3],

$$\eta = \frac{C_A + C_B}{w_{tot}} \tag{3.7}$$

where C_A and C_B are the achievable data rates (capacity) in SP_A's and SP_B's layouts, respectively. They are the sum of the achievable data rates of *all the MUs* subscribed to SP_A and SP_B within the coverage. That is, $C_A = \sum_{i=1}^{nu_A} C_i$ and $C_B = \sum_{j=1}^{nu_B} C_j$, where C_i and C_j are calculated by Eq. 3.6.

3.3.2 X percentile MU throughput

Different from Shannon capacity that is computed over random MU locations, shadow fading and channel fading in every simulation run, 5-percentile and 50-percentile MU throughputs [4] are obtained at the 5% and 50% points of the cumulative distribution function (CDF) curves, respectively. MU throughput is taken from simulations and reflects the bits of information MUs receive in our simulator. We record throughputs of all MUs in the given network, every simulation run, then generate the CDF curve accordingly. The 5% and 50% points are taken from each simulation run and the average values are calculated over the simulation runs and presented in the plots.

[2] The optimal transmit signal covariance matrix is $\Sigma_s = (N_0/2)\mathbf{U}diag(p_1, ..., p_{n_R})\mathbf{U}^H$ where $p_i = (\mu - \frac{1}{\lambda_i})^+$ and μ is chosen such that $\sum_{i=1}^{min(n_T, n_R)} p_i = P_T$. The function $(.)^+$ denotes the larger one of . and 0.

[3] The area spectral efficiency of a cellular system is defined as the achievable data rate per unit area for the bandwidth available. Here we assume the area of SP_A's layout to be the unit of area of interest, so the measure of area spectral efficiency is in terms of bit/s/Hz/(area of SP_A's layout) [47, 48]. "Area of SP_A's layout" is neglected.

[4] We pick 5-percentile and 50-percentile MU throughput to make some results are comparable to ones in the existing work [56].

4.0 RADIO RESOURCES VIRTUALIZATION IN A SIMPLE CELLULAR NETWORK

4.1 MOTIVATION

This chapter is the first step of our research. We aim at deploying RRV in a simple cellular network and investigating how much gain in resource usage efficiency is achievable and under what circumstances.

Virtualization has great potential to improve resources usage efficiency by spectrum sharing while supporting isolation between users/services and enabling customization of applications. In previous chapters, we have mentioned that most existing work on spectrum sharing considered spectrum as normal resources in wired networks which consist of orthogonal slices. In other words, sharing of spectrum occurs only at the level of chunks of frequency. However, spectrum is not like a simple resource such as time slots on a wire or certain bandwidth in a link. Most existing works assume no "inter-cell" interference in any spectrum chunk (no simultaneous usage of spectrum slices in nearby geographical area). In reality, there is chance that a user's QoS requirements (i.e., achievable data rates) can still be ensured when bearable interference occurs within the user's spectrum slices. Therefore, allocation of orthogonal/separate slices may cause waste in spectrum. We should consider radio resources that are a function of factors like geography, signal strength, user device capability and QoS requirement as shared quantity, rather than orthogonal slices. Simultaneous usage of spectrum in a geographical area is more likely in diverse applications (e.g., high-speed wide coverage broadband by SP_A and local applications with small coverage by SP_B or even low-speed supervisory control and data acquisition (SCADA) networks by a third party).

Based on the general system model described in Chapter 3 (see Figure 3.4), a simpler cellular network is considered in this chapter. As illustrated in Figure 4.1, two SPs, SP_A and SP_B that have agreements with an InP that cover an area, can access the InP's frequency band following resource manager's assignments. Through the leased spectrum, one virtual network's coverage is a subset of another. Therefore, those two SPs have chance to use the same spectrum in time and space. We quantify how much gain exclusively comes from RRV in a this simple network. When we consider RRV, transmit power, interference, and the usage scenario (capabilities/needs of devices) become important in determining how much of sharing is possible, or say how much of gain is achievable. This type of potential gain in utilizing spectrum has been neglected so far in the research literature. Results of investigation here are strong proof that shows RRV often leads to better resource efficiencies compared to SSV. MIMO is used to reduce the interference and increase the capacity to the possible extent as explained before. The contribution of the analysis in this chapter can be concluded into twofold.

- RRV gain is investigated as a function of transmit power, separation distance between interfering BSs, cell radius and the degrees of freedom in MIMO space. A "combined SINR matrix" is used to observe relation of RRV gain and MIMO space.
- Possible strategies of customizing virtual networks are proposed and tested, including directional transmissions and customized MIMO settings.

4.2 HIERARCHICAL SHARING

We consider only the downlink in our model shown as Figure 4.1. In a wireless environment, radio propagation (that includes large-scale and small-scale fading) spatially creates "layers" of users. When SP_A and SP_B manage transmissions to certain mobile users (MUs), they may have a chance to use the same frequency bands at the same time in the same area. Suppose SP_B has three layers of MUs, indicated by three different circles in cell B in Figure 4.1. SP_B probably can operate its virtual network on the spectrum which has already been allocated

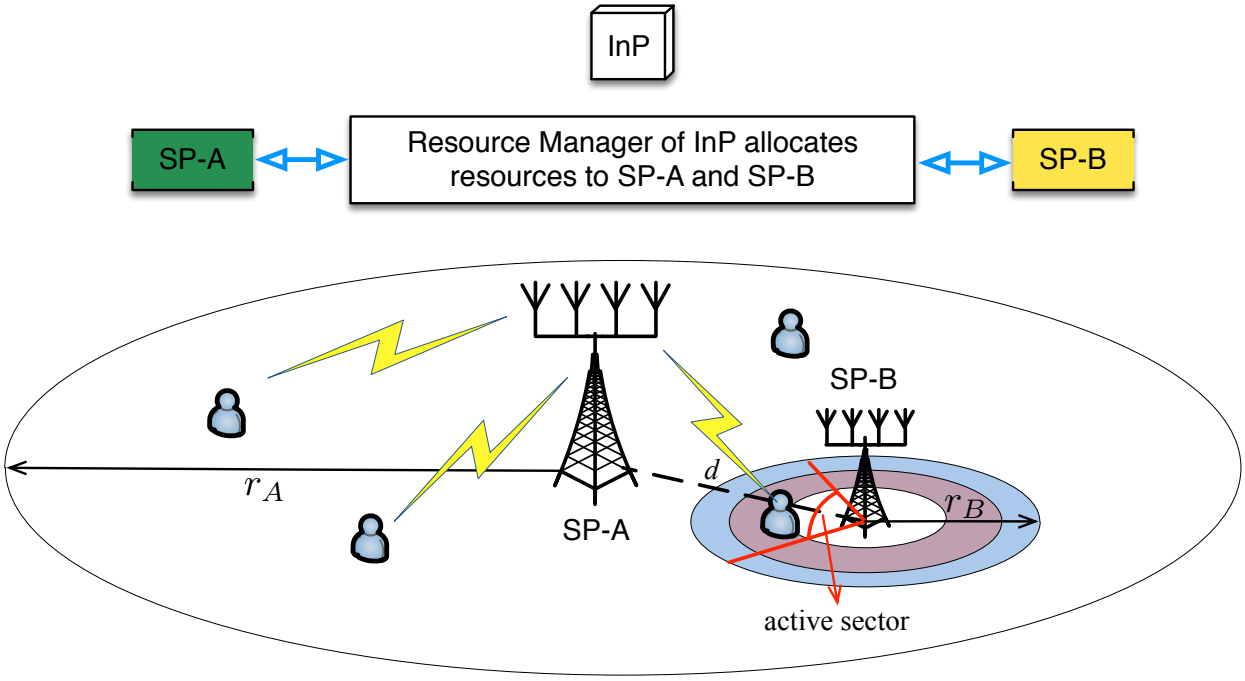

d – distance between two interfering BSs
r_A – radius of the large cell of SP-A
r_B – radius of the small cell of SP-B

Figure 4.1: A two-cell system

to SP_A (and probably being used by SP_A) in the white circle. MUs in this "white layer" can possibly achieve their desired data rate because the received SINR for such users is still high enough. We call this reuse scheme as RRV. The situation of MUs in the "middle layer or middle ring" is not that clear. It is quite likely that some of these MUs are able to reuse the SP_A's spectrum slices, but not all of them. This implies that the SP_B can only partially share spectrum with SP_A in the middle circle, i.e., allow MUs with high SINR to utilize SP_A's spectrum and allocate separate spectrum slices to those with low SINR. As far as the "outer layer" is concerned, most MUs in this outer ring layer will face fierce interference. Hence it is better that the MUs in this layer be assigned (by a scheduler) orthogonal spectrum slices that do not overlap with those of SP_A in every time unit. When SP_A does not use a spectrum slice, SP_B can use it everywhere. In this simplified system, both SSV and RRV generate gains. Obviously, such layers exist in the larger cell as well. Also, we show circular coverage here, but this is not the case in reality. We do not fix any particular coverage area in the evaluations in this chapter since a large scale fading model with shadow fading and small scale fading are used everywhere, except to constrain MUs of different SPs into specific areas to evaluate the capacities they achieve.

As discussed in Section 3.2, we focus on the sharing that is limited in space, thereby the sharing happens between SP_A with the large cell and SP_B with the white circle. RRV gain on the downlink transmission is quantified in terms of answering questions such as: How large can the white circle be? What level should the transmit power be? Hence, in the following study, only MUs in the white circles are considered. *We assume SSV is adopted in system no matter if RRV is allowed in various circumstance.*

4.3 NUMERICAL RESULTS

First, we evaluate the RRV gain in terms of capacity for multiple scenarios. Second, the cumulative distribution functions (cdf) of the singular values of a combined SINR matrix $\mathbf{R}^{-1/2}\mathbf{H}$ (see Eq. 3.2) are presented as a function of the separation distance between the BSs of the small and large cell, the small cell radius, and the available degrees of freedom in

the MIMO channel. A proportional relationship between the combined channel matrix and capacity can be observed by comparing the trends in the cdf as the various parameters change. The combined SINR matrix is a candidate that measures interference level or capacity. The layer (circular rings of Figure 4.1) of a particular MU and the sharing scheme to be applied may be determined based on these numbers. Finally, the potential of MIMO enabled RRV for customization across different virtual networks is investigated. We run simulations based on a two-cell RRV system, as shown in Figure 4.1. r_A and r_B are the radii of the large cell and small cell (used for placing MUs) and d is the separation distance between the two BSs. A MU's coordinate can be expressed as $(l,\ \phi)$ where $l \in (0, r_B \text{ or } r_A)$ and $\phi \in (0, 2\pi)$ and we distribute MUs uniformly over the radius and the angle. Results shown are averages of 10,000 simulation runs that vary locations, ζ, and h_{ij}. Suppose a MU belonging to SP_A is at $(l_i,\ \phi_i)$, the distance between this MU and the BS of SP_B can be calculated as $L_i = \sqrt{{l_i}^2 + d^2 - 2l_i d cos(\phi_i)}$. The combined SINR matrix (that includes transmissions from SP_A and interference from SP_B) can then be generated using Eq. 3.1. We assume that the large cell and the small cell have separate 10 MHz and 5 MHz frequency bandwidth allocation respectively and the total bandwidth is 15 MHz for the RRV system. Unless specified, at each BS, $n_T = 4$ antennas are adopted while $n_R = 2$ antennas are used at each MU. The transmit power P_A is 40 dBm, P_B is the transmit power of the small BS, and $N_0/2 = -178$ dBm. α takes the value of 4 (except for the conditional $\alpha = 2$ cases – see below) and $\zeta = N(0, \sigma)$ where $\sigma = 8$.

4.3.1 RRV and Capacity

We calculate the aggregate spectral efficiency in Eq. 3.7 while varying the power ratio (P_A/P_B) for the seven different RRV scenarios described in Table 1 to obtain insights on how this changes with various parameters. Error bars correspond to one standard deviation of the mean aggregate spectral efficiency over 10,000 runs. Table 1 lists the number of MUs in the large cell and in the small cell respectively.

Table 1: Parameter Settings for Various Scenarios

ID.	r_A	r_B	nu_A	nu_B	d
1	1000	50	100	10	500
2	1000	50	100	20	500
3	1000	50	100	10	800
4	1000	50	100	10	300
5	1000	100	100	10	300
6	1000	100	100	10	800
7	1000	100	100	20	300
SSV only	1000	50	100	10	-

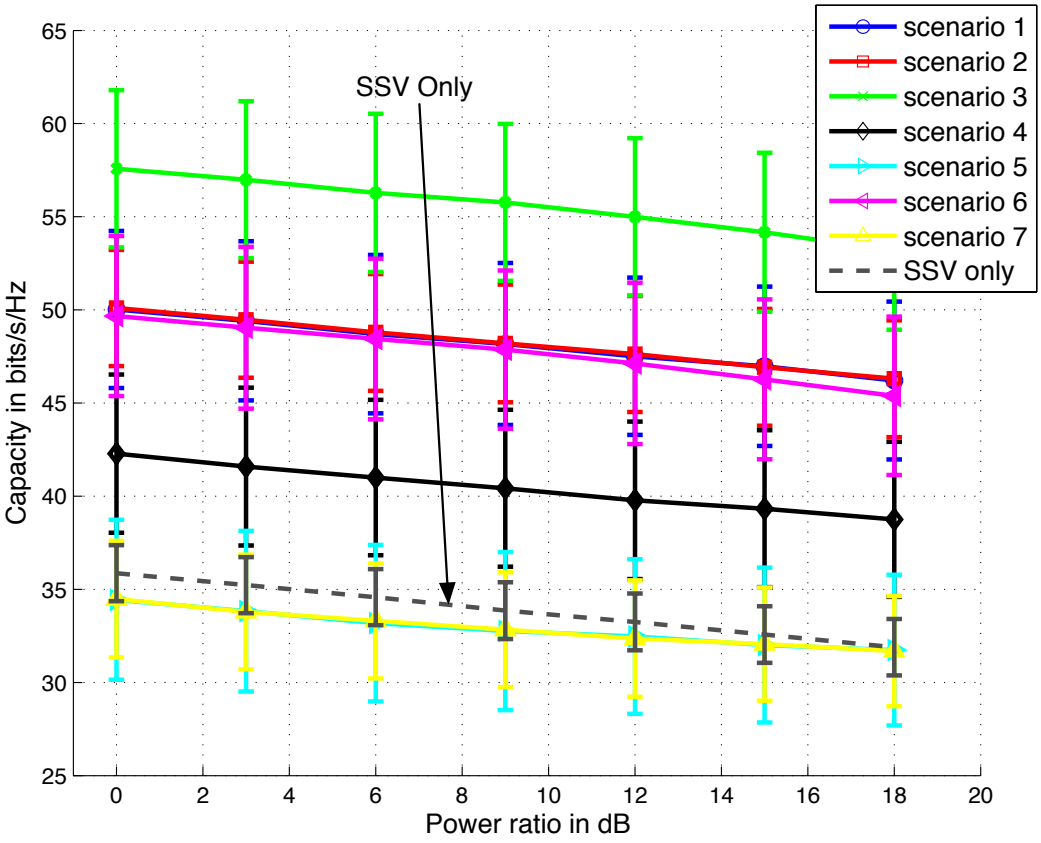

Figure 4.2: Aggregate capacity of two cells with water-filling

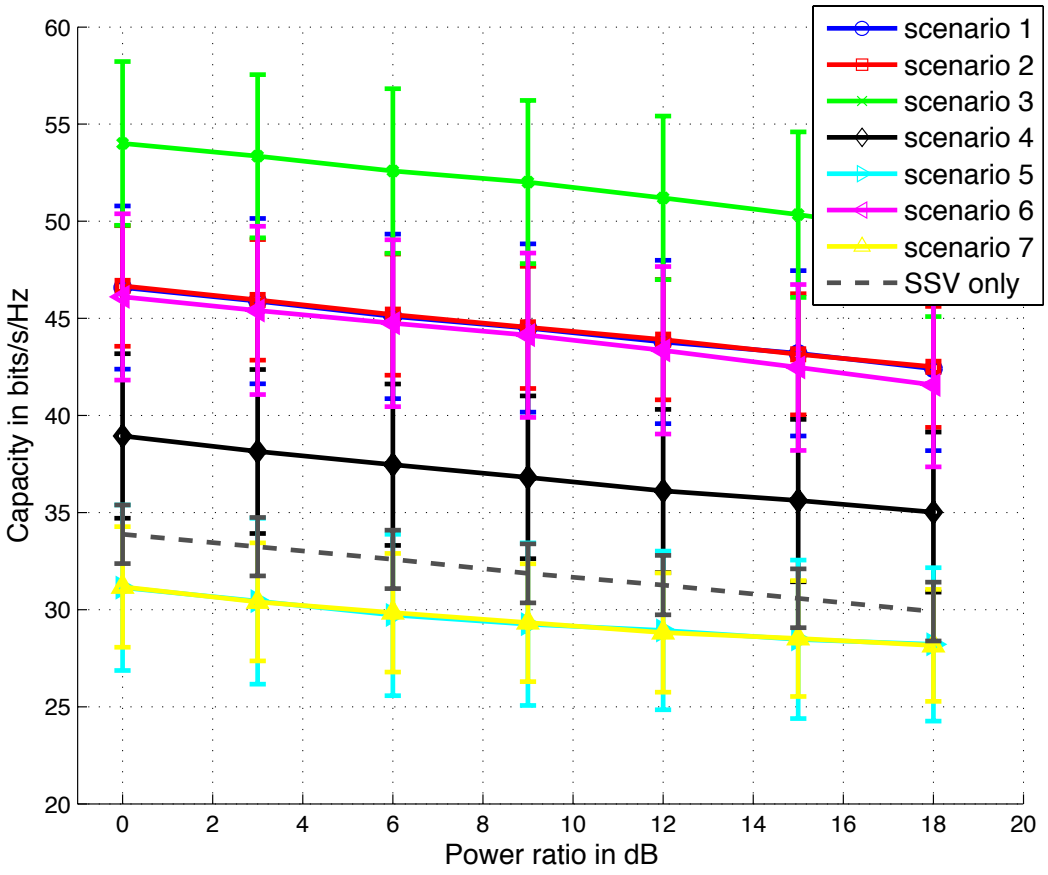

Figure 4.3: Aggregate capacity of two cells with equal power allocation

4.3.1.1 Aggregate Spectral Efficiency

The aggregate spectral efficiency for the water-filling algorithm and equal power allocation [1] is shown in Figures 4.2 and 4.3 respectively. The variation in capacity results primarily due to the location of MUs (but also due to the random fading). We omit error bars in some figures for clarity. Several preliminary conclusions can be perceived here. First, in either the water-filling or equal power allocation case, the spectral efficiency for the SSV only scheme (in Table 1) is mostly below that for all the RRV scenarios with the same parameter settings, which shows there is some gain that exclusively comes from RRV. Second, water-filling outperforms (as expected) equal power allocation approximately by 3 or 4 bits/s/Hz. Third, larger numbers of MUs in the small cell do not significantly affect the aggregate capacity because SPs are assumed to orthogonally and equally share the spectrum amongst their own MU groups. Fourth, the aggregate spectral efficiency increases as the separation distance between two BSs becomes larger but reduces when the small cell's radius increases. This implies that if the two BSs are too close (e.g., closer than 300 meters), they will not be able to adopt RRV (alternatively, the small cell should shrink further to enable RRV). Lastly, increasing the power ratio (P_A/P_B) from 0 to 18 dB changes the efficiency only a little (e.g. 3 bits/s/Hz in scenario 2). That is, the distances from SP_B's BS to SP_A's MUs are such that they make this power ratio as not a very significant factor. On the contrary, the large-scale fading for interference, which depends on the separation distance d and cell radius r_B is influential. Therefore, the separation distance and the cell radius appear to be the two major factors which have influence over the aggregate efficiency.

To have a better view of how these factors affect the aggregate spectral efficiency, we evaluate them using scenario 1 as a baseline. In the cases shown here we keep r_A, nu_A and nu_B fixed and vary two factors at a time from the normalized radius r_B/r_A, the normalized distance d/r_A or the power ratio P_A/P_B. We use different values of α here ($\alpha = 4$ everywhere and $\alpha = 2$ when the distance from the transmitter is smaller than 50m - called conditional

[1] In general, the channel condition is known only by the receiver. In this case, the transmitter allocates power equally over all the antennas to maximize the capacity (this allocation is sub-optimal). The channel capacity in this case would be

$$C = \sum_{i=1}^{min(n_T, n_R)} w \log_2(1 + \frac{P_T \lambda_i}{n_T}) \tag{4.1}$$

.

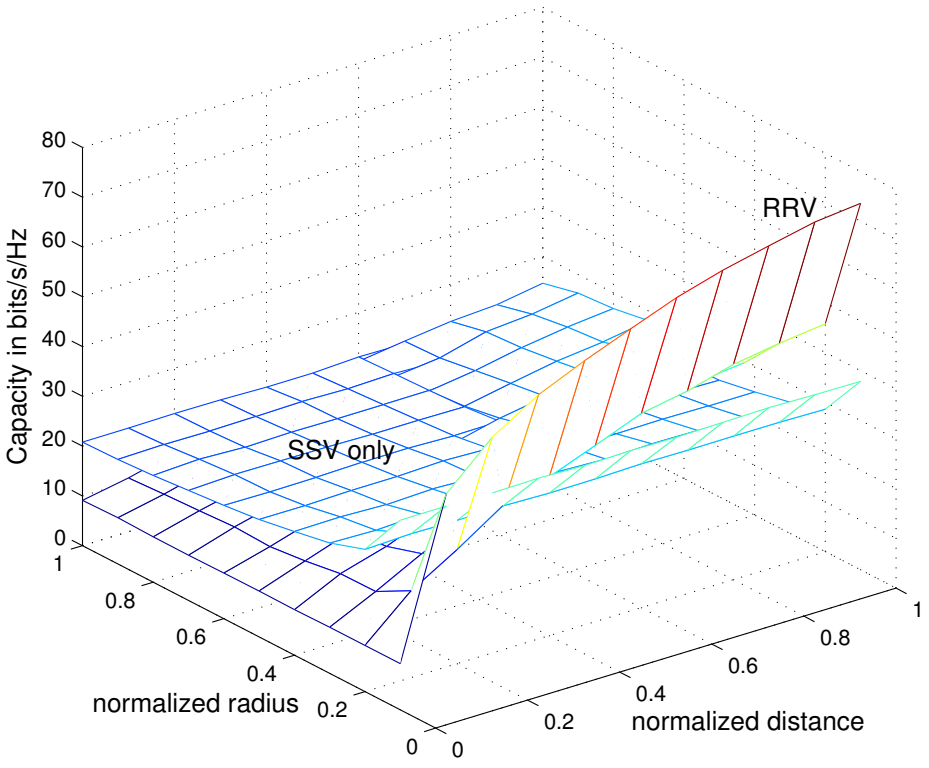

Figure 4.4: Capacity Vs. Distance & Radius ($\alpha = 4$)

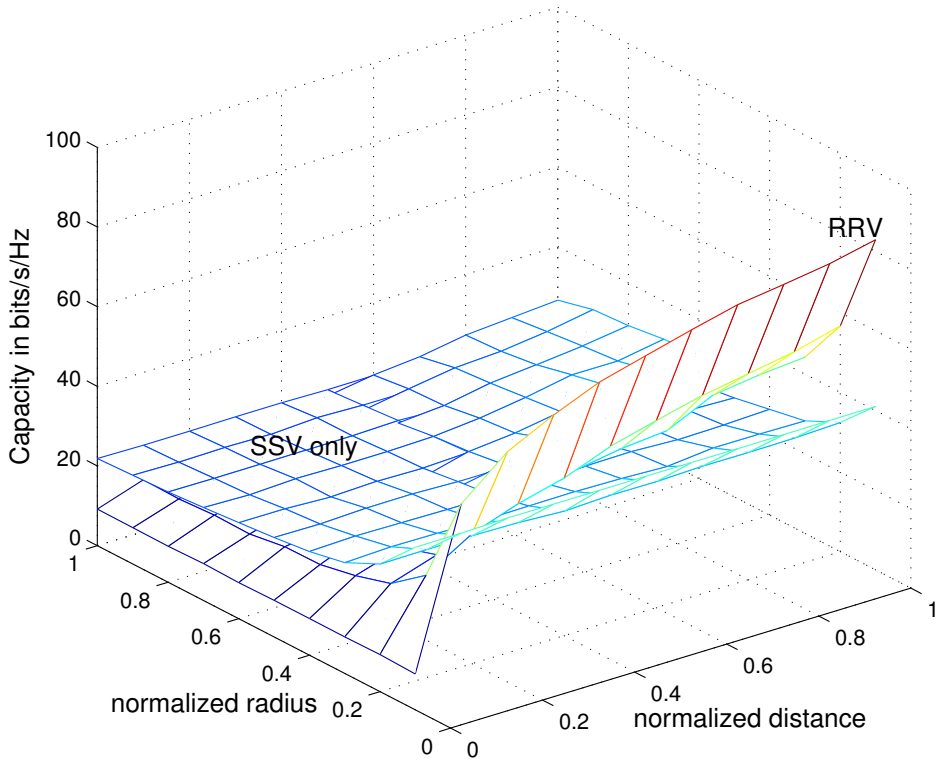

Figure 4.5: Capacity Vs. Distance & Radius (conditional $\alpha = 2$)

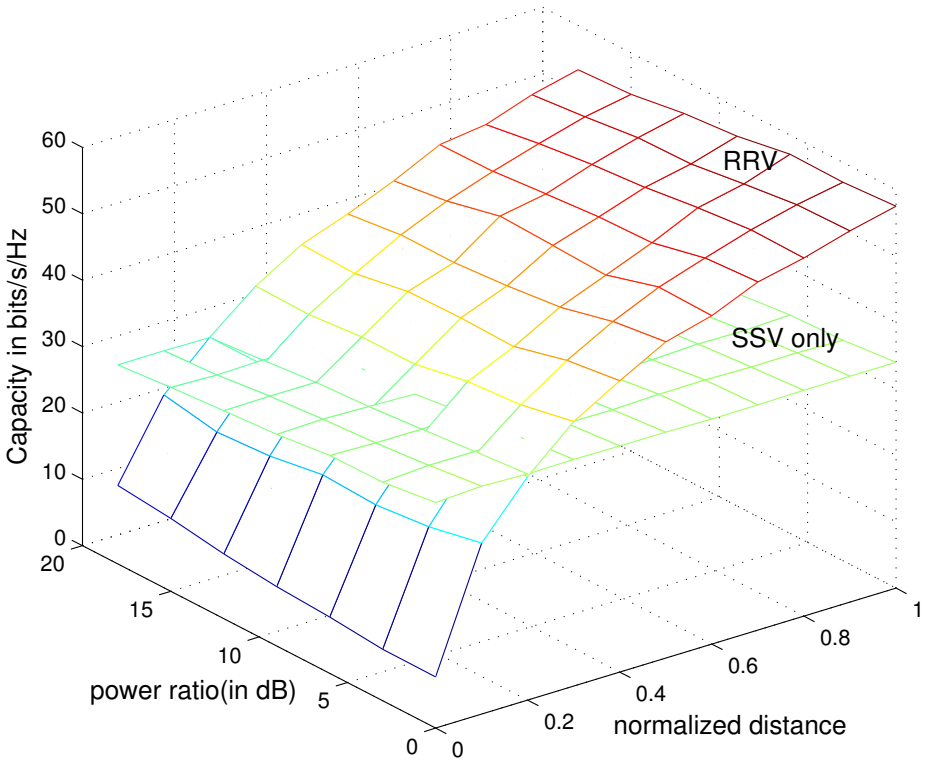

Figure 4.6: Capacity Vs. Distance & Power ($\alpha = 4$)

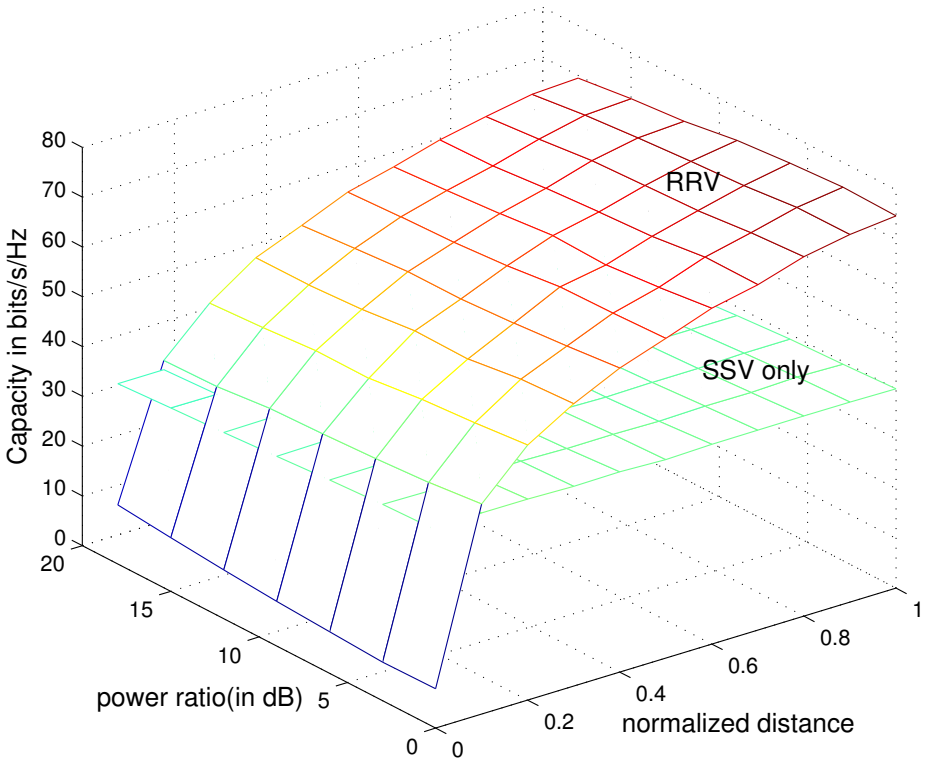

Figure 4.7: Capacity Vs. Distance & Power (conditional $\alpha = 2$)

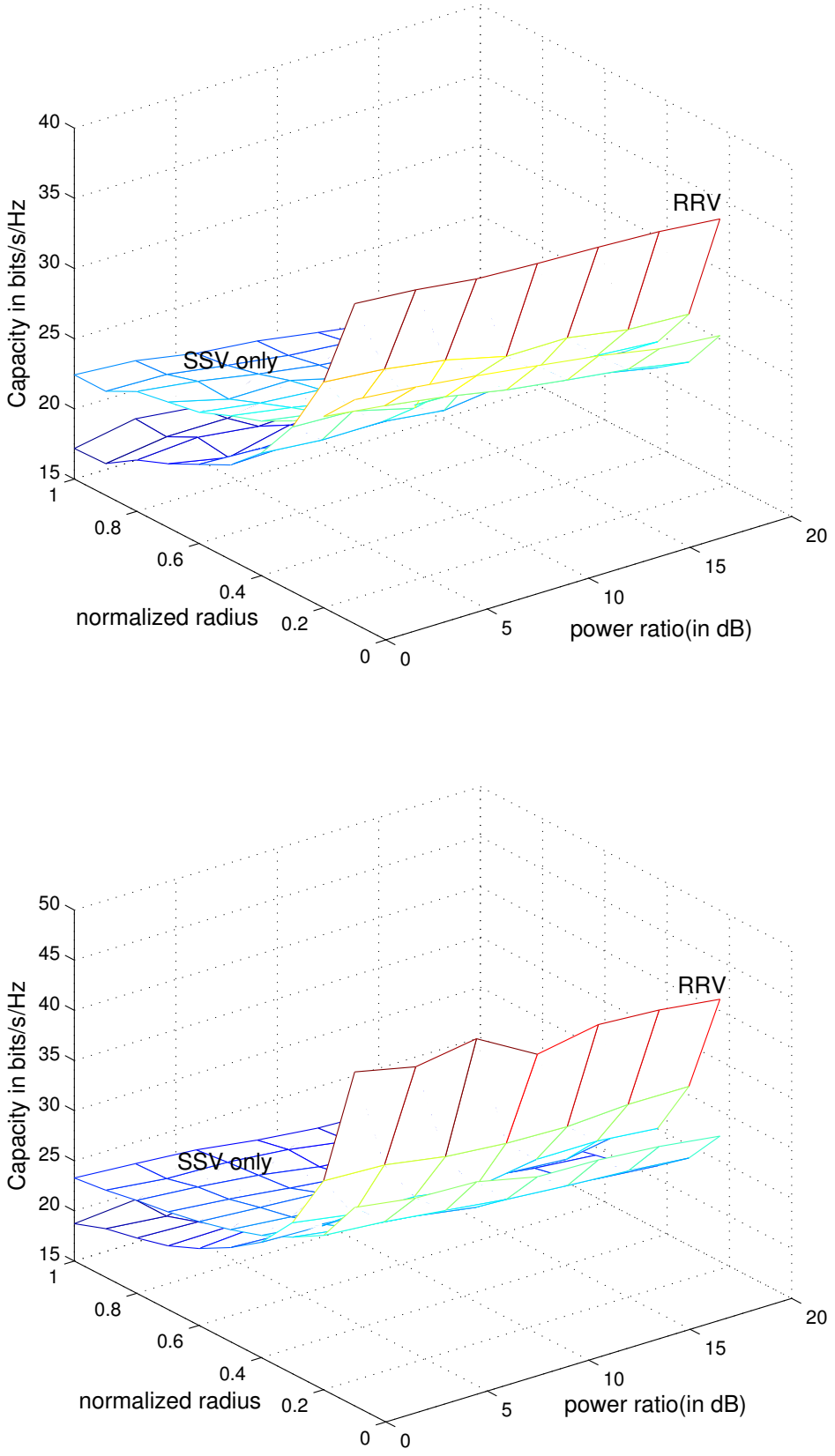

Figure 4.8: Capacity Vs. Power & Radius – top ($\alpha = 4$) and bottom (conditional $\alpha = 2$)

$\alpha = 2$, otherwise $\alpha = 4$). The average results are shown in Figures 4.4, 4.5, 4.6, 4.7, and 4.8. In Figures 4.4 and 4.5 the power ratio is fixed at $P_A/P_B = 10$ dB and we vary the normalized radius and distance. Notice that the RRV gain is dependent on the normalized radius being small for the normalized distance to have an impact. Figures 4.6 and 4.7 show the effects of varying the power ratio and normalized distance with fixed $r_B = 50$. One can see that the power ratio has little effect compared to the normalized distance. In Figure 4.8, the results of varying the normalized radius and power ratio while maintaining the distance fixed at $d = 500$ are shown. Observe that the power ratio has little influence on the capacity and the normalized radius should be relatively small for the RRV gain to be large. From Figures 4.4 to 4.8, the RRV gain is greater when $\alpha = 2$ conditionally than when $\alpha = 4$ universally since the small cell benefits by a smaller α. The service providers can use these results to decide when to switch to partial spectrum sharing or only SSV instead of RRV when it fails to achieve a desired data rate.

4.3.1.2 Individual Cells The average achievable data rate **per MU** of the large cell and small cell are evaluated in Figures 4.9 and 4.10 for all the scenarios using the equal power allocation scheme and $\alpha = 4$. Error bars correspond to one standard deviation of the average achievable data rate per MU over 10,000 runs. Note that MUs of each SP share the available bandwidth orthogonally. MUs in the large cell do not see a large increase in achievable data rate across the scenarios. The available bandwidth for SP_A's MUs does not increase much in the large cell which has 100 MUs in all scenarios. In the small cell however, the average data rate per user falls severely from scenario 1 (blue) to scenario 2 (red) because the number of MUs doubles in the small cell. Further, in most scenarios the achievable data rate is higher than the SSV only scheme for the small cell. It appears that most benefits, when they occur, are for MUs in the small cell.

We hypothesize that MUs of the large cell that are further away from the BS face excessive interference from the SP_B BS and this impacts their average data rates. To test this, we use a sectored scenario. We assume that the cell of SP_B is divided into three sectors (each 120°, shown in Figure 4.1) and RRV is used only in the one that faces the BS of SP_A (where SP_A's MUs have better channels). The achievable data rate per MU is still calculated over

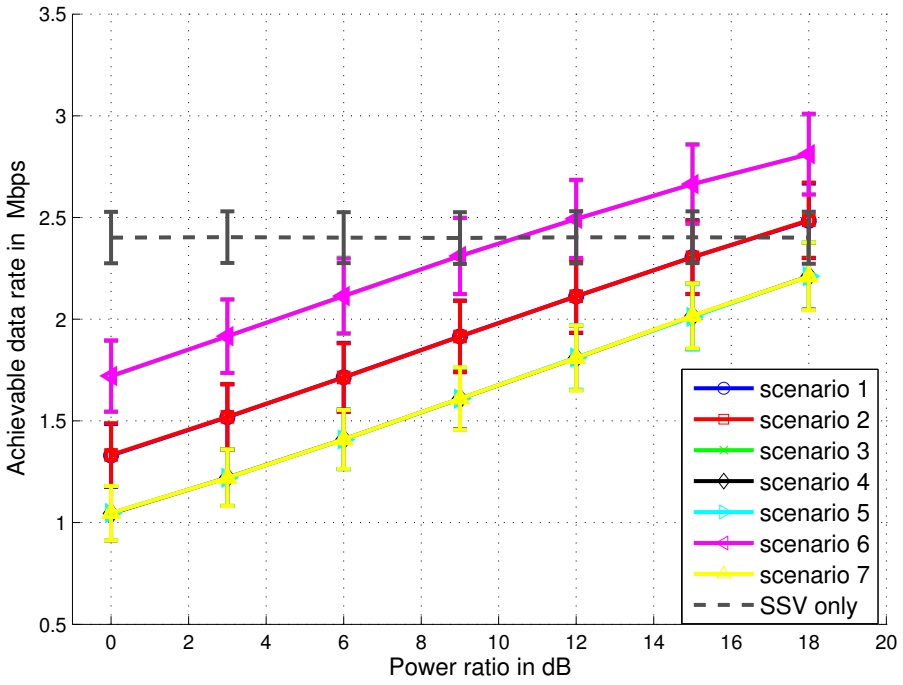

Figure 4.9: Achievable data rate at large cell (per MU)

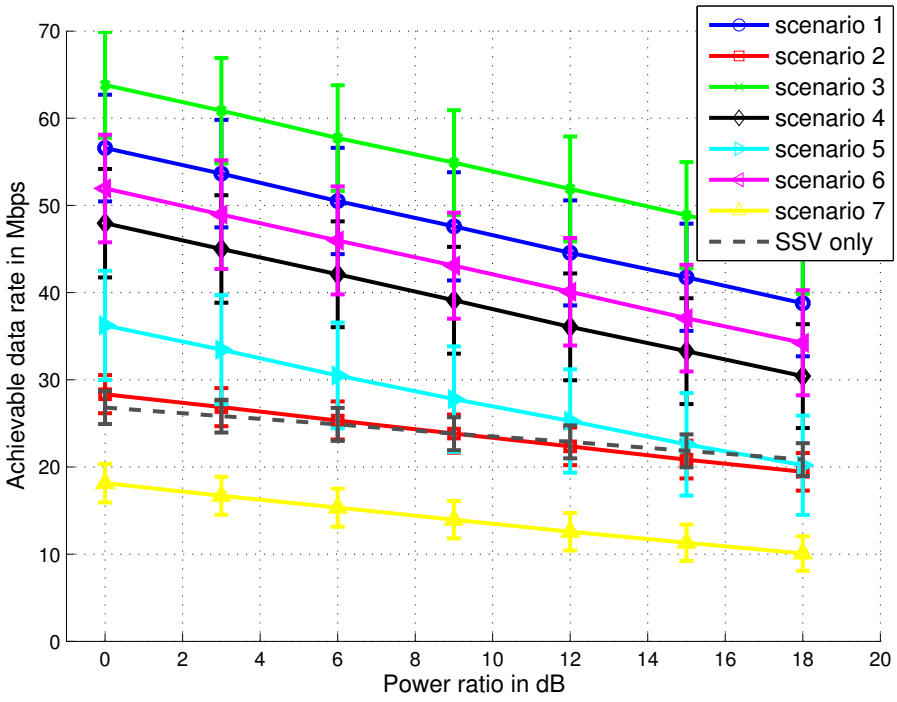

Figure 4.10: Achievable data rate at small cell (per MU)

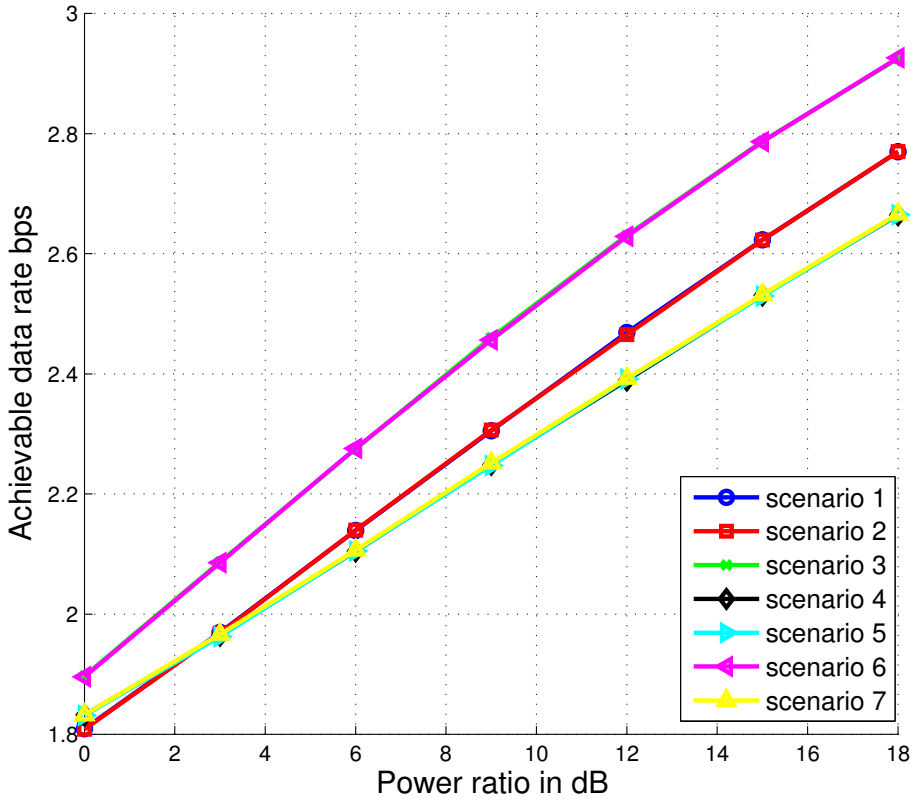

Figure 4.11: Average achievable data rate (per MU) at large cell with RRV employed in only one sector

the seven scenarios in Table 1 with unchanged parameters. In the small cell, the achievable data rate (average) for MUs of SP_B does not change. However, for the data rate of MUs of the SP_A large cell improves as shown in Figure 4.11 compared with Figure 4.9. The achievable data rate curves with the same separation distance d still group up together and are indistinguishable. However, after the small cell moves closer toward the large cell's BS (i.e., d is 300m in scenarios 4,5, & 7), the achievable data rate per MU is improved compared to the omnidirectional case implying that MUs at the edge of the large cell suffer the most under RRV.

An interesting observation can be made from Figures 4.9 and 4.10. A minor change of data rate with the power ratio implies that even if SP_A accidentally or intentionally increases its transmit power in the RRV system, it will not cause a serious damage to MUs of SP_B. On the other hand, if SP_B intentionally transmits at a high power level, what SP_A needs to do is to adjust its own power carefully to keep the desired data rate for its MUs. This aspect, while not fully explored here, becomes important when virtualization of the wireless network considers the ***isolation*** between various services under intentional or accidental misbehavior.

4.3.2 Analyzing the Combined SINR Matrix

In an RRV system, estimating the channel condition is important as it helps the resource manager to decide when RRV should be invoked. We consider the combined channel matrix $\mathbf{R}^{-1/2}\mathbf{H}$ here due to its relationship with capacity. From Eq. 3.3, $\mathbf{R}^{-1/2}\mathbf{H}$ is also a function of the separation distance d, transmit powers P_A and P_B, cell radii r_A and r_B, and available degrees of freedom (minimum number of antennas at BS or MU) in the MIMO channel. The singular values of combined channel matrix are essentially the orthogonal sub-channel gains in a MIMO channel (λ_i in Eq. 3.6) which represent the sub-channel quality. However, they do not include any information on the available bandwidth. Taking the amount of bandwidth into consideration provides the capacity for a given MU. Therefore, the rank of this combined channel matrix is also crucial, as it is the number of sub-channels possible (available degrees of freedom in MIMO channels). We sum all the singular values to reveal the "volume" of

the MIMO channel and average it by the number of MUs in each cell while observing the singular value distributions, but how the available degrees of freedom in the MIMO channel affects the combined channel matrix is considered next. The impact of separation distance d and small cell radius r_B are examined as these two factors have a larger influence on capacity. For a fair comparison, the distribution of MUs in the area is kept fixed for both cases. For the singular value vs separation distance d case, $r_A = 1000$m, $r_B = 50$m, and P_B is 10 dB less than $P_A = 1$W. For the singular value vs radius of small cell r_B case, $r_A = 1000$m, $d = 500$m, and P_B is the same as in the previous case. All the other parameters in the simulation remain. Hence, $d = 500m$ in Figure 4.12 and $r_B = 50m$ in Figure 4.14 have the same distribution and both of them stand for scenario 1 in Table 1.

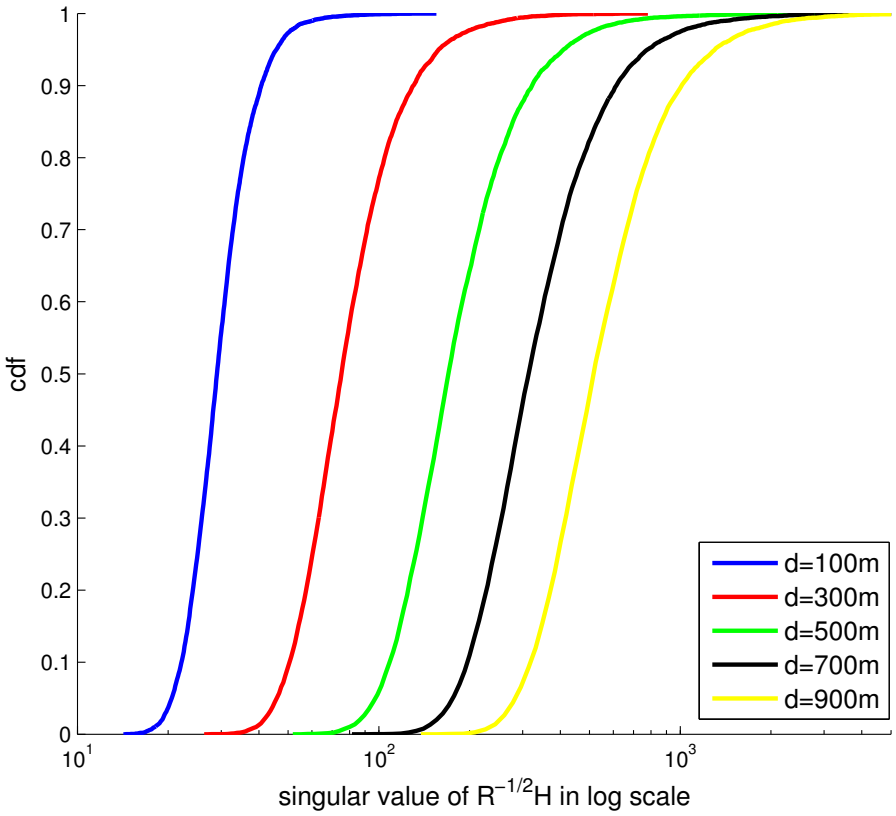

Figure 4.12: CDF of singular values at different separation distance (for MUs in the large cell)

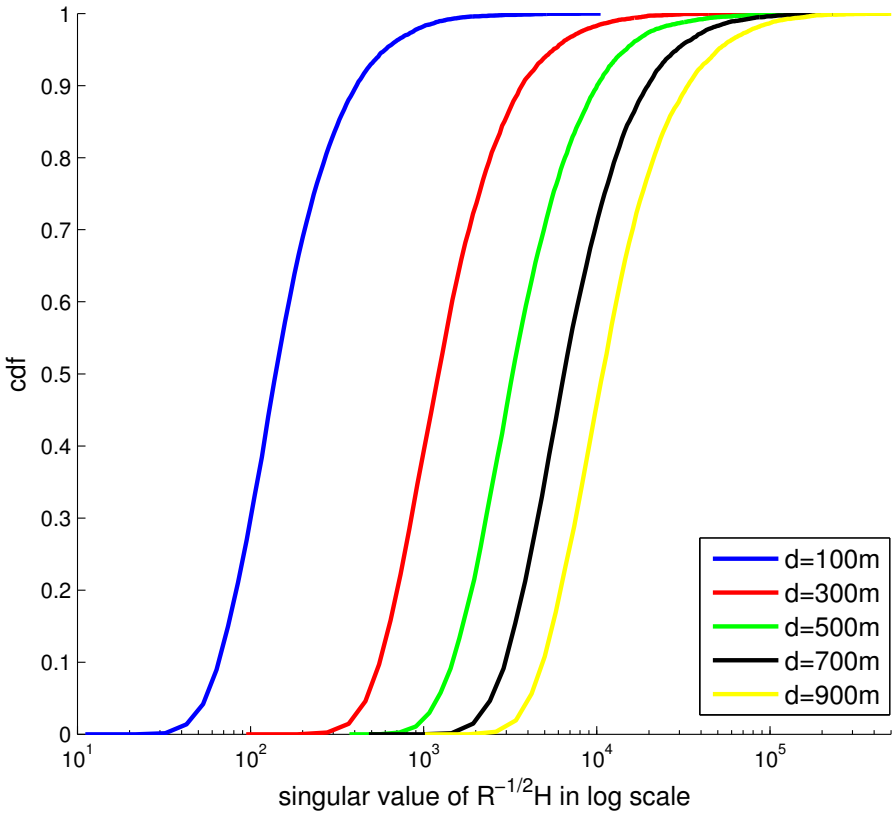

Figure 4.13: CDF of singular values at different separation distance (for MUs in the small cell)

The distribution of singular values of the combined matrix $\mathbf{R}^{-1/2}\mathbf{H}$ shifts towards the right as the separation distance d becomes larger (as shown in Figure 4.12 and 4.13) both for MUs in the large cell and in the small cell (for the same locations of MUs for each d). This means, increasing the separation distance improves both the combined matrix and the resulting capacity (shown in Figure 4.9 and Figure 4.10). Figures 4.14 and 4.15 show that expanding the small cell only degrades the capacity of itself not of the large cell, which matches what is shown in Figure 4.9 - the capacity curves cluster with the same d value no matter what the value of r_B is. As for the small cell, for the same number of MUs, the more compact the distribution of MUs, the higher the capacity those MUs can achieve. This conclusion can also be obtained from Figure 4.10 as well and is intuitive.

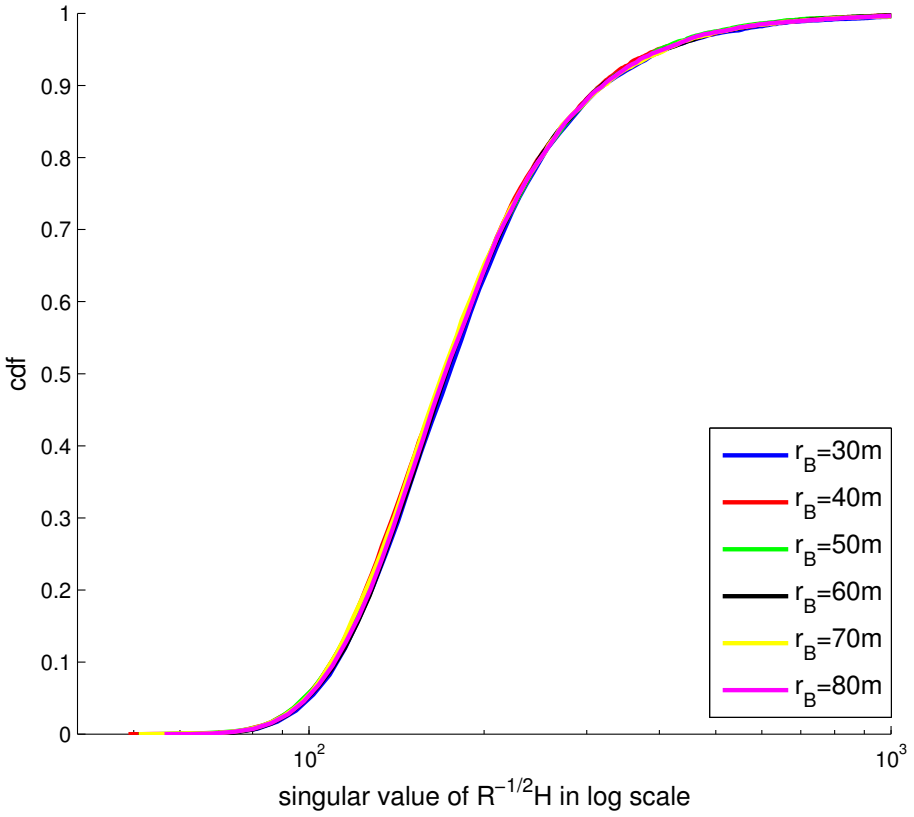

Figure 4.14: CDF of singular values at different radii of small cell (for MUs in the large cell)

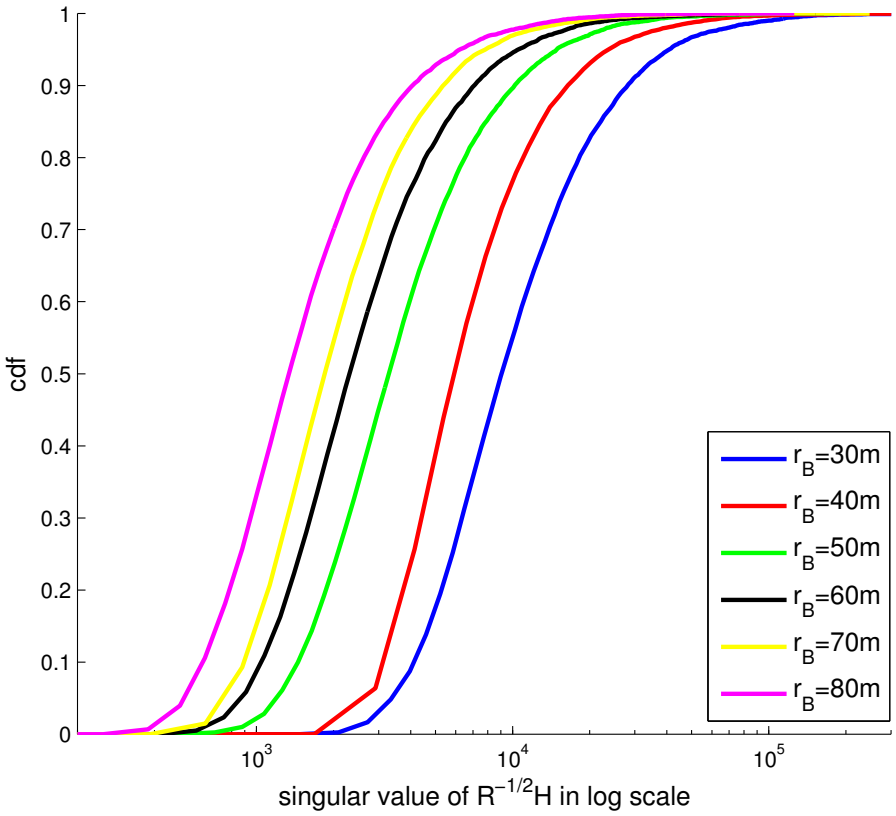

Figure 4.15: CDF of singular values at different radii of small cell (for MUs in the small cell)

4.3.3 Customization in RRV

The essence of a virtualized network includes enabling SPs to customize their own networks based on the requirements of their MUs. Customization in this paper assumes that the devices in each SP's network can be different [2]. Here, we evaluate the relationship between the available degrees of freedom in the MIMO channel and the combined channel matrix. As shown in Eq. 3.6, the rank of the MIMO channel limits the system capacity in terms of the number of orthogonal sub-channels. Meanwhile, the singular values affect the capacity through the SINR in the sub-channel. Thus, the combined channel matrix not only facilitates estimation of capacity but also offers an opportunity for SPs to combat interference in an RRV system.

The combined SINR matrix $\mathbf{R}^{-1/2}\mathbf{H}$ is a function of separation distance, cell radii, and available degrees of freedom in the MIMO channel. The proportional relationships between this matrix and the separation distance d and the cell radii r_B are shown in Figures 4.12,4.13, 4.14, and4.15. Since large-scale fading (path loss) dominates the signal (in the received signal strength as well as the received interference), a change in capacity with either the separation distance or the radius of the small cell is clear. The small-scale fading in the MIMO channel does not impact the average received power (the small-scale fading is averaged out over the transmit signal block) but it impacts the singular values λ_i. The capacity will be significantly improved only if more antennas are adopted at the BSs and MUs of both SPs. Furthermore, if only the number of transmit antennas increases, it still improves the targeted sub-channel gain but it also causes an increased interference to the second SP's network which simultaneously operates in the same spectrum bands. Therefore, the relationship between the number of antennas at the large BS, the small BS or MUs is not straightforward. This is the focus of the investigation in this section. We set the number of antennas at the three points as (x, y-z), where x, y and z stand for the number of antennas at the large cell's BS, the small cell's BS, and MUs in the small cell respectively). MUs in the large cell still use 2 antennas.

In Figures 4.16 and 4.17, the large cell BS has 4 antennas and its MUs have 2 antennas.

[2]In general, customization also includes the ability of a virtual network to adjust itself to meet the need for multi-class traffic as well as adaptation to a variant environment with multiple SPs.

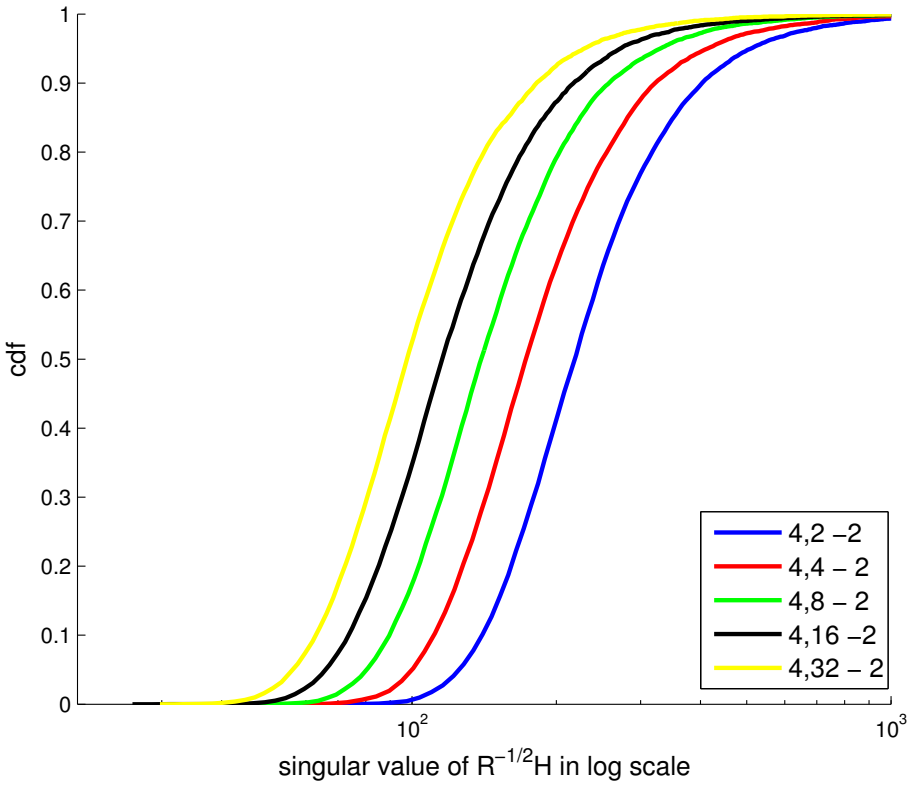

Figure 4.16: CDF of singular values (as seen by MUs in the large cell) with 2 MU antennas in the small cell, but varying numbers of BS antennas in the small cell

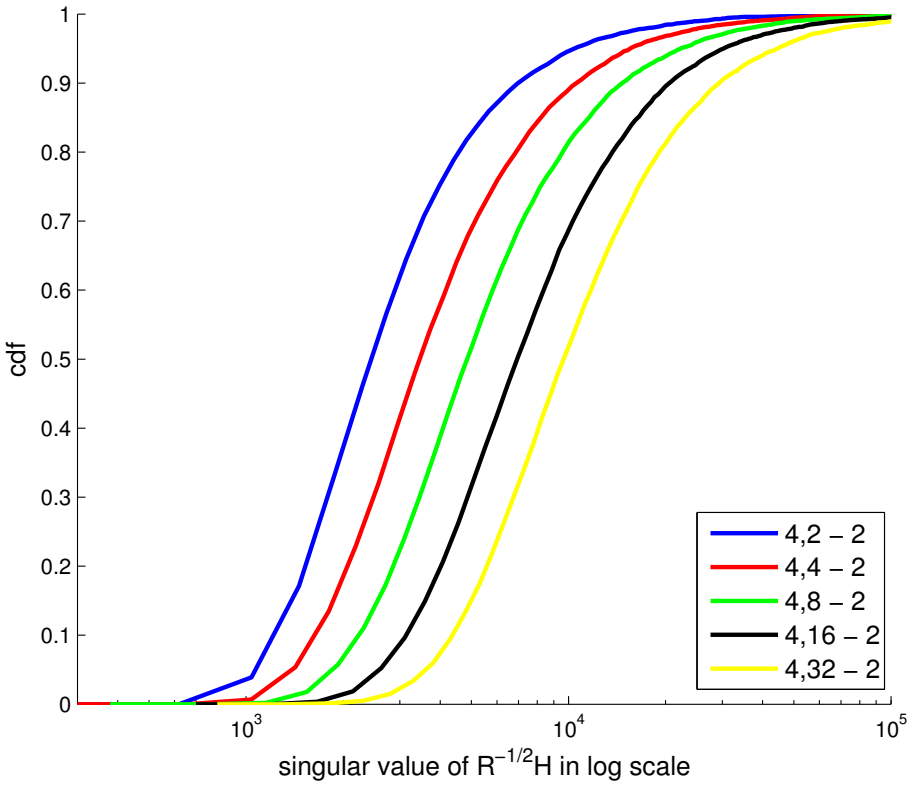

Figure 4.17: CDF of singular values (as seen by MUs in the small cell) with 2 MU antennas in the small cell, but varying numbers of BS antennas in the small cell

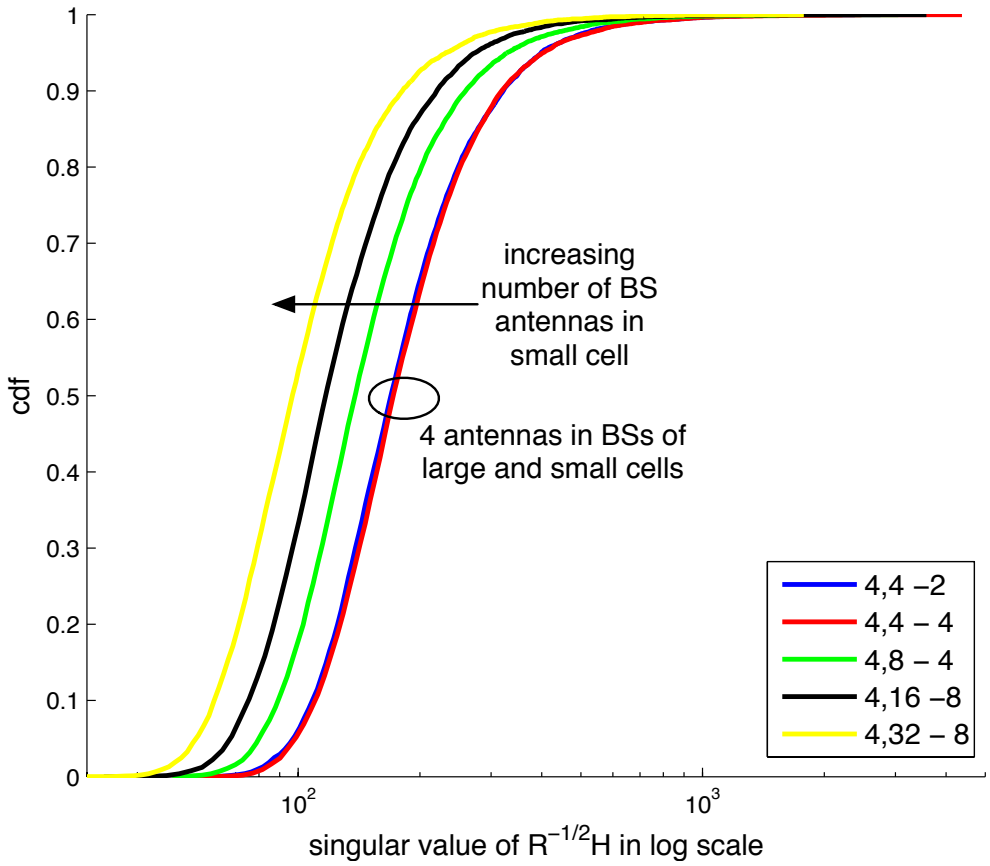

Figure 4.18: CDF of singular values (as seen by MUs in the large cell) with varying numbers of MU and BS antennas in small cell

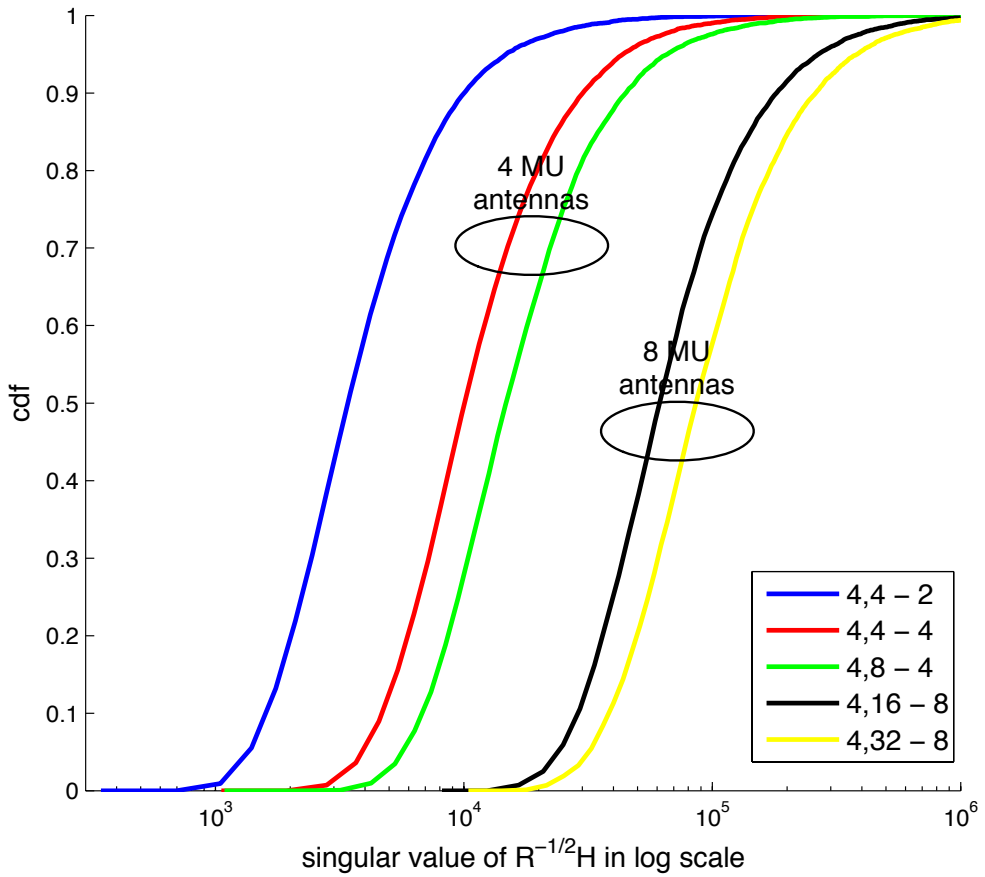

Figure 4.19: CDF of singular values (as seen by MUs in the small cell) with varying numbers of MU and BS antennas in small cell

The small cell's MUs all have only 2 antennas, but the small cell's BS has varying numbers of antennas. The best singular value distributions for the large cell and the small cell lie at the (4, 2-2) and the (4, 32-2) values, respectively. That is, the large cell benefits from fewer BS antennas in the small cell, but the small cell suffers if it reduces the number of BS antennas! The opposite effect may be expected if we change the number of BS antennas in the large cell. On the positive side, even when the small cell uses more antennas to transmit, the large SP is not significantly impacted on average as illustrated in Table 2.

Next, we assume MUs in the small cell are able to install up to 8 antennas. The capacity in the large cell remains stable as long as the ratio x/y is unchanged (Figure 4.18 - cases 4,4-2 and 4,4-4). The rest of the singular value distributions for the large cell remain the same as the ones shown in Figure 4.16 as expected since the change in number of MU antennas in the small cell does not impact the interference faced by the MUs in the large cell. The distribution of singular values in Figure 4.19 cluster with the available degrees of freedom in MIMO channel ($min(n_T, n_R)$) for the small cell (singular values of 4 MU antennas are together, 8 MU antennas are together). The greater the available degrees of freedom in MIMO channel, the higher the aggregate system capacity. This is a relatively strong proportional relationship which can be seen in Table 2. The capacity in the (4, 4-4) case is almost twice of that in the (4, 4-2) MIMO channel, and the capacity in the (4, 16-8) case is much more than four times that of the (4, 4-2) case. Thus from a customization point, it may be better for SP_B to use MUs with more antennas than a BS with more antennas to avoid interference to the large cell.

4.4 DISCUSSION AND CONCLUSIONS

We show that it is possible to share "radio resources" rather than simply spectrum slices across service providers when we consider virtualizing wireless networks. We evaluate the downlink capacity of two service providers occupying the same geographical area, but perhaps offering different services. One service provider is assumed to have a much larger coverage and transmit power. The amount of spectrum that can be shared through simultaneous use

Table 2: Achievable data rate (in bps) per MU

MIMO channel	SP_A	SP_B
(4, 2-2)	1.7325	47.1777
(4, 4-2)	1.7316	47.2488
(4, 8-2)	1.6691	48.5423
(4, 16-2)	1.6621	48.3901
(4, 32-2)	1.6414	48.6210
(4, 4-4)	1.7300	93.6539
(4, 8-4)	1.6831	98.4671
(4, 16-8)	1.6638	221.6121
(4, 32-8)	1.6538	224.3495

depends on the geography and transmit powers (at a minimum). It is certainly possible to have radio resource sharing gains in a variety of circumstances. It appears that the primary factor that may impact such sharing is the interference from the smaller service provider to the mobile users of the larger service provider (affecting isolation in a virtualized network). This may be mitigated by using directional transmissions (or using disjoint spectrum slices in specific directions). There are also opportunities for customization of services at the device level. Using different MIMO settings may provide different tradeoffs between capacities across service providers. We have not considered the uplink in this work, nor have we considered interference that may be caused in a multi-cell scenario. The channel matrix assumes that the fading is independent and identically distributed while there are possible correlations in real channels. Investigation of interference in a multi-cell is presented in the next chapter.

5.0 ON CONFIGURING A FFR VIRTUAL NETWORK

5.1 MOTIVATION

In this chapter, we investigate the use of RRV with configurations to give a framework, which provides suggestions to a resource manager about configuring radio resources to meet SPs' demands and capabilities.

We recall that wireless network virtualization is a solution that breaks down the old fixed network architecture towards better efficiency, customization, and isolation. Implementing it on an existing physical network implies that we don't tear down the existing one and built up a brand new one, instead, we just remove the "fixed" way of using resources and add a new management to dynamically realize multiple architectures on limited physical resources. However, there is a price at removing the "fixed" way especially in wireless networks. Interference caused by careless sharing may lead to worse efficiency and damage performance for all parties in the system. Hence, wireless network virtualization also requires proper resource configuration to ensure every SP's system performance.

To better exploit radio resource usage efficiency, we propose RRV and claim that some "overlap" slices of spectrum could be used by all SPs with careful planning (see Figure 3.3). In Chapter 4 we illustrate (albeit in a simple scenario) why spectrum should be considered as a "radio resource" and that RRV often leads to better resource efficiencies compared to SSV. Then a key issue is how we manage cellular networks considering RRV. The one question to ask is how can we configure the network to enable RRV to achieve the best resource utilization? Unfortunately, there is no definite or simple answer yet. The configuration problem becomes even more complicated as the network architecture becomes more complicated, such as when frequency reuse is adopted. For example, the resource manager has to decide what

power level (in a given slice of spectrum) should be assigned to a given SP in a given cell. It has to determine how many antennas a given SP (or MUs) can use in a given cell. It has to decide how these may change depending on the distances between infrastructure entities like BSs).

Here we start answering the above question by examining fairly involved scenarios that include a range of configuration cases. Shown as Figure 5.1, we consider an InP's cellular network with radio resources being shared between two SPs. One SP is deployed with the assigned spectrum in 3 large cells and it applies FFR in these cells. The other SP operates in a smaller cell using the assigned spectrum. The smaller cell is a subset of one of the 3 large cells. In practice, it is likely that many SPs may operate in many different sized cells. The general sharing problem is depicted in Figure 3.4 in Section 3.2. However we focus on simultaneous usage of spectrum across SPs. Simultaneous usage can be possibly limited in many spectrum slices or in small areas near base stations (BSs). Most SPs would be configured to use dedicated/orthogonal slices of spectrum for much of their coverage (SP_A and SP_C in Section 3.2). Further, our focus is on the more complex problem of SPs that may be configured to use the "overlapping" slices of spectrum (see the low half of Figure 3.3). Therefore we extract the sharing between SP_A and SP_B from the general problem in Section 3.2.

Multiple-input Multiple-output (MIMO) is also considered here to understand how system capacity may change with capabilities of SPs and their subscribers. To summarize all cases and changing parameters, we develop configuration maps that a resource manager can find proper configuration according to SPs' demand and abilities. Last but not least, we discuss some potential unsolved issues in radio resources virtualization at the end of this chapter.

The contribution of this part of our work can be viewed from two aspects. From a technical perspective, our investigation of the RRV scheme provides a framework that evaluates the resource efficiency, and potentially the ability of customization and isolation in a virtual wireless network. The results of this evaluation can be seen as a manual or guideline showing possible network configurations of SPs' for a resource manager. On the other hand, pricing of radio resources that may be dynamically leased by a SP from an InP, the cost of reconfig-

uration and management of the network, service agreements between SPs and InPs, hinge on the ability to manage the radio resources appropriately. Hence, our technical evaluation of scenarios can assist in such economics and policy decisions.

5.1.1 Fractional Frequency Reuse and Radio Resource Virtualization Cases

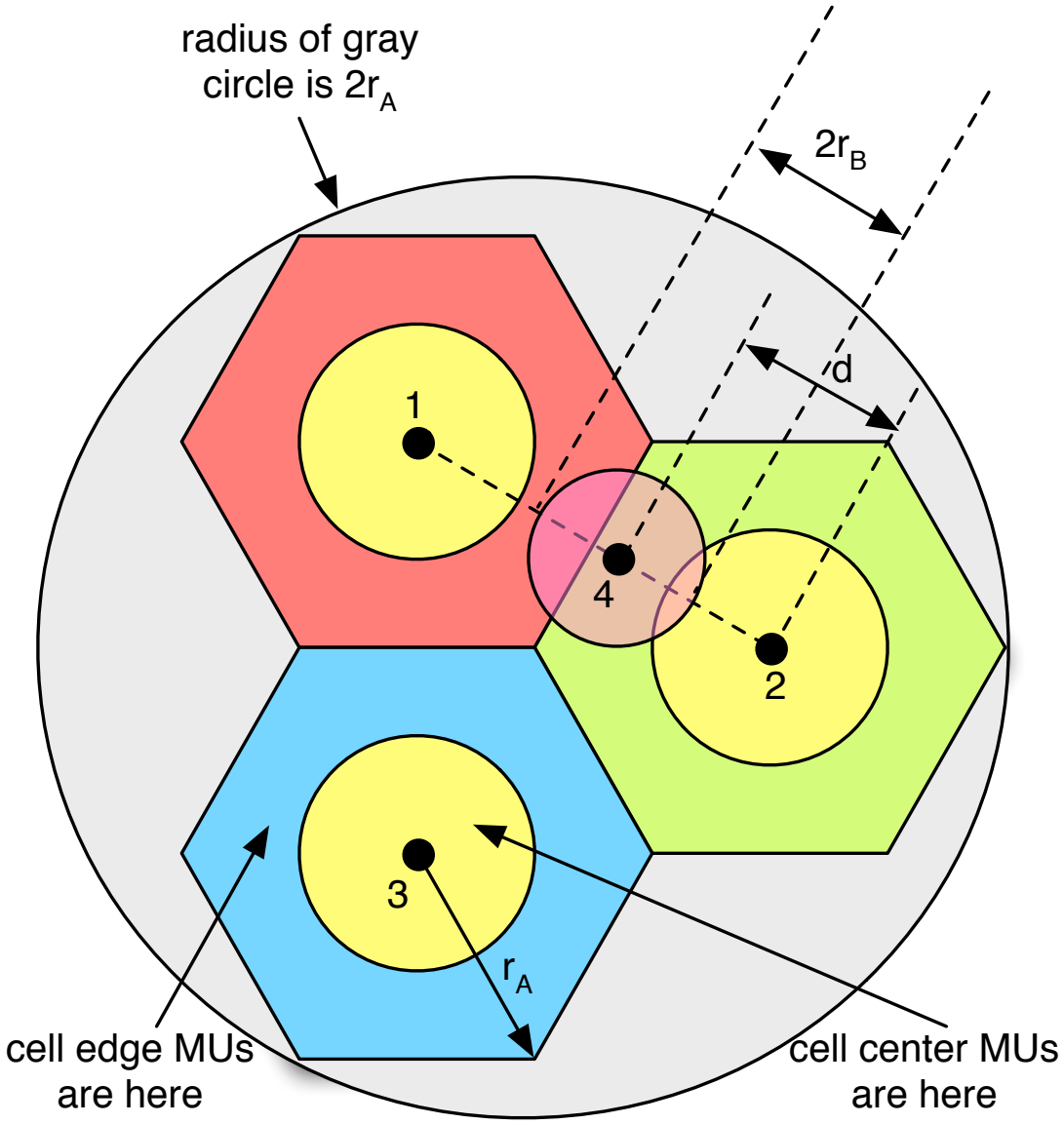

Figure 5.1: 2D-Schematic of multicell virtual system with FFR

We consider a geographical area where two SPs co-exist - SP_A and SP_B (gray area shown

in Figure 5.1). The resource manager configures SP_A to deploy FFR in BS-1, BS-2, and BS-3. We will refer to this as SP_A's layout, where the center of three cells utilize the same frequency band f_0, and the other frequency bands are divided equally into three parts: f_1, f_2 and f_3, then distributed to the edges of cells 1, 2 and 3 orthogonally. For now, we assume that BS-4 is located along the dashed line in Figure 5.1 and we call this SP_B's layout in the system. Parameters d, r_A, and r_B indicate the distance between BS-4 and BS-2, the radius of cells created by BS-1, BS-2, BS-3 and the radius of the cell created by BS-4, respectively.

Note that the cells in Figures 5.1 are only schematics. Inversely, the cells are not hexagonal or circular in shape. The way in which we associate a MU with a BS in our simulations is as follows. In SP_A's layout, MUs are uniformly distributed within the gray area in Figure 5.1, and the received signal strength (RSS) values from the three macrocells are determined for every MU. The BS that a MU should be attached to is based on the largest RSS. If the MU receives a signal with RSS smaller than a minimum received signal power, it is not attached to any of the three base stations. A minimum received signal power threshold P_{th_A} is set by the operators depending on the equipment deployed and target data rates. If a MU's RSS (including path loss and shadow fading factor) is larger than Pr_{th_A} but smaller than $2Pr_{th_A}$ (3 dB larger than threshold), we call it a cell edge MU[1]. Otherwise, it is a cell center MU. In SP_B's layout, MUs are uniformly distributed in the small cell. We make no comparison of receive powers and assume all MUs subscribed to SP_B associate with BS-4. BS-4 is configured to use all of the spectrum allocated for it throughout its coverage area (i.e, there is no separation into cell center and cell edge).

Figure 5.2 shows several possibilities that a resource manager can consider for configuring spectrum among the base stations for the two SPs. Suppose that w_A Hz of spectrum is allocated to the SP_A's layout and w_B Hz to the SP_B layout in the case of orthogonal spectrum allocation. The total bandwidth available for configuration by the resource manager is $w_{tot} = w_A + w_B$. When FFR used by SP_A, in SP_A's layout, a proportion bp_c of bandwidth is utilized by the center area of all cells (colored yellow) while the rest of the bandwidth (a proportion bp_e) is equally divided into 3 chunks (colored blue, green, and red), each of which

[1]The cell edge number is considered as part of the FFR configuration and is changed later in simulations

is allocated to one cell edge (as shown in Figure 5.1), such that $bp_c + bp_e = 1$ [2]. This high level view is shown as the general set up at the top of Figure 5.2. We now describe the five cases (listed below the general set up in Figure 5.2) that are investigated in our simulations.

- **Case I – RRV:** In this case, there is no spectrum planning in SP_A's layout. The system is configured such that MUs can access the entire w_{tot} Hz spectrum in a time unit in all of the four cells served by BS's 1-4. Note that this has the highest potential for interference.
- **Case II – Freq. reuse + RRV:** The cells (BSs 1-3) in SP_A's layout are configured to use $\frac{1}{3}w_{tot}$ each orthogonally (traditional frequency reuse with a reuse factor of 3). No FFR is applied (i.e., the spectrum allocated to a BS is used throughout the cell). The cell of BS-4 in SP_B's layout is configured to use all of the spectrum in a time unit.
- **Case III – RRV + FFR:** As described above, the center area of any cell in SP_A's layout is configured such that center MUs can access $bp_c w_{tot}$ of the bandwidth and the amount of frequency bandwidth used by cell edge MUs is $\frac{1}{3}bp_e w_{tot}$. SP_B's layout is configured such that its MUs can access the entire w_{tot} Hz spectrum in a time unit.
- **Case IV – Center + RRV:** The center area of any cell in SP_A's layout is configured such that center MUs can access $bp_c w_{tot}$ of the bandwidth and the amount of frequency bandwidth used by cell edge MUs is $\frac{1}{3}bp_e w_{tot}$. SP_B's layout is configured such that its MUs can access, in a time unit, only the portion $b_{pc} w_{tot}$ Hz spectrum used by the center areas in each cell in SP_A's layout.
- **Case V – FFR / SSV:** This configuration corresponds to separate spectrum virtualization – it ensures that there is no sharing between the two SPs. SP_A is configured to use FFR with its own spectrum to protect cell edge MUs from severe interference. This case has the lowest potential for interference. In practice, the boundary between w_A and w_B changes over time, but we keep it fixed in our simulations.

[2] We assume for simplicity in each case that each SP manages frequency bands in frequency division multiplexing fashion for its MUs. In other words, there is no intra-cell interference (like LTE). Thus, with FFR, the available bandwidths for each of SP_A's center MU and edge MU are $bp_c w_{tot}/(nu_{Ac_k})$ and $\frac{1}{3}bp_e w_{tot}/(nu_{Ae_k})$ respectively. The available bandwidth for each of SP_B's MU is $w_{tot}/(nu_B)$. The numbers nu_{Ac_k}, nu_{Ae_k} and nu_B are numbers of the users in the center area of Cell k, edge area of Cell k and SP_B's layout respectively. Note that $nu_{A_k} = nu_{Ac_k} + nu_{Ae_k}$ and $nu_A = \sum_k nu_{Ac_k} + \sum_k nu_{Ae_k}$. In reality, the bandwidth allocation to individual users will be more complex (e.g., physical resource blocks in LTE-like systems).

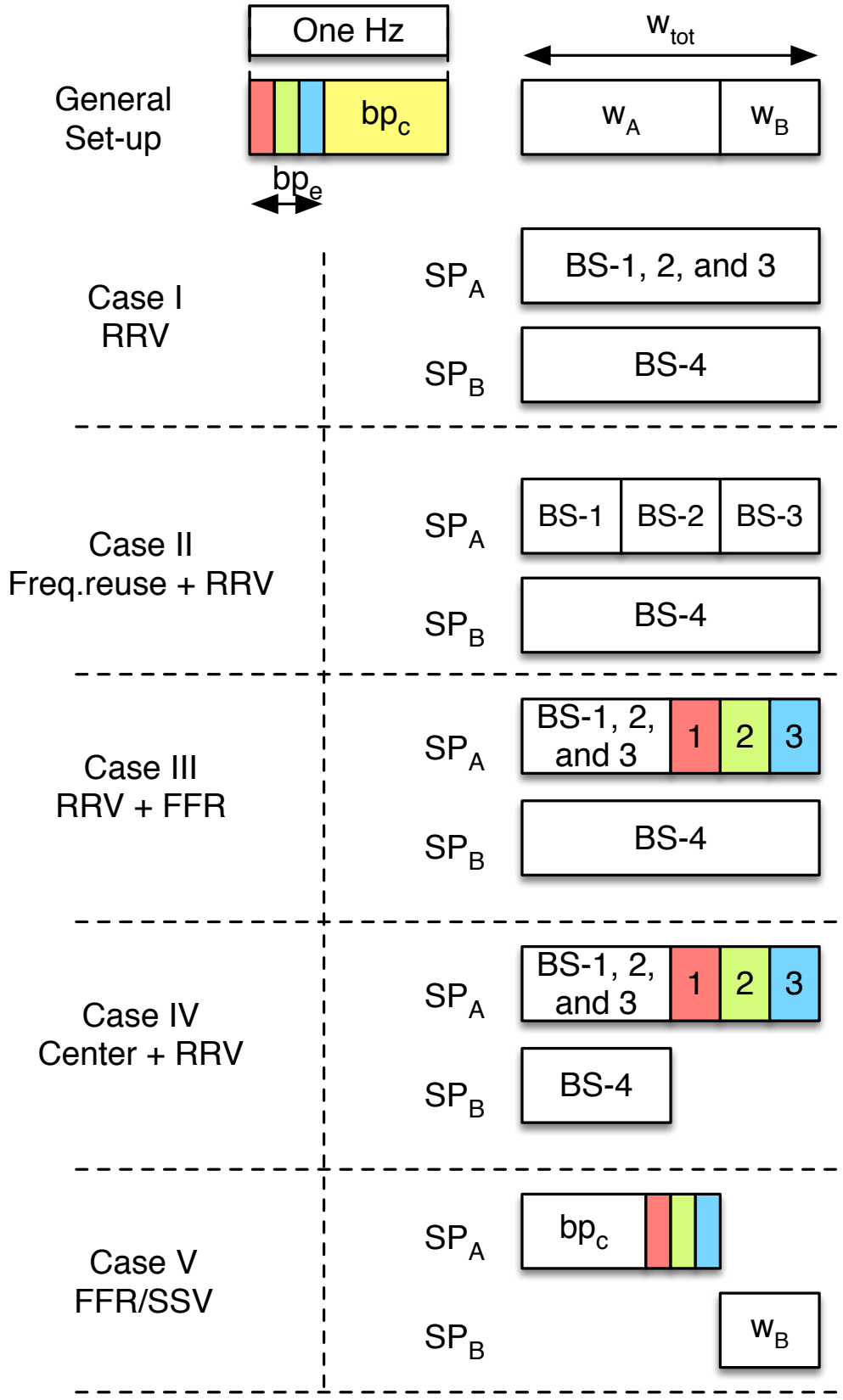

Figure 5.2: Radio Resource Allocation Cases

Please note from Figure 5.2 that the sharing of radio resources can have intricate configurations. Immediately, it is not obvious as to which configuration will be suitable and under what circumstances. Clearly, the interference is maximum in Case I and minimum in Case V. The amount of available bandwidth per MU for SP_A is w_{tot}/nu_A if frequency bands are universally reused in the SP_A layout (Case I). nu_A is the total number of SP_A MUs. In that case, many concurrent transmissions will cause excessive interference and degrade system performance. For all cases, the amount of available bandwidth for each MU (SP_A's center MU, edge MU and SP_B's MU) is summarized in Table 3. With traditional frequency reuse (Case II), frequency bands are divided equally according to a reuse factor (into 3 cells in our model resulting in a $\frac{1}{3}w_{tot}$ bandwidth per cell). This reduces interference between the cells in SP_A's layout, but reduces the capacity as well. With FFR (Case III), the amounts of available bandwidth for each "center MU" and "edge MU" are $\frac{b_{pc}w_{tot}}{nu_{Ac_k}}$ and $\frac{\frac{1}{3}b_{pe}w_{tot}}{nu_{Ae_k}}$ respectively, where nu_{Ac_k} refers number of center MUs and nu_{Ae_k} denotes the number of edge MUs in Cell k. In Case IV, only the center area of the cells served by BSs 1, 2, and 3 in SP_A's layout share the spectrum with SP_B reducing the amount of bandwidth that each MU in SP_B's layout gets to $\frac{b_{pc}w_{tot}}{nu_B}$ bandwidth. However, the interference to SP_A's cell edge MUs reduces. Case V doesn't allow simultaneous usage of spectrum between SPs so MUs only access their SP's spectrum. FFR partition dominates the spectrum allocation in SP_A's layout (influential FFR parameters will be discussed later). It is inconclusive that which configuration is generally preferable because the achievable data rate per MU depends on how much radio resources is shared, interference level, as well as factors b_{pc}, b_{pe}, nu_{Ac_k}, and nu_{Ae_k}. We note that the range of cell edge affects the values of nu_{Ac_k} and nu_{Ae_k}.

5.2 SIMULATION RESULTS AND ANALYSIS

Simulations to analyze the five cases are based on a multi-cell FFR virtual system, as shown in Figure 5.1. MUs in the SP_A layout are distributed uniformly over the radius of the gray area ($2r_A$) and the angle (2π). The distances between a MU and BSs of Cell 1, 2 and 3 and the corresponding receive powers Pr_{A1}, Pr_{A2} and Pr_{A3} are calculated. SP_A decides which

Table 3: Available frequency bandwidth per MU

Spectrum Scheme	SP_A center	SP_A edge	SP_B
Case I: RRV	$\frac{w_{tot}}{nu_{A_k}}$	$\frac{w_{tot}}{nu_{A_k}}$	$\frac{w_{tot}}{nu_B}$
Case II: Freq. reuse + RRV	$\frac{1}{3}\frac{w_{tot}}{nu_{A_k}}$	$\frac{1}{3}\frac{w_{tot}}{nu_{A_k}}$	$\frac{w_{tot}}{nu_B}$
Case III: RRV + FFR	$\frac{b_{pc}w_{tot}}{nu_{Ac_k}}$	$\frac{1}{3}\frac{b_{pe}w_{tot}}{nu_{Ae_k}}$	$\frac{w_{tot}}{nu_B}$
Case IV: Center	$\frac{b_{pc}w_{tot}}{nu_{Ac_k}}$	$\frac{1}{3}\frac{b_{pe}w_{tot}}{nu_{Ae_k}}$	$\frac{b_{pc}w_{tot}}{nu_B}$
Case V: FFR	$\frac{b_{pc}w_A}{nu_{Ac_k}}$	$\frac{1}{3}\frac{b_{pe}w_A}{nu_{Ae_k}}$	$\frac{w_B}{nu_B}$

cell any given MU is associated with according to the strongest RSS from BS's 1, 2, and 3. If none of the received powers at the MU is larger than $P_{th_A} = P_A r_A^{-\alpha}$ (P_A is transmit power of BSs 1 to 3), we assume this MU is not supported in SP_A's layout. Around 20% MUs are dropped from the simulation with this assumption. In SP_B's layout, we distribute MUs uniformly over the radius of the small cell (r_B) and the angle (2π), and no further decision process is used. Results shown are averages of 10,000 simulation runs that vary locations, ζ, and h_{ij}. The complex channel matrix (for either the transmission from the intended transmitter or interference from any interfering transmitter) is generated using Eq. 3.1. We assume that $w_A = 10$ MHz and $w_B = 5$ MHz and so, the total bandwidth $w_{tot} = 15$ MHz. At each BS, $n_T = 4$ antennas and at each MU, $n_R = 2$ antennas are assumed unless otherwise discussed. The transmit power $P_B = 1$W is the transmit power of BS-4. BSs 1, 2, and 3 have a power $P_A = P_B \times$ Power Ratio where the power ratio scales the transmit power P_A compared to P_B. The value of $N_0 = -174$ dBm/Hz [57]. The path-loss exponent α takes the value of 4 and $\zeta = N(0, \sigma)$ where $\sigma = 8$. Unless specified, the FFR spectrum assignments are $bp_c = \frac{32}{50}$ and $bp_e = \frac{18}{50}$, which means $f_0 = \frac{32}{50}w_A$, $f_1 = f_2 = f_3 = \frac{6}{50}w_A$ ($w_A = 10$ MHz). If the received power at a MU is no larger than $2P_{th_A}$ (3dB higher than P_{th_A}), it is defined as a cell edge MU in SP_A's layout.

Table 4: Parameter Settings for Various Scenarios

ID	Radius of BS-4	Distance *d* of BS-4 from BS-2		Remarks
1	50m	500m	Case III	BS-4 has small radius, is at different distances from BS-2
2	50m	800m		
3	50m	300m		
4	100m	500m		BS-4 has larger radius, is at different distances from BS-2
5	100m	800m		
6	100m	300m		
SSV 1	50m	-	Case V	BS-4 has two different radii, MUs have better channel in smaller cell
SSV 2	100m	-		

5.2.1 General Trends

We first examine the general trends using Case III and Case V. We pick these cases as our primary objective is to look at configurations that employ FFR and either use virtualized radio resources or perform orthogonal spectrum sharing. In subsequent sections, we consider all five cases. Since results will depend on transmit powers and other parameters, we set up six scenarios, summarized in Table 4. The radius $r_A = 1000$m. The first three scenarios in Table 4 have a small radius ($r_B = 50$m) for BS-4 while scenarios 4–6 use a radius of $r_B = 100$m for BS-4. Also, we consider that BS-4 is at different distances $d = 500, 800, 300$m from BS-2 (see Figure 5.1). However, the separation distance d doesn't matter when separate/orthogonal spectrum sharing (Case V) is used. This is different from any other case since Case V is the only case in which no sharing happens between SPs. Hence, we list two scenarios for Case V in Table 4 separately. In each scenario, there are almost 300 MUs subscribed to SP_A (100 per base station, but around 20% of the MUs at the edge of the gray circle in Figure 5.1 are dropped) and 10 MUs subscribed to SP_B.

The **aggregate** spectral efficiency in Eq. 3.7 is determined from simulations for the scenarios described in Table 4 and shown in Figure 5.3. The x-axis in this figure corresponds to the ratio P_A/P_B. Error bars correspond to one standard deviation of the mean over 10,000 runs. The variation in capacity results primarily due to the varying locations of MUs (and also due to the random fading). We see that the aggregate spectral efficiency in Case III is better than that in Case V for most of the scenarios. This gain comes exclusively from RRV (simultaneous use of interfering spectrum) indicating that it is possible to exploit RRV for better spectrum usage than using orthogonal-only slices with SSV that has been considered in the most of the existing work on wireless virtual networks. Figure 5.3 also provides some insights that are not obvious, assuming that aggregate spectral efficiency is the metric of interest.

- RRV with FFR is *not necessarily* the best option always. However it is better than FFR/SSV in several scenarios.
- Increasing the power ratio (P_A/P_B) from 0 to 18 dB changes the average aggregate spectral efficiency minimally (it is essentially flat).

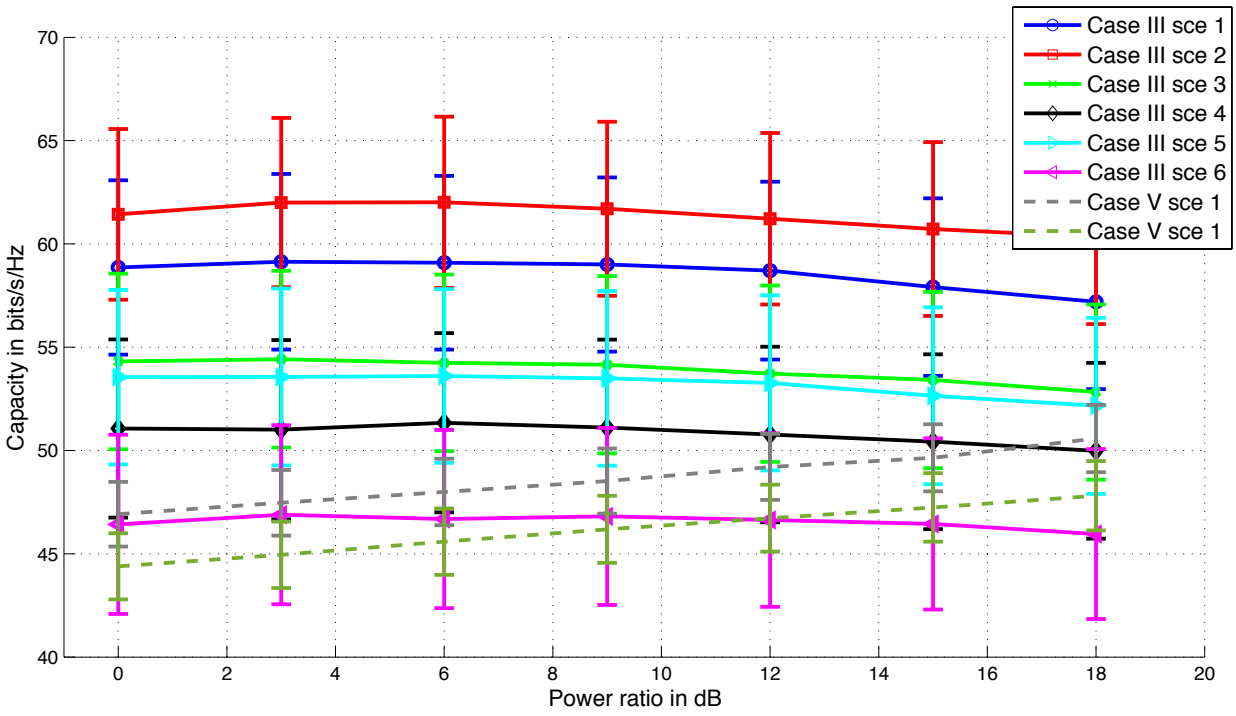

Figure 5.3: Aggregate spectral efficiency of the multi-cell system

The reason for the second observation is that the distances from BSs 1, 2, and 3 to SP_A's MUs are such that they make this power ratio not a very significant factor. On the contrary, the separation distance d and cell radius r_B are influential. However, the way in which they impact capacity are different for SP_A and SP_B's MUs which will be discussed next.

While aggregate capacity is useful, how the cases and scenarios would matter to each SP is important. This would determine the configuration that is provided by the resource manager. The average achievable data rate for **each MU** in SP_A's and SP_B's layouts are shown in Figure 5.4 for all the scenarios in Table 4. The per MU data rate in SP_A's layout clusters together and appears to be mostly independent of the scenario. Further, sharing of spectrum provides limited gains since MUs of each SP share the available bandwidth orthogonally. So, the extra available bandwidth for SP_A's MUs is not significant since SP_A's layout has almost 300 MUs. When the power ratio is lower than 9 dB or so (this ratio varies slightly across scenarios), the capacity for MUs in SP_A's layout with RRV is worse than with SSV only. Therefore, it may be necessary for the resource manager to carefully consider the options to ensure sufficient capacity for MUs in SP_A's layout.

In SP_B's layout, for most scenarios, the achievable data rate is higher with RRV than with SSV only. The capacity in SP_B's layout substantially increases due to the extra spectrum that MUs subscribed to SP_B get through RRV and it is the main contributor to the increase in aggregate capacity. The capacity increases with the separation distance d, but reduces when the small cell's radius r_B increases, i.e., they both impact the capacity. For instance, Scenarios 3 and 5 from Table 4 have very similar capacity values, although the numbers are not identical. In Scenario 3, the cell radius $r_B = 50$m is small, but the separation distance $d = 300$m is also small. In Scenario 5, the cell radius $r_B = 100m$ is large, but the separation distance $d = 800$m is also large. When r_B is small, MUs are closer to BS-4 and the interference from BS's 1,2, and 3 is small compared to the desired received power. When r_B is large, the desired received power is smaller, and the interference may be larger for some MUs. This interference can be made smaller if the separation distance is large, i.e., the MUs of SP_B are much farther away from the major interfering base station (BS-2). We also note here that d is the distance between BS-2 and BS-4 (see Figure 5.1). We keep it less than r_A in our simulations (which means the BS-4 is within BS-2's coverage). The performance

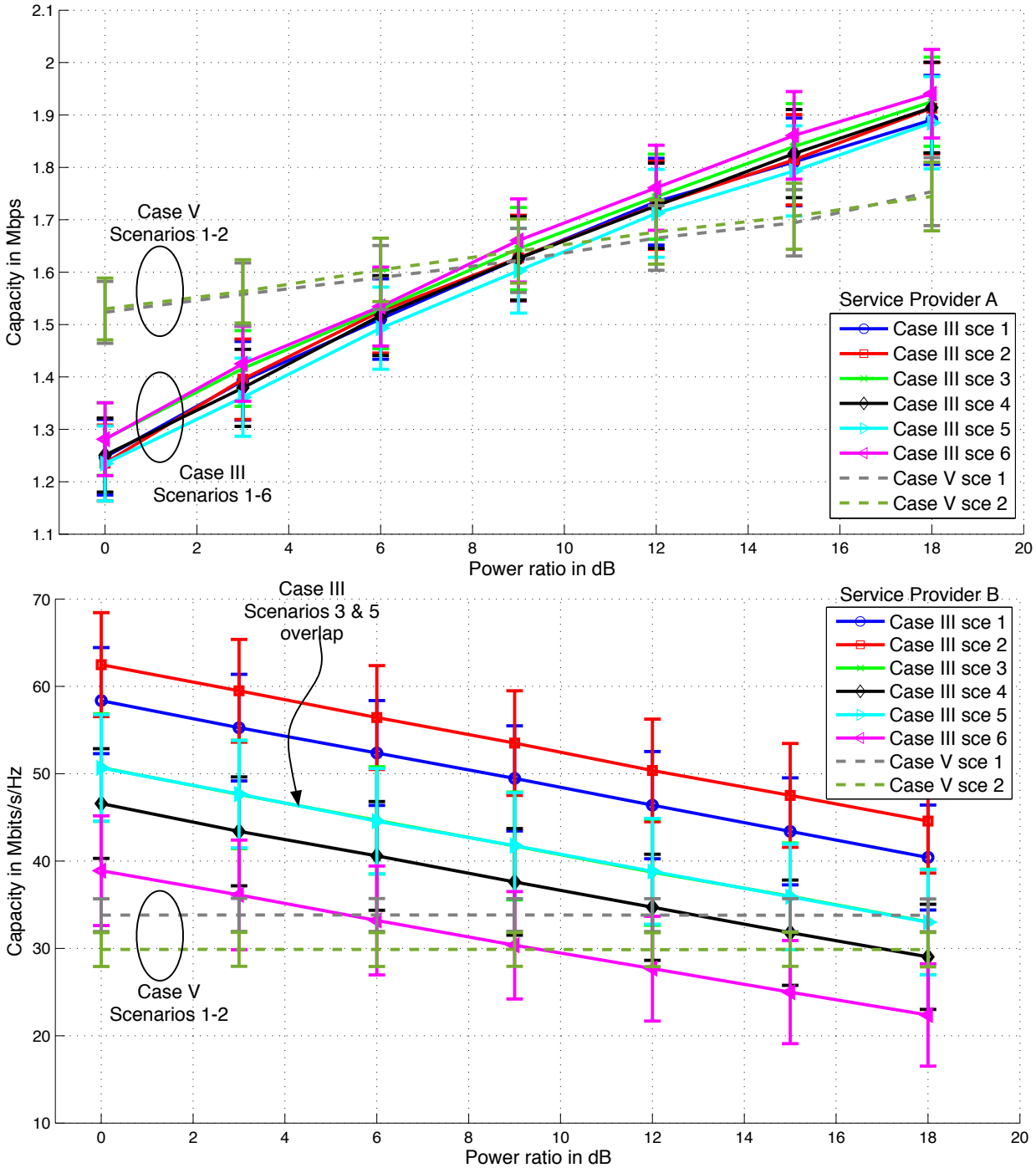

Figure 5.4: Achievable data rate (per MU) – top (SP_A's layout) and bottom (SP_B's layout)

would be similar when d is larger than r_A (BS-4 would move into BS-1, but the impact is the same).

5.2.2 Comparison of Cases

Next, we consider a comparison of the various cases described in the previous section, with the six scenarios in Table 4 to get some insights into how a resource manager may pick configuration options.

Figures 5.5 and 5.6 provide the comparisons of the various cases for two power ratios (P_A/P_B) of 3 dB and 15 dB. In the former, the larger cells (BS-1, 2, and 3) operate at a power that is only 3 dB higher than BS-4, while in the latter, this value is 15 dB. From Figure 5.4, we see that FFR/SSV (case V) may be better for SP_A's layout when the power ratio is 3 dB, but not if the power ratio is 15 dB. In these figures, we only plot the *average capacity per MU* and do not show the variability to avoid clutter. There is variability across cases and scenarios as shown in Figure 5.4. In each figure, the top graph shows the results for MUs in SP_A's layout while the bottom shows the results for MU's in SP_B's layout. We make the following observations from these plots.

- The scenario (size of BS-4's cell or its distance d from BS-2) does not impact the capacity per MU for MU's in SP_A's layout in a perceptible way. However, the cases (how spectrum is shared) matter substantially. This is NOT the case for MUs in SP_B's layout.
- The power ratio P_A/P_B is an important factor, that can change the capacities for the MUs (though it is not as important to change the aggregate spectral efficiency). The power ratio is disproportional between the MUs subscribed to SP_A and SP_B. The capacity of MUs subscribed to SP_B can go up from 30–40 Mbps (when the power ratio is 15 dB) to 30–60 Mbps (when the power ratio in 3 dB). On the contrary, MUs in SP_A's layout see a decrease from a maximum of 2.3 Mbps to 1.8 Mbps respectively.
- The best strategy for configuring spectrum resources for MUs in SP_A's layout is NOT the best strategy for MUs in SP_B's layout and vice versa. For instance, Case IV (Center + RRV) is the best spectrum configuration for MUs in SP_A's layout in all scenarios. However, Case I (RRV), Case II (Freq. reuse + RRV) and Case III (FFR + RRV)

behave comparably for MUs in SP_B's layout. In fact, for the MUs in BS-4, it does not matter (on average) much how the spectrum is configured for use by MUs in SP_A's layout as long as all of the spectrum is configured for use by them. They are affected only in Cases IV and V when their share of spectrum is reduced.

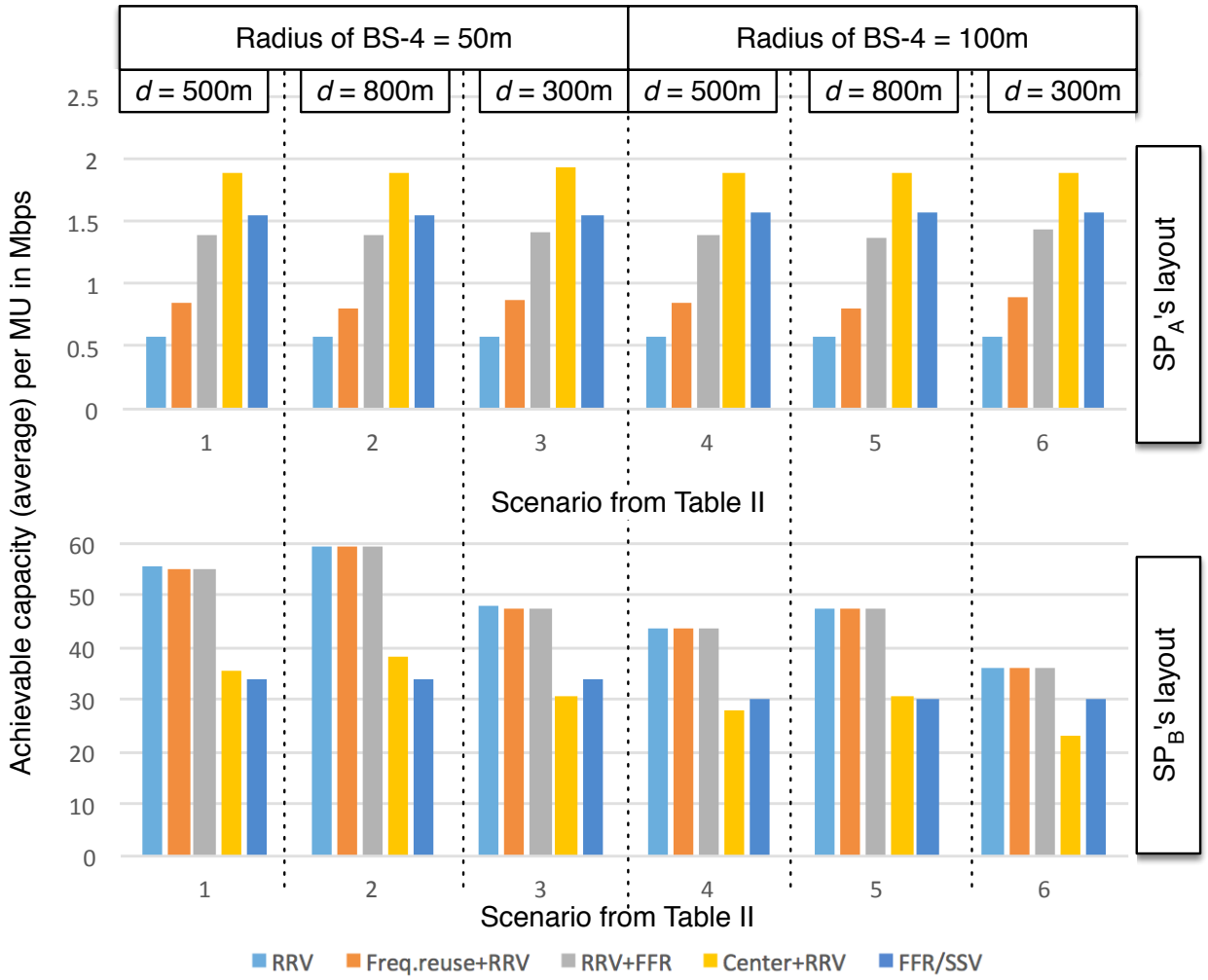

Figure 5.5: Comparison of achievable data rate per MU in SP_A and SP_B's layouts for a power ratio of 3 dB

To understand the results better, we plot the average capacity per MU in SP_B's layout versus the average capacity per MU in SP_A's layout for the various cases, scenarios and power ratios of 3 dB and 15 dB in Figure 5.7. Ideally, we would like to see results in the top right corner of these plots. That is, MU's in both SP_A's layout and SP_B's layout see high capacity,

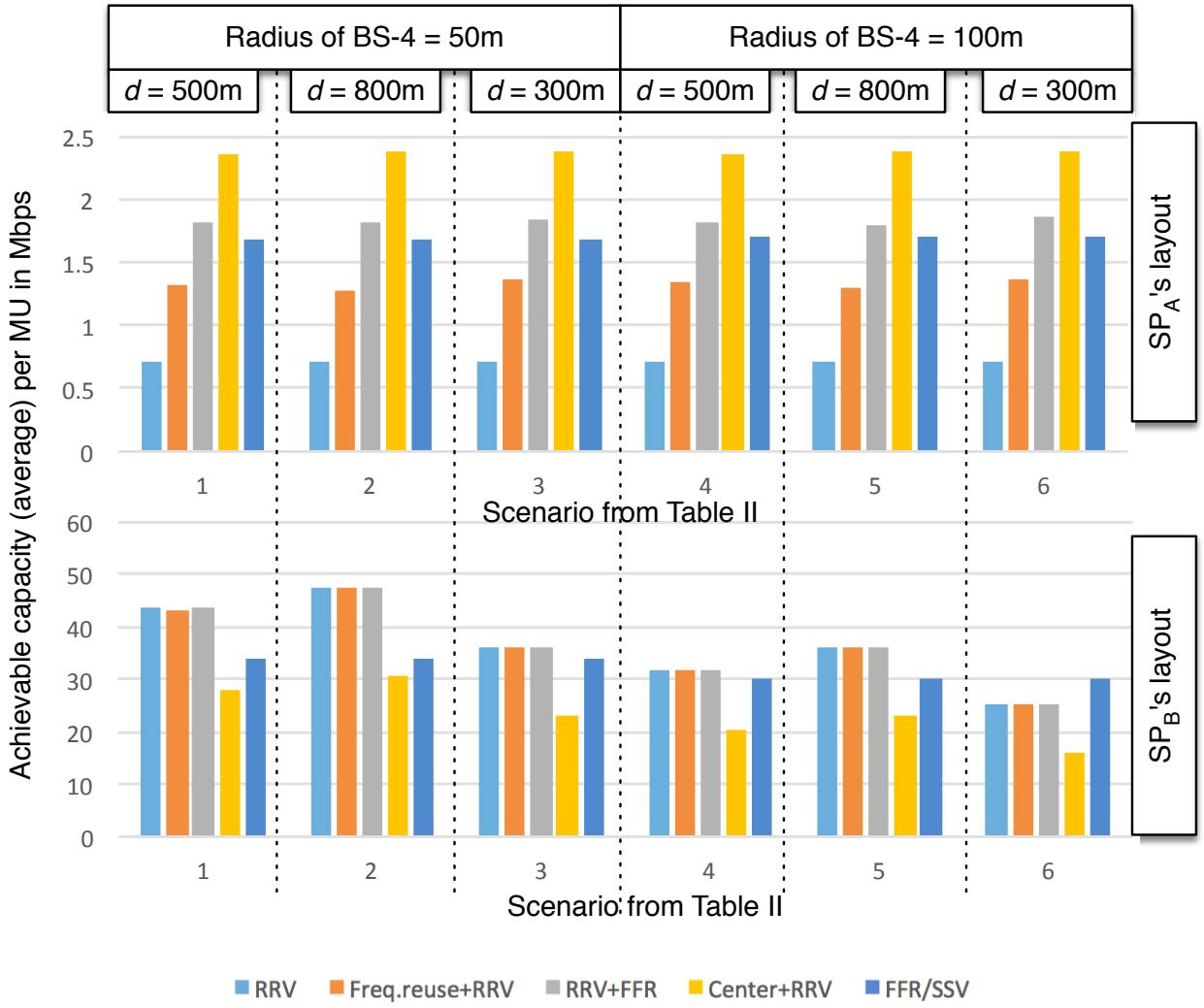

Figure 5.6: Comparison of achievable data rate per MU in SP_A and SP_B's layouts for a power ratio of 15 dB

but clearly, that is not feasible for all scenarios and cases. However, the average capacities show some interesting trends that can be used from a resource manager's perspective towards configuring a virtual network based on the SPs' requirements (capacities).

- The influence of the power ratio is clearer in Figure 5.7. When the power ratio increases from 3dB to 15dB, SP_A's capacities are higher while SP_B's capacities are lower (the average capacity points shift toward the lower right corner).
- The average capacities follow similar patterns if the power ratios P_A/P_B of 3dB and 15dB are considered separately. For SP_A, scenarios belong to the same case do not see varying average capacities (capacity points for a given case – e.g., RRV + FFR – but different scenarios align almost vertically). However, the average capacity varies across cases (vertical lines are separated and occur at different capacities for MUs of SP_A). For the MUs of SP_B, the average capacities vary across both cases and scenarios. Scenario 2 with small r_B and large d is the best in every case for SP_B. Cases in which SP_B can share all of the radio resources (Case I, II and III) are most beneficial.
- We can say that if SP_A's demand is the resource manager's primary concern, the preferred configuration options would be Center + RRV regardless of the scenario. On the other hand, a resource manager trying to increase SP_B's capacity in the hotspot would discard the Center + RRV and FFR/SSV options.
- FFR + RRV provides the greatest aggregate capacity (most towards the top right corner) and mutual benefits for both SPs. Therefore, it is a desirable configuration, almost always. Orthogonal spectrum sharing through FFR/SSV helps SP_A when the power ratio is low (3 dB, as observed previously), but the benefits are only minimally better than the FFR + RRV case. Especially when SP_A is able to transmit at a relatively high power level, FFR + RRV is the best option.

5.2.3 Configuration Map

We can view Figure 5.7 as a *configuration map* for use by the resource manager. We have drawn dotted lines to separate various cases and scenarios – this splits the figures into a

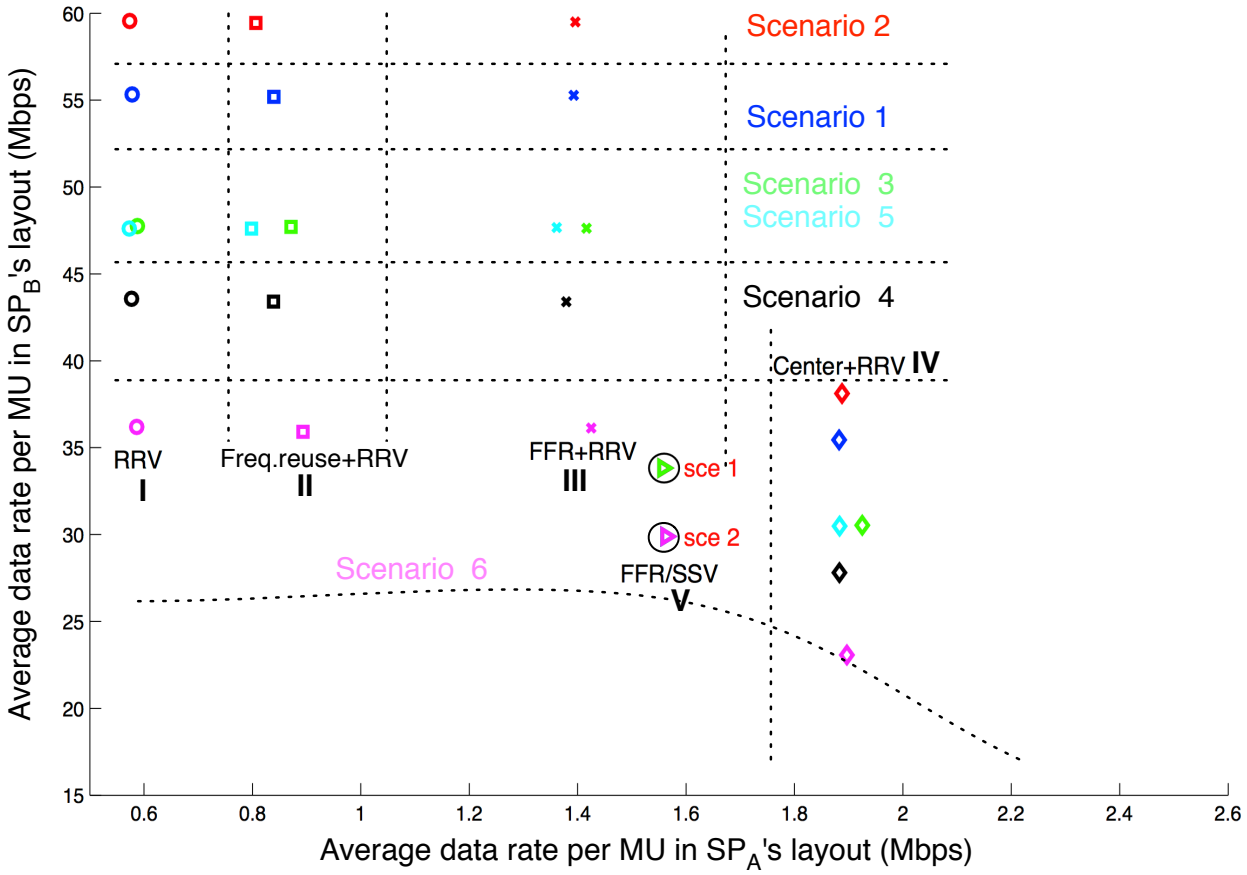

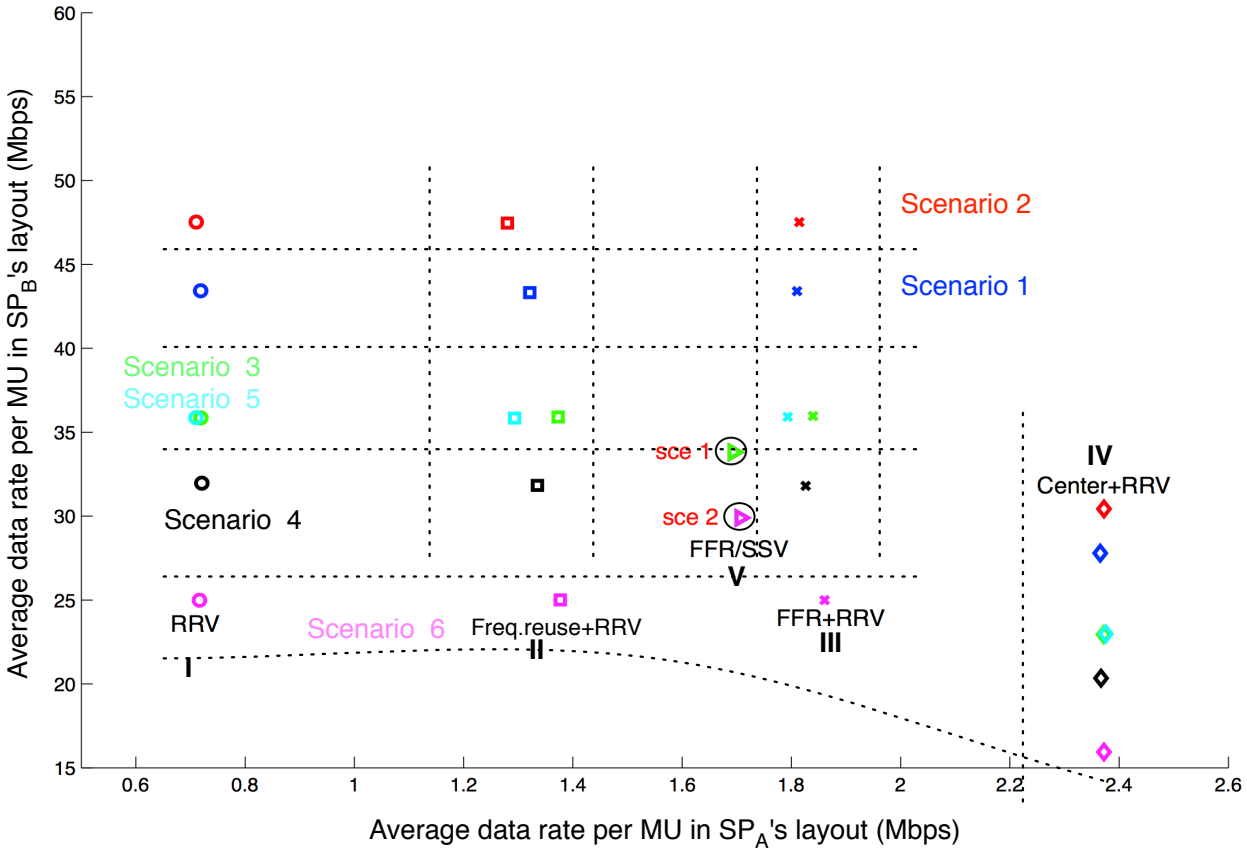

Figure 5.7: Capacity in SP_A v.s. capacity in SP_B layouts – top (3dB) and bottom (15dB)

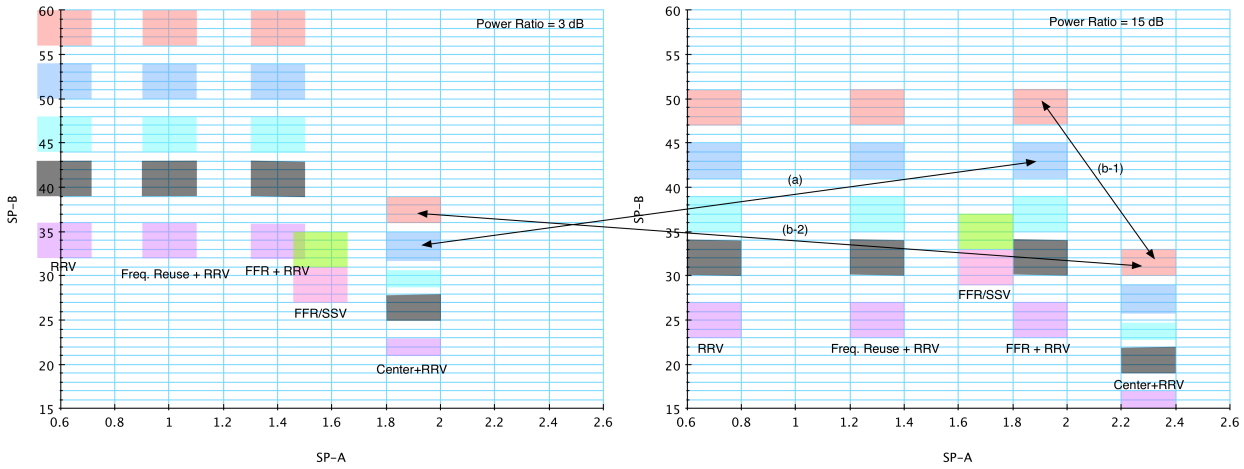

Figure 5.8: Using configuration map by resource manager

tabular format where every point can represent the demands of the two SPs and includes tradeoffs between them.

We redraw this configuration map for clarity in Figure 5.8. The associated scenario and case show the network environment and configuration. A resource manager could choose or switch between configurations to adjust the sharing according to the SPs' requirements. We explain this through two simple examples:

- a) Let us suppose that in a given time unit, the network environment is similar to scenario 1 (blue dots). SP_A reports that its required capacity is no less than 1.8 Mbps and SP_B has a demand in the hotspot that is no less than 35 Mbps per MU. The configuration options are either Case IV: Center + RRV or Case III: FFR + RRV. With the Center+RRV option, the power ratio should be 3 dB. However, if the resource manager chooses FFR + RRV, it has to configure SP_A to transmit at least 15dB higher than the power of SP_B in BSs 1, 2, and 3. Note that Center+RRV shares a smaller slice of the spectrum.
- b) Suppose the network environment is similar to scenario 2 (red dots). In a given time unit, the capacity demands of SP_A and SP_B are around 2Mbps and 20Mbps per MU in their layouts. The configuration applied by the resource manager is Case IV: Center + RRV with a power ratio of 15dB. If there is a spike in SP_B's hotspot (BS-4's) demand

to 35 Mbps, the resource manager (based on the service agreement) may reconfigure the network in the next time unit to Case III: FFR + RRV reducing the capacity per MU of SP_A to 1.85 Mbps and increasing it to 47 Mbps for SP_B by allocating more spectrum for use by SP_B while increasing the interference to MUs of SP_A. Alternatively, the resource manager could stay with Case IV and reduce the power ratio to 3 dB. We observe that in each case, the cell edge MUs in SP_A's layout are likely to be impacted negatively.

5.2.4 Impact of Number of Antennas

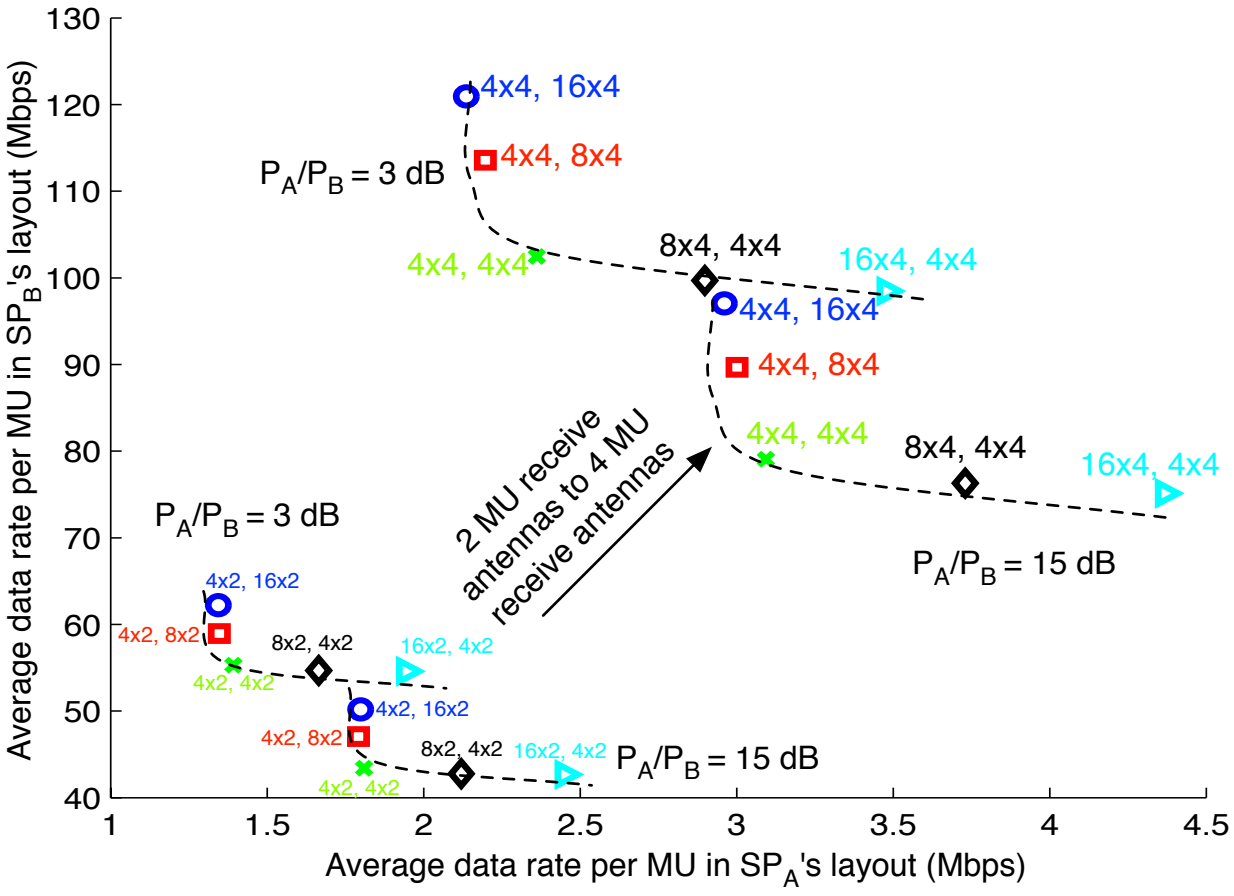

Figure 5.9: Capacity in SP_A layout v.s. capacity in SP_B layout for various MIMO settings

MIMO settings as an important part of configuration has a major influence on system and per MU achievable capacity. We assume all sub-channels created through MIMO are

dedicated to the same MU (eq. 4 to 6), hence capacity proportionally increases as the number of sub-channels ($min(n_T, n_R)$) [58]. Due to hardware limits, it may not be practical to implement more than 2 antennas at the MUs. However, we do consider 2 and 4 antennas at the MU while changing the number of antennas at BSs 1, 2, 3, together and BS-4 to examine the ability of MIMO in combating interference. We use scenario 1 of case III as representative and plot the average capacities in Figure 5.9. In this figure, a pair of products $x \times y, p \times q$ indicates the number of BS transmit antennas $\times$ the number of MU antennas of SP_A and SP_B respectively. We observe the following:

- The trend of capacities of MUs of SP_A and MUs of SP_B for the power ratios of 3 dB is the same as the trend for 15dB. In the two upper curves, when the number of SP_A's antennas is fixed (e.g., 4), as the number of antennas used at SP_B's BS-4 is doubled, the average capacity per MU for SP_B increases by 7 to 10 Mpbs (around 7%). The capacity per MU of SP_A drops only slightly even though more antennas are transmitting in BS-4. A similar result is observed when when SP_B uses a fixed number (e.g., 4 antennas) while SP_A doubles the number of antennas. For example, when the power ratio is 3dB, the average capacities for MUs of SP_B barely change but the capacity for MUs of SP_A increase from 2.35Mbps to 3.5Mbps after the number of antennas is quadrupled. This may be a configuration strategy that can be adopted by a resource manager to quickly improve a SPs' capacity.

- If device heterogeneity can be exploited (which is a possibility in the future), we see that the curves can be moved towards the right top corner in Figure 5.9 by configuring the system differently with increasing numbers of mobile antennas.

5.3 DISCUSSION

In this section, we discuss some outstanding issues partially. Further study is required to understand these issues in the context of radio resource virtualization.

5.3.1 Isolation

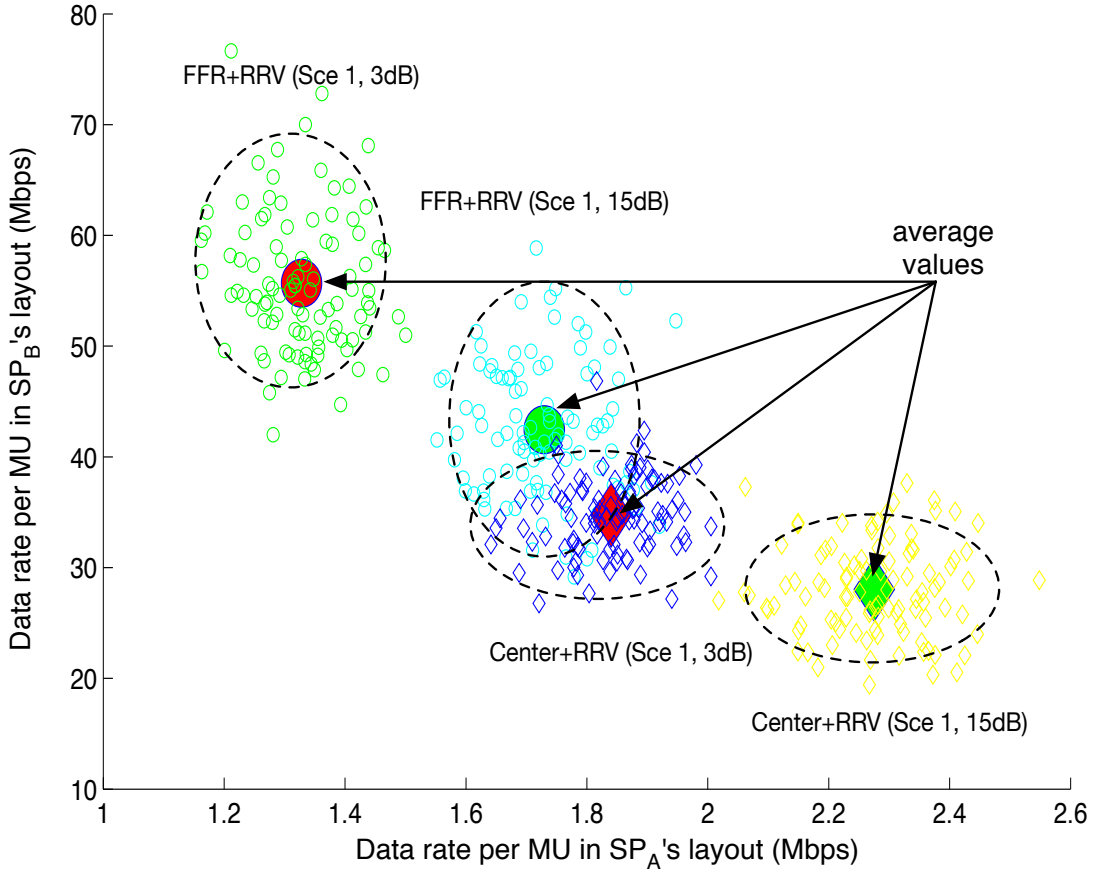

Figure 5.10: Variation in Capacity

In Figures 5.5–5.7, we have only shown the average values of the capacity for MUs over several simulation runs. There is appreciable variability around this mean value. Figure 5.10 shows this for two cases, both Scenario 1, for power ratios of 3 dB and 15 dB. The plot only includes 100 runs to avoid clutter and the average values reflect this, compared to the 10000 runs in the previous results. Clearly, the variability has impact on the achievable data rates for MUs of the two SPs due to the varying locations of MUs and the varying channel conditions. The resource manager and InPs may be able to use data to provide probabilistic service agreements that provide average capacity values with certain probabilities. This also alerts us to the fact that misconfigurations of one or both SPs will have considerable

impact on the isolation between them. If SPs are allowed to configure the hardware with the parameters supplied by a resource manager, and they behave selfishly or maliciously, the impact may be worse.

The challenges of isolation between SPs needs substantial thought and it is part of our ongoing work.

5.3.2 Impact on cell-edge users due to FFR in SP_A's layout

There are two factors that impact the capacity of cell edge MUs - how much spectrum is allocated to them and how we define the cell edge. The cell edge is defined by a dB value that is larger than P_{th_A}. The average fraction of cell edge MUs at varying cell-edge ranges are listed in Table 5. The fewer the cell edge MUs, the more spectrum they have (since the spectrum is partitioned in a deterministic manner). We examine Case III, Scenario 1 here [3]. The transmit power ratio is 10dB.

Figure 5.11 shows the average achievable data rates over *all MUs* and over only *cell edge MUs*. As more spectrum ($82\% = \frac{41}{50}$) is allocated to center MUs, the overall capacity (achievable data rate per MU) has a mild improvement. At the same time, the average data rate per cell edge MU drops. The cell edge capacity per MU drastically falls with the increasing edge area because more MUs share a limited spectrum. On the contrary, the overall average data rate does not change much even when the cell center area shrinks. Note that here we provide 3 cases of partitions with changeable edge area to give an impression of the interaction between those parameters. The optimal partition in virtual FFR system requires more detailed evaluation metrics like user satisfaction [59]. We used a 3dB threshold in our simulations since the cell edge MUs have almost the same capacity as the overall MUs in each cell when $64\% = \frac{32}{50}$ of spectrum is allocated to center MUs.

[3] We also examined the overall and cell edge performance for other scenarios. The results are neglected here due to the high similarity to Figure 5.11.

Table 5: Percentages of cell edge MUs

cell edge range	1dB	2dB	3dB	4dB	5dB	6dB
percentage	0.043	0.091	0.141	0.194	0.248	0.304

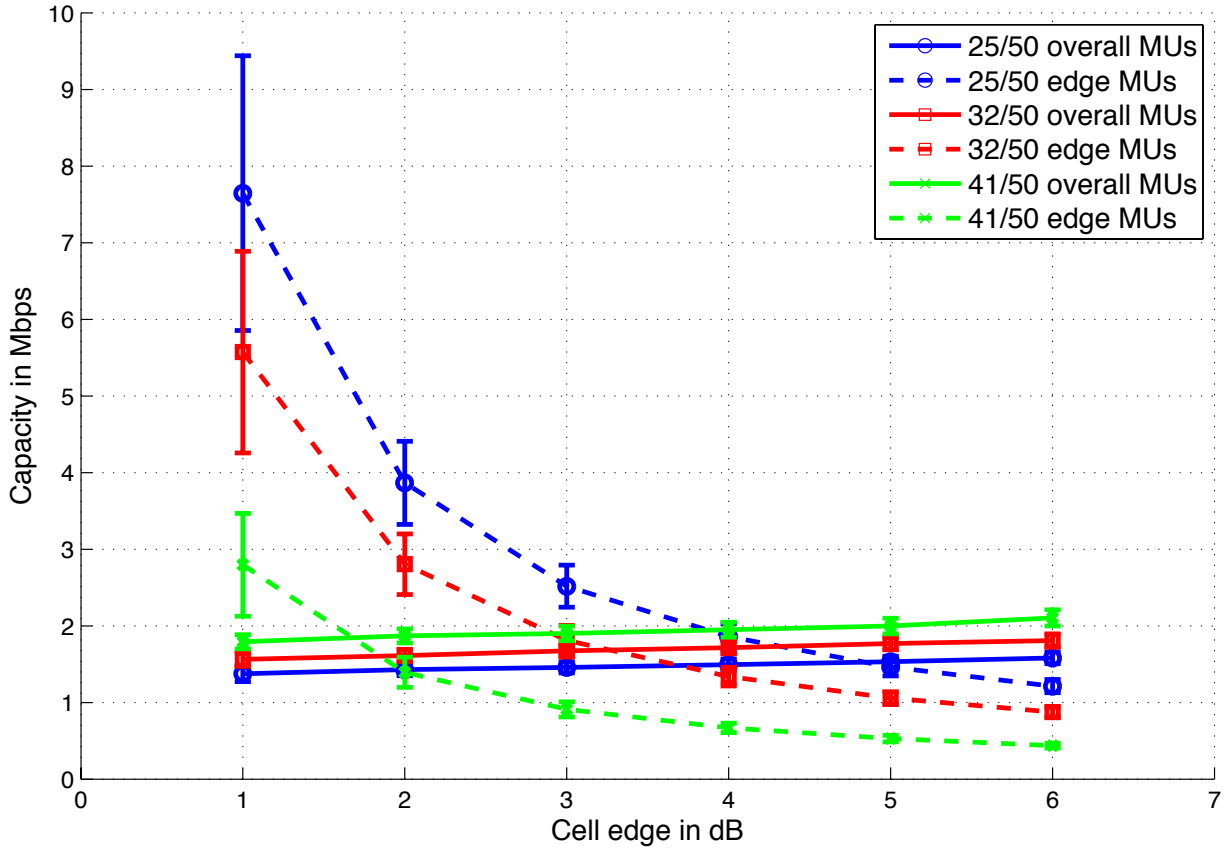

Figure 5.11: Achievable data rate per MU for cell center MUs and cell edge MUs

5.3.3 Other Issues

We consider only the overlapping slice shown in Figure 3.3 when it is accessed by more than one SPs. From a SP's perspective, the service agreements can be estimated based on the assigned dedicated spectrum from the InP in every time unit. Spectrum that is configured for RRV usage can be seen as an additional resource and provides an upper bound of predicted capacity. An example for spectrum planning is when an SP configures its network assuming only SSV is available and leaves some potential hotspots to RRV. Also, the time scale of virtualization is an essential problem. Study in this field needs to strike a balance between the abilities of cellular hardware and gains in the capacity of virtualization. One example is whether or not BSs can switch from "center+RRV" to "FFR+RRV" in small time scales, due to limitations on RF amplifiers or other hardware. These are beyond the scope of this dissertation.

For simplicity, the system model in this paper assumes the transmit powers are the same in all spectrum slices allocated to a given SP. If a snapshot is taken, the BSs transmit to MUs of the same group (e.g., SP_A center MUs, SP_A cell edge MUs, and SP_B MUs) at the same power level. This need not be the case and the powers may be tuned to different MUs. The other assumption made here is that the orthogonally-divided frequency slices for one SP are distributed randomly to its MUs. In reality, this might not be the best case. The interference level and channel conditions in different frequency slices may be different. Cells 1, 2 and 3 may operate at different transmit power levels. As a result of these differences, the interference seen by SP_B's MUs may be different. Further, different definitions of cell edge are possible in Cells 1, 2 and 3.

The consequence of these changes is that units of spectrum assigned to MUs could be differentiated by interference levels. The tradeoff of capacities will boil down to the MU level instead of an SP level. For instance, every slice of spectrum may have a particular RSS level which indicates the power level that another transmission can apply at the same time. The resource manager will have to configure concurrent transmissions in a given spectrum slice based on the MUs' required capacities. Since MIMO has already been considered, the number of antennas set by every pair of transmitter and receiver can also vary to meet the

request of a service. Scheduling based on channel quality (e.g., the proportional fair (PF) scheduler in LTE [60]) also may impact capacity. With channel quality information of MUs in every time unit, the system schedules radio resources to MUs which have good channel conditions. It may be possible to group MUs to achieve pareto optimality as described in [61]. Our future work will be along this line to deploy more flexible configurations to facilitate efficient radio resource virtualization.

5.4 CONCLUSIONS

In this Chapter, we use simulations to examine the problem of radio resource configuration when wireless networks are virtualized. We evaluate several scenarios with several spectrum sharing cases that include fractional frequency reuse. The chapter provides a framework for a resource manager to configure radio resources between two different service providers operating in the same geographical area. The configuration of a virtualized wireless network is unlikely to have a definite "closed form" single solution. Proper configuration depends on the network architecture, capabilities of the network/end-devices and demands of the players, and it changes dynamically. Reasonable configurations appear to be capable of leading virtualization towards higher efficiencies, better isolation across SPs, and customization of services. Configurations investigated are references for future cellular networks with similar advanced technologies.

6.0 A CASE STUDY: LTE NETWORK VIRTUALIZATION

6.1 MOTIVATION

In this chapter, we develop a LTE system-level simulator and integrate RRV in the radio resource management to provide some insight when virtualization is deployed in a LTE system.

In Chapters 4 and 5, we have discussed the potential benefits of RRV as well as how the benefits are influenced by network configuration in a relative complex cellular environment. Apparently, SSV (top half in Figure 3.1) does not fully exploit the use of spectrum nor does it always provide the highest efficiency. RRV (lower half in Figure 3.1) allows SPs to reuse some amount of spectrum in the same time interval in overlapping geographical areas. In Chapter 4 we show that RRV often leads to better resource usage efficiencies than SSV. Chapter 5 gives a framework to tradeoff between SPs by configuring virtual networks. Until now, we have used Shannon's capacity with simulations that provide an upper bound of physical channel performance. However, Shannon capacity-based analysis neglects everything that is above the physical channel and the upper bound may not be convincing enough for the RRV usage. Some important procedures in cellular downlink transmissions have great influence on system capacity, like scheduling, buffering, coding and modulation. Further, in previous study, spectrum assigned to a SP is assumed to be equally divided and randomly distributed to the given SP's MUs - that is, there is no intra-SP interference. In reality, the bandwidth allocation to individual MUs is more complicated and depends on the air-interface of a given RAT. Towards this, we undertake a case study of RRV with LTE in this chapter. We also explore the problem of how a resource manager can configure radio resources for SPs to meet their respective needs. This is a challenging problem when radio resources and interference

play a role in what capacity a SP can actually get and how this may impact the capacity of a different SP.

In this chapter, we consider a two-SP virtual system and extensive system-level simulations are conducted following 3GPP guidelines. Performances of SSV and RRV are evaluated with multiple scenarios and deployment parameters. Also, we discover that time domain (TD) muting techniques, widely studied for enhanced inter-cell interference coordination (eICIC) for a single operator in 3GPP, can be used in a different way in a virtualized setting by a resource manager. The resource manager can employ TD muting to change configurations for different SPs to meet their demands in different time units. The usage of TD Muting subframes is very similar to the almost blank subframes (ABS) of eICIC but it serves a completely different purpose in virtualization. In the case of eICIC, ABS is combined with cell range extension (CRE) and the objective is to support picocell-edge mobile units (MUs) by changing the coverage of picocells and larger macrocells. The idea is to handoff MUs to picocells to improve the aggregate capacity of a single SP. Work in [56] studied the optimum combination of parameters in eICIC. However, in the case of virtualization, the coverage of each SP is deterministic and MUs do not switch between SPs. TD Muting helps in reconfiguring the sharing between SPs that are affected by interference. In this chapter, TD Muting is included and seen as an important part of the configuration provided by the resource manager to SPs. Of course, it is also possible to configure SPs without any TD muting. To differentiate this scheme from the general RRV scheme, we call the former as "TD Muting RRV" and the latter as "unconditional RRV". Also, we propose a novel major-interferer time domain (MI-TD) muting RRV that differentiate the muting patterns of subframes at every small eNB to further improve the efficiency.

6.2 RADIO RESOURCE MANAGEMENT WITH VIRTUALIZATION

LTE adopts advanced radio resource management (RRM) techniques to increase system capacity. A core feature of RRM, radio resource *scheduling*, plays a fundamental role in realizing the improvement in system performance. This feature distributes radio resources

among MUs with fine time and frequency resolutions, taking into account channel conditions and quality of service requirements. In a similar manner, the integration of a *virtual resource manager* with functions similar to LTE's RRM can improve the system performance compare to simply using RRM as is in a virtual network.

6.2.1 LTE Downlink Radio Resource Management

The air-interface of LTE is based on orthogonal frequency division multiplexing (OFDM) [62]. LTE supports two types of frame structures for two different duplexing schemes – frequency division duplex (FDD) and time division duplex (TDD). In this chapter, we assume the more common FDD scheme, where one frame is composed of ten consecutive identical subframes. At the physical layer, radio resources are allocated in both the time and frequency domain. The smallest radio resource unit that can be assigned to an MU for data transmission is a resource block (RB). An RB occupies 0.5 ms in the time domain and has 12 subcarriers which occupy $12 \times 18\text{kHz} = 180\text{kHz}$ in the frequency domain. A transmission time interval (TTI) corresponds to 1 subframe in the time domain and lasts 1 ms (2 time slots). Each frame has 10 subframes. Within every time slot (0.5 ms), there are 7 OFDM symbols (if a normal cyclic prefix is applied). In the frequency domain, the number of RBs varies according to the system available bandwidth (e.g., a 5 MHz channel can have 25 RBs and a 10 MHz channel can include 50 RBs). We only consider downlink transmissions in our simulations.

A typical LTE system makes extensive use of RRM procedures such as link adaptation, hybrid ARQ (HARQ), power control and channel quality indicator (CQI) reporting [63]. These functions are placed at the physical and MAC layers, and strongly interact with each other to improve the usage of available radio resources. However, not all of the modules in RRM are included in our simulator. Here we only describe the main RRM features that we have included in our simulator.

- CQI reporting: CQI reporting enables information about the quality of the downlink channel (observed by an MU) to be available at the BS (which is called an evolved Node B (eNB) in LTE). MUs generate CQI reports that provide a measure of the downlink channel conditions experienced by MUs. Such reports are sent to their associated eNBs.

An eNB uses CQI reports within its resource scheduling and link adaptation algorithms. If a proportional fair (PF) scheduler [60] is used, then MUs reporting high CQI values relative to the average CQI are more likely to be scheduled. Far scheduling also accounts for the historical throughput achieved by an MU.

- Adaptive modulation and coding (AMC): AMC selects the proper modulation and coding scheme (MCS) whose objective is to maximize the MU throughput with a given target block error rate (BLER) [64]. AMC is more likely to allocate advanced modulation (e.g., 64-QAM) and high coding rate (i.e., less redundancy) leading to high throughput to MUs reporting high CQI values. CQI values range from 1 to 15 and they indicate 16 combinations of modulation schemes and code rates. The sizes of transmission blocks (TB) are determined by the combination of the modulation scheme and coding rate and the CQI reference resource.

Note that besides the functions described above that are in our simulator, LTE RRM also enables power control and HARQ. AMC usually works with power control to save energy [64]. HARQ applies the stop-and-wait algorithm (at the lowest layer possible to avoid latency) and combines erroneous frames with retransmissions for diversity [65]. But these features are out of the scope of our work.

Following the RRM procedure, an eNB sends TBs of information to scheduled MUs. The sizes of TBs (in bits) is defined by the MCS tuple and it is related to the downlink channel conditions of MUs. The throughput of an MU depends on the sizes of TBs, CQI reference resource and how many subframes are scheduled for it. The CQI reference resource is a specific set of RBs in the frequency domain and a single subframe in the time domain. The set of RBs in frequency domain covers the entire available channel bandwidth when a wideband CQI is reported [66].

6.2.2 Scheduling in LTE RRV System

We develop a LTE system-level simulator for a virtualized setting that includes only the aforementioned RRM features. Our simulator considers two main RRM functions – CQI computation (PF scheduler is used), and AMC. The whole downlink scheduling process

can be described as a sequence of operations as follows: In every TTI/subframe, each MU measures its channel condition, computes its CQI according to the PF scheduling mechanism and reports to the resource manager of the virtual network. Then the resource manager picks the most proper MU and schedules resources based on the CQI information. Here CQI information reflects the measured channel signal to interference plus noise ratio (SINR) and is a measure of the MU's throughput. The PF scheduler chooses MUs with high throughput relative to the average MU throughput observed until this TTI/subframe. CQI information is also used by the AMC module to select the proper MCS. MUs experiencing high SINR are served with high bit rates. To simply evaluate AMC throughput, an adjusted Shannon capacity formula based on the work in [13] is used. This formula has been previously used to benchmark capacity in LTE links with interference. It takes into account the system bandwidth efficiency and SINR efficiency to approximate throughput with a formula that is similar to the Shannon-capacity evaluation. The bandwidth efficiency is determined based on system parameters, and the SINR efficiency is extracted from detailed link level studies [13]. Results of this simulator are compared, when it is possible, with other LTE ones already present in literature [56] (see Appendix) for validation.

In the next section, we describe the implementation of these RRM functions and the TD muting strategies that we adopt in the virtualized setting of Figure 6.1.

6.3 SYSTEM MODEL

A schematic of the virtual LTE network examined in this chapter is depicted in Figure 6.1. Two SPs, SP_A and SP_B, co-exist in an area. A resource manager is responsible for providing the spectrum assignment (or alternatively configuring the SPs with the spectrum) that is dedicated to SP_A, SP_B respectively and more importantly, also responsible for RRV (spectrum used by both SPs in the same space at the same time). Within the RRV spectrum, SPs configure transmissions strictly following values of parameters (such as transmit power or time slots to be used) that also come from the resource manager. If spectrum is shared between cells with the similar sizes simultaneously in space, it is likely that the interference

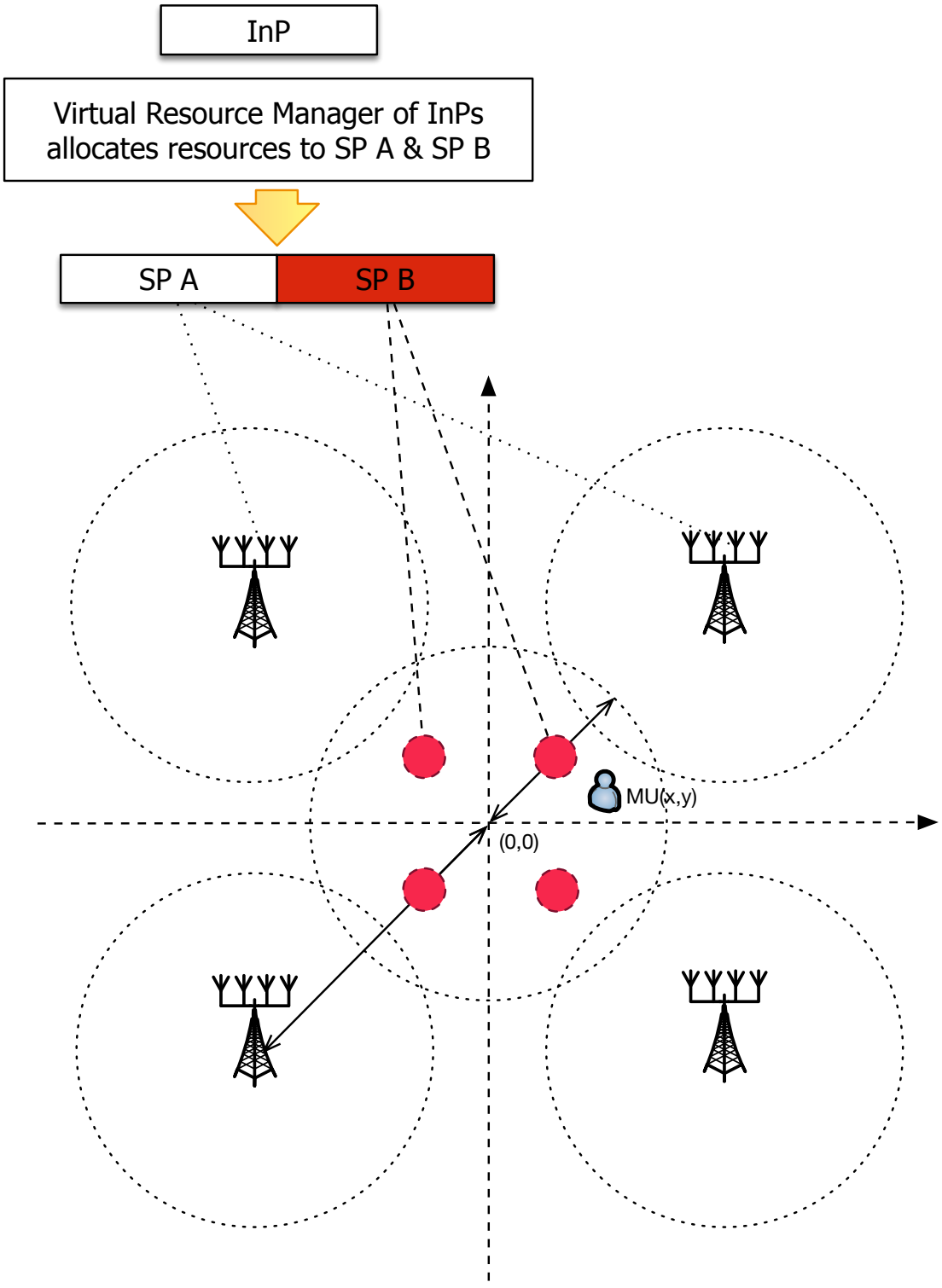

Figure 6.1: System model of LTE simulator

will be too high. Hence, we assume that the two SPs have cells with heterogeneous sizes. SP_A's operation is in the large cell (four other large cells, not shown in the figure, are implemented in the simulation to add co-channel interference) shown in Figure 6.1 with relatively high transmit power P_A on the downlink. SP_B owns four small cells (that is, the frequency reuse factor is 1) in the coverage of SP_A's large cell and transmits at a lower power level P_B.

6.3.1 RRV configuration in the LTE Network

Inherent from conventional LTE RRM, every eNB has its own resource manager module that operates scheduling, while those resource managers exchange information extensively over X2 interface. So we can also view these separately located resource management entities as one single "virtual" resource manager, similar to the resource managers we assumed in Chapters 4 and 5. Such a virtual resource manager is still responsible for providing the spectrum assignment and configuration to each SP in every TTI. The purpose of this design is to facilitate virtualization but keep minimum modifications to the existing LTE system.

As already mentioned, a physical resource block (PRB) is the smallest unit of radio resources in frequency and time in LTE networks. In each transmission period (e.g., 40 subframes [1]), a resource manager determines PRB groups for SSV (dedicated spectrum that is orthogonal for SP_A and SP_B as shown in the top figure of Figure 3.1) and RRV (overlapping spectrum in the bottom figure of Figure 3.1).

An important responsibility of the resource manager is to provide proper configurations for SPs in each transmission period. In the orthogonal PRB groups which do not interfere with each other, SPs can provide services to their subscribers, if necessary at their own expense. For example, SP_B's MUs will not be affected if SP_A transmits at an extremely high power level since the SPs are configured to use orthogonal slices of spectrum. Of course SP_A has to manage the interference it causes to its own neighboring cells. However, the resource manager will have to configure SPs to use the appropriate parameters within the RRV PRB groups to maintain the service level agreements that may be in place. A correct configuration depends on each SP's QoS requirement at a time, the agreements between each

[1]The periodicity of 40 subframes maximizes the protection of common channels, including uplink hybrid automatic repeat request (HARQ) performance.

SP and the InPs in the serving region, and the abilities of the subscriber equipment of each SP (e.g., how many antennas MUs of a given SP may have). Thus, the configuration could include transmit power, MIMO settings and TD Muting portion, and could also change in every transmission period.

The selection of parameters in configuration like transmit power and MIMO settings are fairly straightforward, while the TD Muting portion is more tricky although it has been well known as part of eICIC for a *single service provider*. The portion of TD Muting subframes is a major part of the configuration chosen by the resource manager as we show later. An example of TD Muting is shown in Figure 6.2 where SP_B only transmits critical system information and common reference signals (CRSs) in TD Muting subframes. SP_A transmits all the time. Through this coordinated configuration across SPs, we expect SP_A's MUs to get better throughput due to fewer subframes that face high interference from transmissions of SP_B. Note that here we assume that TD Muting only occurs at SP_B's BSs, but in general, the same idea can be applied to both SPs. In the TD muting RRV, we don't differentiate muting patterns between cells of SP_B (all cells of SP_B use the same frequency bands from the InP). Four cells operated by SP_B are muted within the same subframes, also they transmit at the same time. However, an MU of SP_A most likely receives strong interference from only one eNB of SP_B. Muting all of SP_B's eNBs would cause waste of radio resources usage. To further seek mutual benefit for both SPs, we propose MI-TD muting RRV scheme shown as Figure 6.3, which *distinguishes the small cell that generates the strongest interference to a SP_A MU and then only mutes that specific small cell when the given MU is scheduled.* In Figure 6.3, MU 1 is scheduled within subframes 0, 2, 8, 1 and 3. The eNB of SP_B that generates the most interference is muted accordingly in those subframes.

Note that frequency domain scheduling is not under consideration, we assume all available RBs are assigned to the MU selected by the time-domain PF scheduler.

6.3.2 Throughput Evaluation

We assume that all MUs in the system are active at all time and eNBs use a frequency domain PF scheduler to choose an MU to communicate with. MUs are selected such that

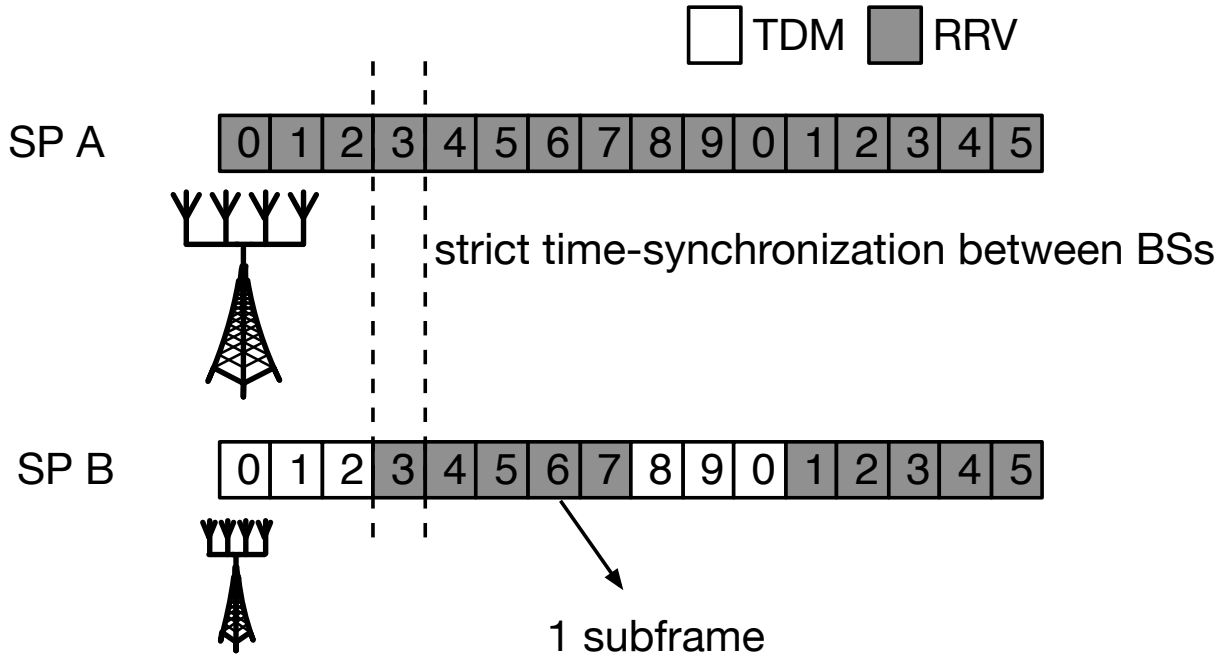

Figure 6.2: TD muting RRV at SP_B

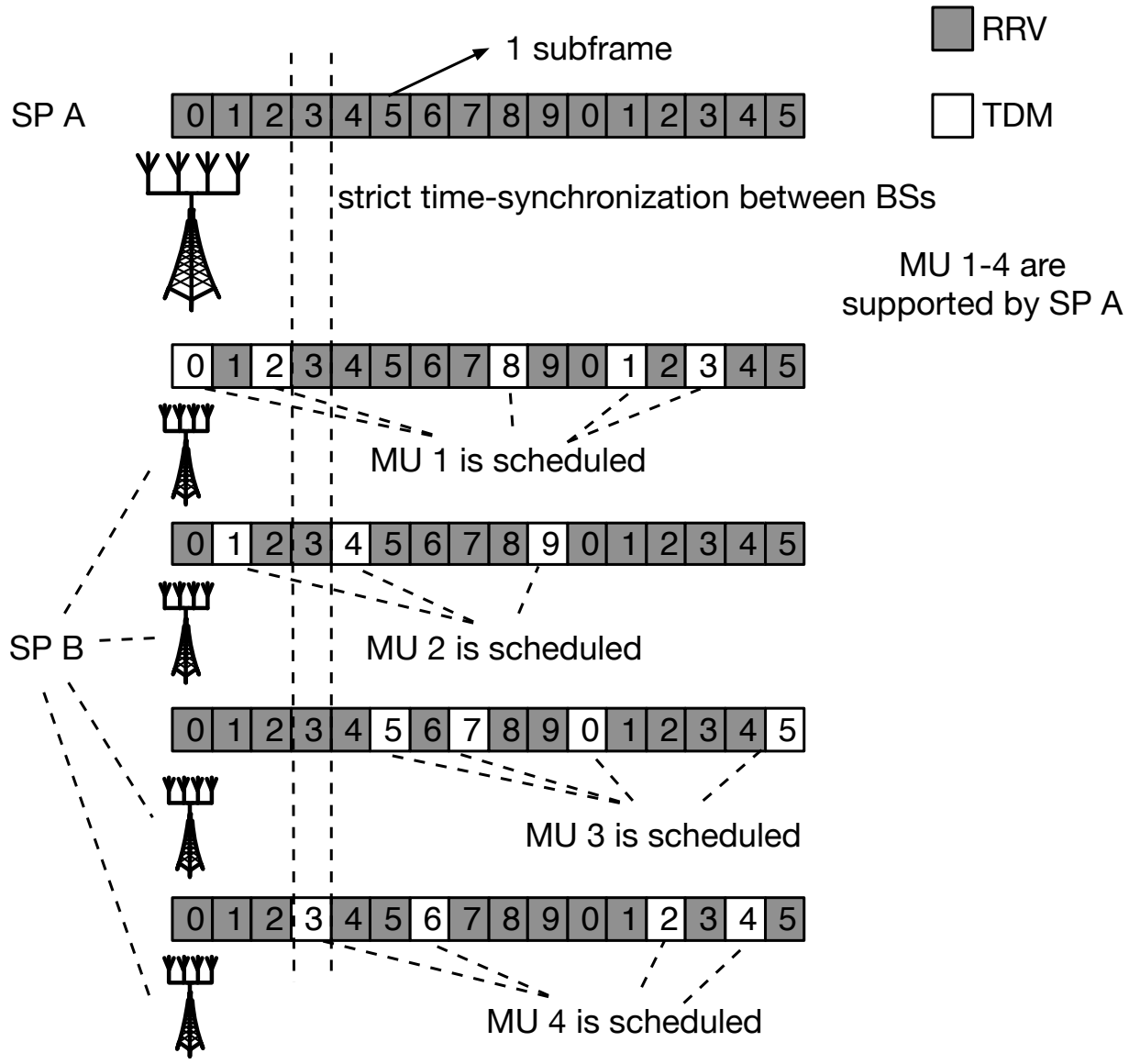

Figure 6.3: MI-TD muting RRV at SP_B

they have the maximum throughput in the current TTI relative to the average throughput until this TTI at the desired physical resource block group, i.e., they have

$$\text{Max}_k\{Throughput_{k,t}/AvgThr_{k,t}\}, \tag{6.1}$$

where k is the MU index, t indicates the time/subframe, $Throughput_{k,t}$ is the MU throughput at time/subframe t, and $AvgThr_{k,t}$ is the average MU throughput until time/subframe t. The value of $Throughput_{k,t}$ is estimated from the channel quality information (CQI) and an adjusted Shannon capacity formula, which is discussed in the following.

In a real LTE system, the standards define 15 different MCSs, driven by 15 channel quality indicator (CQI) values. The defined MCSs include code rates that are as small as 1/13 and as high as 1 combined with 4-QAM, 16-QAM and 64-QAM modulation schemes [67]. The throughput of every MU is determined by fast link adaption by the chosen MCS in each transmission, and the CQI of the MU's link indicates the appropriate MCS. To simplify this process, in this chapter, we use an adjusted Shannon capacity formula to estimate the throughput of each link based on [13]. The system bandwidth efficiency and the SNR efficiency of LTE system are taken into account in the formula to adjust the Shannon bound to be close to the LTE capacity. The bandwidth efficiency is calculated based on system parameters and the SNR efficiency is extracted from link-level measurement (curve fitting) [13]. Since here MIMO is enabled, the bandwidth efficiency and SNR efficiency are specified based on the usage of MIMO. The estimation of each link's throughput is [13]

$$C = \eta_{BW} w \log_2 \det[(\mathbf{I}_{n_R} + \eta_{SNR}(\mathbf{R}^{-1/2}\mathbf{H})P_R(\mathbf{R}^{-1/2}\mathbf{H})^H] \tag{6.2}$$

where w is the available bandwidth for one particular MU, P_R is the receive power and equal to $P_T - Pathloss$. Path loss exponent and shadow fading component are considered when P_R is calculated. Two Path loss models are used in large cells and small cells respectively (see Table 6). η_{BW} indicates bandwidth efficiency, and η_{SNR} refers SNR efficiency. $\mathbf{H}$ is the complex channel gain matrix, consisting of h_{ij} (note here $\mathbf{H}$ is different from $\mathbf{H}$ in Chapter 3). h_{ij} is the Rayleigh fading channel gain of the channel between the ith transmit

antenna and the jth receiving antenna. N is the thermal noise with variance $N_0/2$. $\mathbf{R}$ is the interference and thermal noise combined matrix, which is given as:

$$\mathbf{R} = \sum_k \mathbf{H}_{Ik}\mathbf{H}_{Ik}^H P_{Ik} + wN_0\mathbf{I}_{n_R} \tag{6.3}$$

where $\mathbf{H}_{Ik}$ is the interfering channel matrix from interfering Cell k. For example, an MU of SP_A faces interference from 4 SP_B eNBs, as well as 4 other eNBs operates by SP_A shown in Figure 6.1. Also, an MU of SP_B's receives interference not only from SP_A eNBs but also other 3 SP_B eNBs. P_{Ik} is the kth interferer's power that ends at the given MU's receiver. $\mathbf{I}_{n_R}$ is an identity matrix of dimensions. The rest of the computation is the same as the process introduced in Chapter 3, please see Eq. 3.3 to Eq. 3.6 for further computation steps.

6.3.3 Scheduling

The entire scheduling process consists of five steps. 1) Every MU measures the downlink channel, computes the CQI and sends it to the virtual resource manager. 2) The virtual resource manager performs PRB allocation based on the CQI information from MUs. 3) The AMC module selects the proper MCS for the scheduled MU. 4) Information of the scheduled MU, the allocated RBs, and the selected MCS are sent back to the MUs through the control channel (that is similar to the physical downlink control channel – PDCCH). 5) Every MU reads the PDCCH and accesses the transmitted data only if it is scheduled.

Within any TD muting subframe, MUs of SP_A[2] may experience significantly lower level of interference from normal subframes. It is necessary to report separate CQI values for TD muting subframes and normal subframes. The virtual resource manager of SP_A then can match the CQI information with muting status of the subframe for AMC and scheduling. Therefore in TD muting RRV, we assume all SP_A MUs report separate TD muting CQI metric for the TD muting subframes from normal subframes. In normal subframes, all interference from SP_A's eNBs and SP_B's eNBs are taken into account when we calculate CQI values. On the other hand, in TD muting subframes, most of interference from 4 SP_B eNBs are removed from the TD muting CQI metric (number of interfering BSs decreases in

[2]In either TD muting RRV or MI-TD muting RRV, scheduling process for all SP_B MUs remains.

Eq. 6.3). SP_A uses the TD muting CQI metric to perform AMC and resource scheduling. For a SP_A MU facing strong interference from SP_B BS/BSs, a much higher value is expected in TD muting subframes due to low average throughput in its history. MUs that are located close to SP_B's BSs have higher chance to be scheduled in those TD muting subframes.

As we do not have a cyclic pattern (like every first 3 out of 8 subframes in TD muting RRV) in MI-TD muting RRV, SP_A's eNB does not know which eNB of SP_B will be muted in the next TTI until it completes scheduling. Therefore we slightly modify the working flow of the scheduler described above to adapt to this tricky situation. Every SP_A MU reports CQI values only for MI-TD muting subframes. CQI values are computed through Eq. 6.2 to Eq. 6.3 while the strongest interference from SP_B is removed. Besides, an MU needs to inform the virtual resource manager of the SP_B's eNB that generates the strongest interference. At any TTI, the PF scheduler of virtual resource manager selects a MU according to MI-TD muting CQI values for SP_A. After that, the virtual resource manager informs the corresponding eNB of SP_B to mute in the next subframe and uses the MI-TD muting CQI value within the AMC module.

6.4 SIMULATION RESULTS AND ANALYSIS

A network as shown in Figure 6.1 is built in our simulation. Three network layouts with different sizes of cells and different distances between interfering cells are considered to understand the benefits of RRV and how to use TD Muting in the virtualized setting. The simulation parameters and details of the three network layouts are summarized in Table 6. R indicates the cell radius of the large cell where SP_A is configured to operate, and N_A is the number of MUs of SP_A. We assume the cell radius of each of the four small cells is $50m$ and each cell serves 10 subscribers. The four small cells are placed at a distance $R/2$ from the eNB of the large cell and are 90° apart from each other. In the virtualized setting, SP_A and SP_B together have 15 MHz of bandwidth. With SSV, they have 10 and 5 MHz of bandwidth respectively. At each eNB, $n_T = 4$ antennas and at each MU, $n_R = 2$ antennas are assumed. In this chapter, we assume that when RRV is enabled, it exists in *all*

Table 6: System parameters

Network Layout	**Description,** R**,** N_A
1	1000m, 100
2	1000m, 20
3	500m, 20
Parameters	**Settings**
MU distribution	uniformly distributed
Transmission power	SP_A variable (P_A)
	SP_B $30dBm(P_B)$
Bandwidth	SP_A 10MHz, SP_B 5MHz
Subframe Duration	1ms
	(11 data plus 3 control symbols)
Simulation Duration	1000ms
Pathloss model	distance$>$ $50m$:
	$128.1 + 37.6log10(d[km])$
	distance$<$ $50m$:
	140.7+36.7log10(d[km])
Shadow fading	distance$>$ $50m$:
	Log-normal, std=8dB
	distance$<$ $50m$:
	Log-normal, std=10dB
Antenna setting	SP_A 4×2, SP_B 4×2
Bandwidth efficiency	0.76 [13]
SNR efficiency	1.05 [13]
Packet scheduling	PF scheduler
TD muting proportion	0, 1/8, 2/8, 3/8, 4/8, 5/8, 6/8

PRB groups unless muted and we do not test different MIMO settings (changing n_T, n_R). As n_T, n_R increase, the throughput of an MU increases if the channel coefficients h_{ij} are independent and identically distributed. The four eNBs of the small cells transmit at the same power P_B and the BS of the large cell has a power $P_A = P_B \times$ Power Ratio where the power ratio scales the transmit power P_A compared to P_B. Simulations results are averaged over 1000 runs. The 5th percentile and 50th percentile MU throughput are measured as evaluation metrics. They correspond to 95% of the MUs achieving a certain throughput or 50% of MUs achieving a certain throughput.

6.4.1 Performance of SP_A

From Figures 6.4 to 6.6, MU throughputs of SP_A for SSV, unconditional RRV and TD Muting RRV with different TD Muting muting portions are compared across the 3 network scenarios. Both 5%-ile and 50%-ile MU throughputs are shown. In general, unconditional RRV (can also be seen as TD Muting RRV with 0 TD Muting subframes) is worse than either SSV or TD Muting RRV as interference from SP_B exists in all subframes. In contrast to unconditional RRV, SSV doesn't allow simultaneous usage of spectrum by the large and small cells and thereby no interference between SP_B and SP_A occurs in any subframe (note that there is still co-channel interference from 4 large cells not shown in the figures). However, with SSV, in each subframe, the scheduled MU of SP_A only gets a portion of the entire system bandwidth which is 10 MHz out of 15 MHz while that of SP_B gets only 5 MHz of bandwidth. Since SSV outperforms unconditional RRV across all 3 scenarios, it is necessary to consider interference coordination/muting for MUs subscribed to SP_A. Otherwise, it appears that virtualization only harms the system performance in the large cell. Implementing TD Muting RRV is one way of addressing the reduction of interference.

A comparison between SSV and TD Muting RRV changes depending on the network layout and this is somewhat expected. From Figures 6.4 to 6.6, we can conclude several observations as follows. First, SSV outperforms more cases of TD Muting RRV (cases with lower TD Muting portions) in the 50%-ile MU throughput than it does in the 5%-ile MU throughput. For example, the 5%-ile MU throughput of SSV is better than TD Muting RRV

until the TD Muting portion increases up to 5/8 (i.e., 5 of 8 sub frames from the small BSs are muted). Five cases of TD Muting RRV (TD Muting portion ranging from 2/8 to 6/8) are possibly better than SSV when 50%-ile MU throughput is evaluated in Figure 6.4. This implies that TD Muting RRV improves at least half of the MUs' capacity. However there are some MUs facing fierce interference probably because they are located close to SP_B's BSs. For such MUs, the additional bandwidth from virtualization does not help as they barely get scheduled and suffer from very poor SINR that limits their throughput even when they are scheduled.

Second, as the TD Muting portion increases, SP_B pauses transmission in more subframes. Consequently, the system performance of SP_A is improved accordingly. However, 1/8 TD Muting RRV does not provide observable improvement compared to unconditional RRV since only one of 8 sub-frames are muted by eNBs of the small cells. There is a small difference that can be seen in SP_B's throughput in Figure 6.7 and 6.8 (discussed in the next subsection).

Third, the throughput increases as the transmit power increases as expected. For instance, in Figure 6.6, the 50%-ile MU throughput is boosted up to 8 Mbps when the transmit power is 24 dB $+P_B$ (30 dBm) = 54 dBm for 3/8 TD Muting RRV compared to 1.35 Mbps at transmit power 30 dBm.

Fourth, besides the aforementioned factors, the distances between interfering cells and number of MUs in the system also affect the system performance. If we compare network layouts 1 and 2, the number of MUs of SP_A decreases by 5 times (100 MUs in Network Layout 1 and 20 MUs in Network Layout 2). Thus, every MU gets 5 times more opportunity to be scheduled. Hence, the MU throughput is roughly 5 times higher in Figure 6.5 than it in Figure 6.4. However, from Network Layout 2 to Network Layout 3, we shrink the cell range of SP_A, but the system performance almost remains unchanged. It is because the co-channel large cells (not shown) and all the small cells are closer to the BS (see Figure 6.1) increasing the interference even as the the received signal strength is higher.

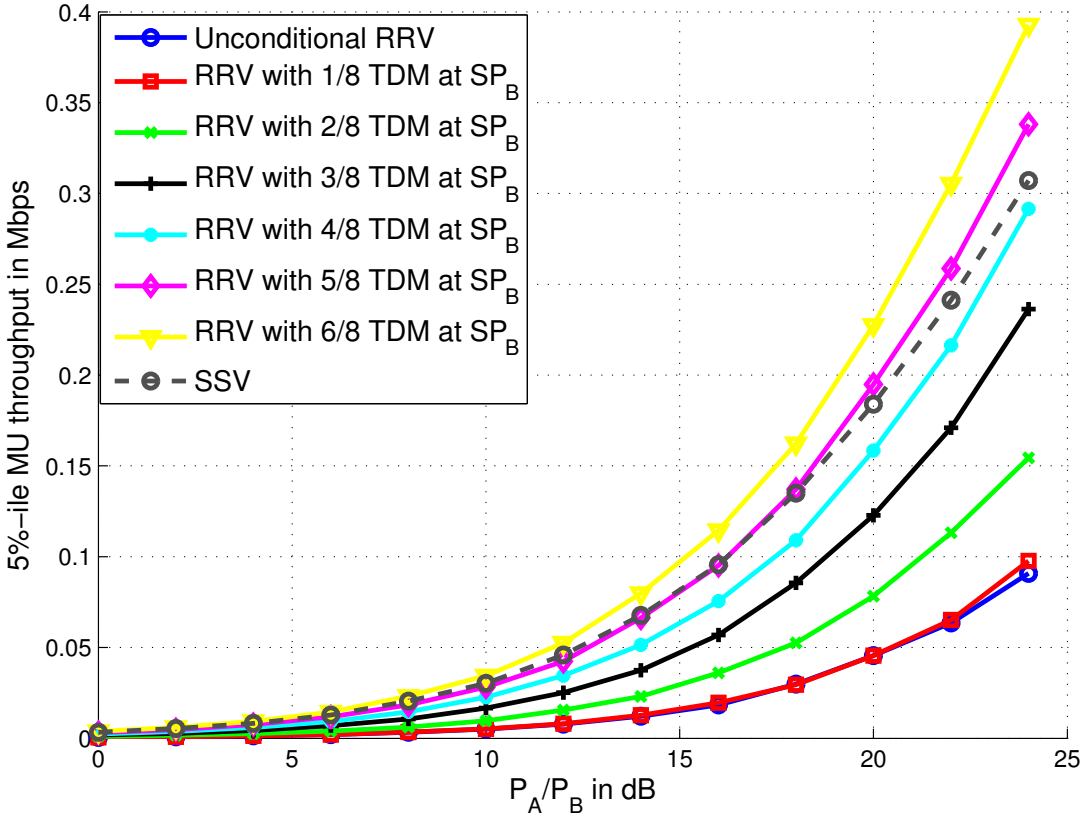

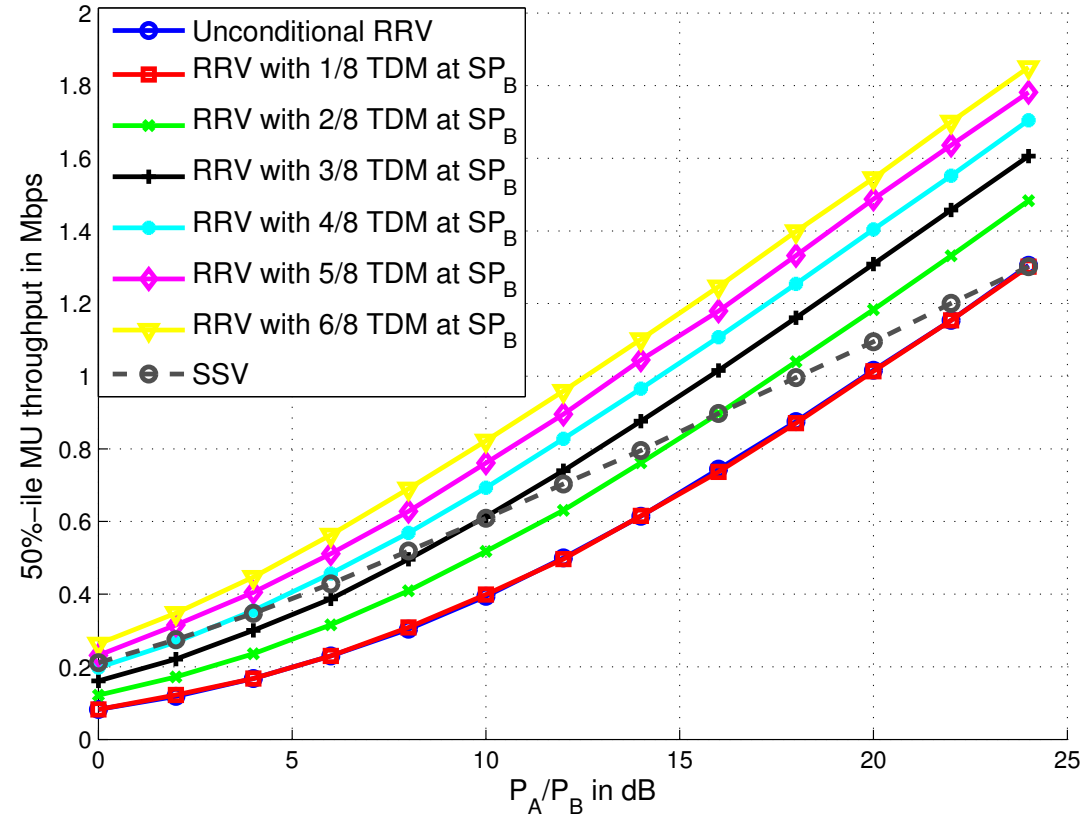

Figure 6.4: SP_A performance for Scenario 1 – top (5%-ile) and bottom (50%-ile)

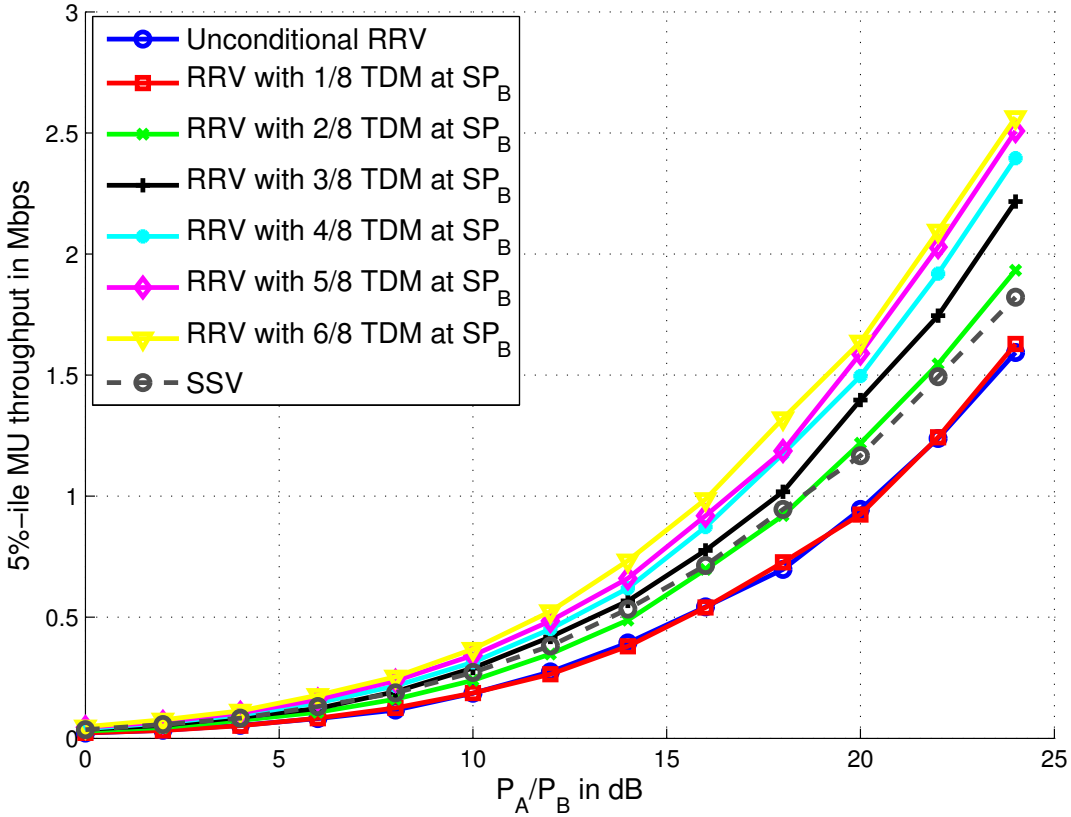

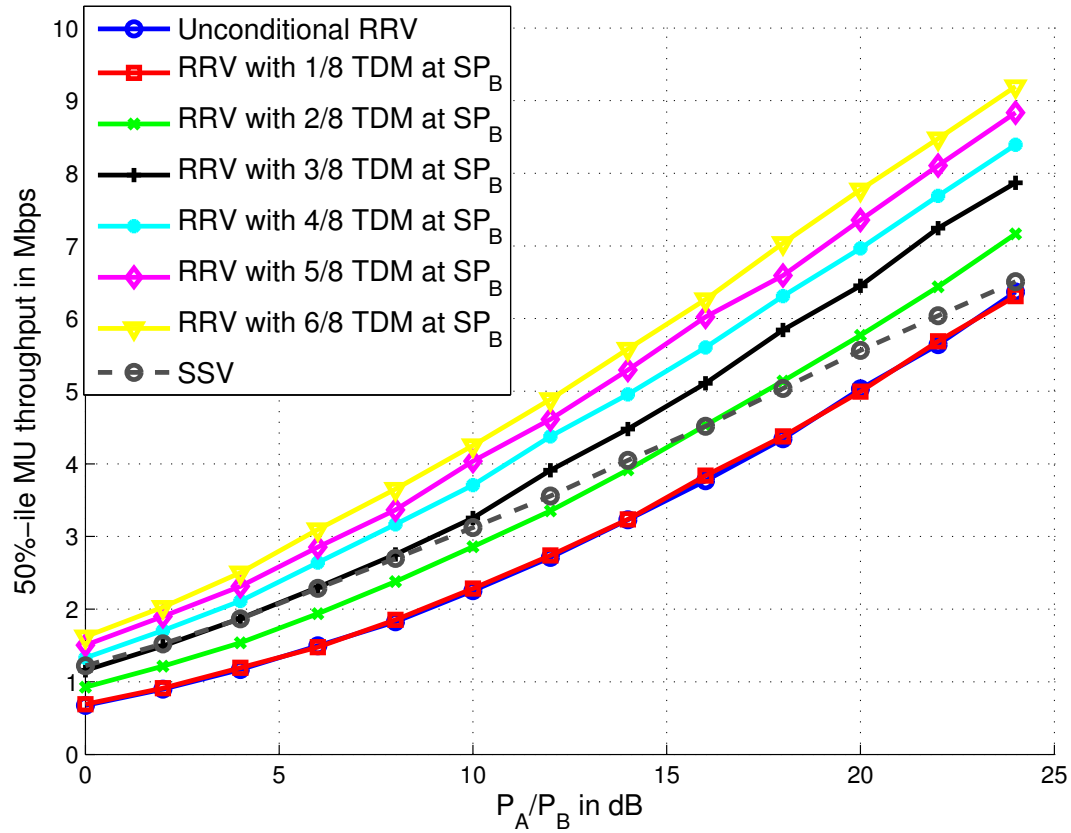

Figure 6.5: SP_A performance for Scenario 2 – top (5%-ile) and bottom (50%-ile)

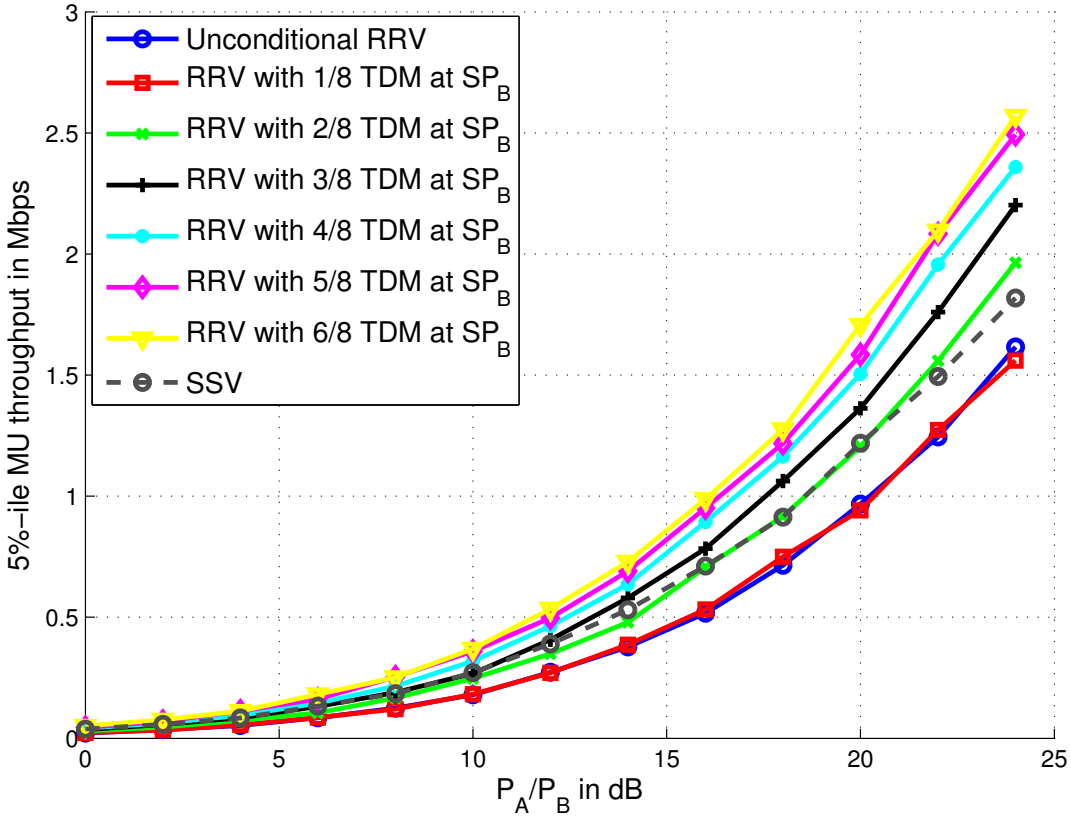

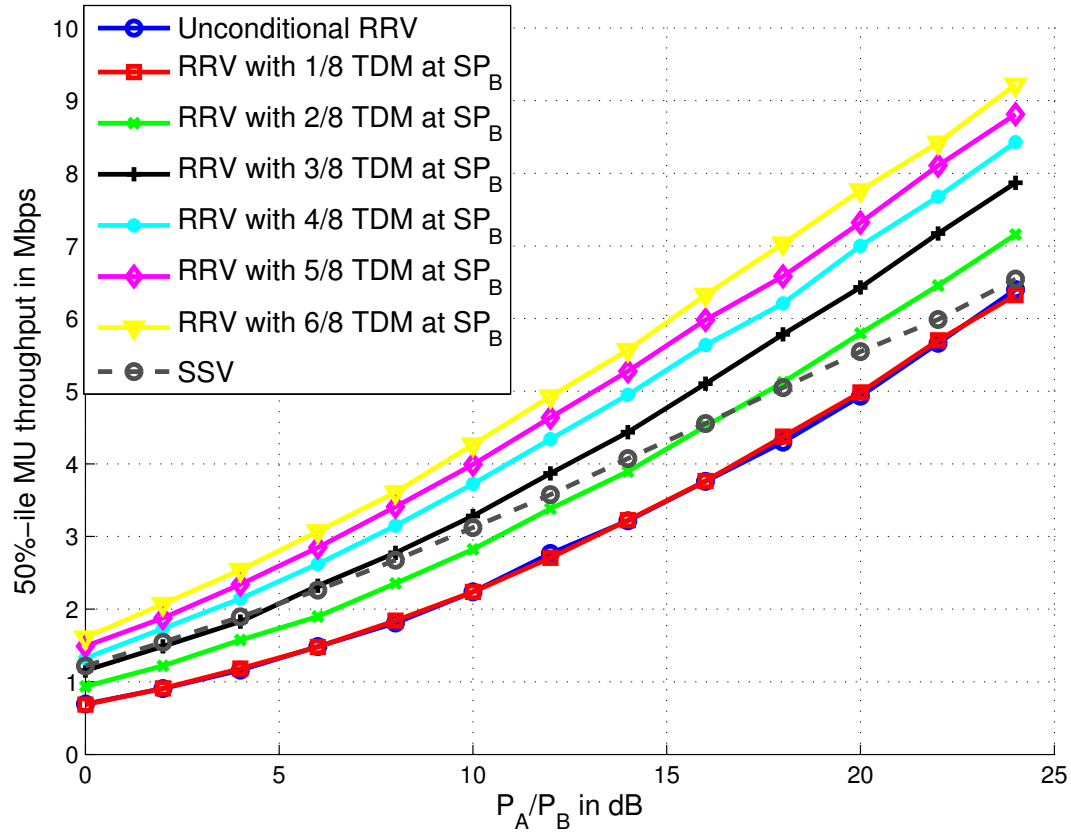

Figure 6.6: SP_A performance for Scenario 3 – top (5%-ile) and bottom (50%-ile)

6.4.2 Performance of SP_B

SP_B's system performance is shown in Figures 6.7 and 6.8. Since only the number of MUs subscribed to SP_A changes between Network Layouts 1 and 2, it does not affect the system performance of SP_B and we do not show the results for Network Layout 2 for SP_B here. Some of the previous observations still exist, like the effect of transmit power and the TD Muting portion, but in an inverse manner. The throughput of MUs subscribed to SP_B decreases as the transmit power at SP_A increases, and the more subframes are muted. Unlike what occurs at SP_A's side, virtualization benefits SP_B that operates 4 small cells and has smaller portion of spectrum with SSV. As SP_B MUs are distributed densely within small cells, their channel SINR conditions are normally good and the extra available bandwidth from virtualization obviously improves the capacity. In Figure 6.7 only 5%-ile MU throughputs of 5/8 and 6/8 TD Muting RRV are completely lower than that of SSV and only 50%-ile MU throughput of 6/8 TD Muting RRV is completely below SSV throughput. In other cases of TD Muting RRV, when SP_A's transmit power is under certain threshold (for example 40 dBm for 4/8 TD Muting RRV in Scenario 1), it is better to use TD Muting RRV instead of SSV. As cells are closer in Scenario 3 and the interference is higher, the system performance of SP_B drops a bit compared to Network Layouts 1 and 2.

Here is an interesting observation if we jointly analyze the system performances of both SP_A and SP_B. Using Network Layout 1 as an example, 5%-ile SP_A throughput of 5/8 and 6/8 are slightly better than SSV (see Figure 6.4) however the corresponding TD Muting RRV cases for SP_B are below SSV (see Figure 6.7). This means that significant improvement at one SP may occur at the sacrifice of the other SP. Hence the resource manager needs to carefully configure the network according to both SPs' requirements which we explore next.

6.4.3 Configuration Maps

We consider the three schemes in our virtual LTE system-level simulator, which are unconditional RRV, TD Muting RRV and SSV. These schemes achieve various system capacities with different network parameters in a particular networking scenario. For example, in Network Layout 2, RRV with 4/8 TD Muting can ensure that 50% of SP_A MUs obtain 5 Mbps

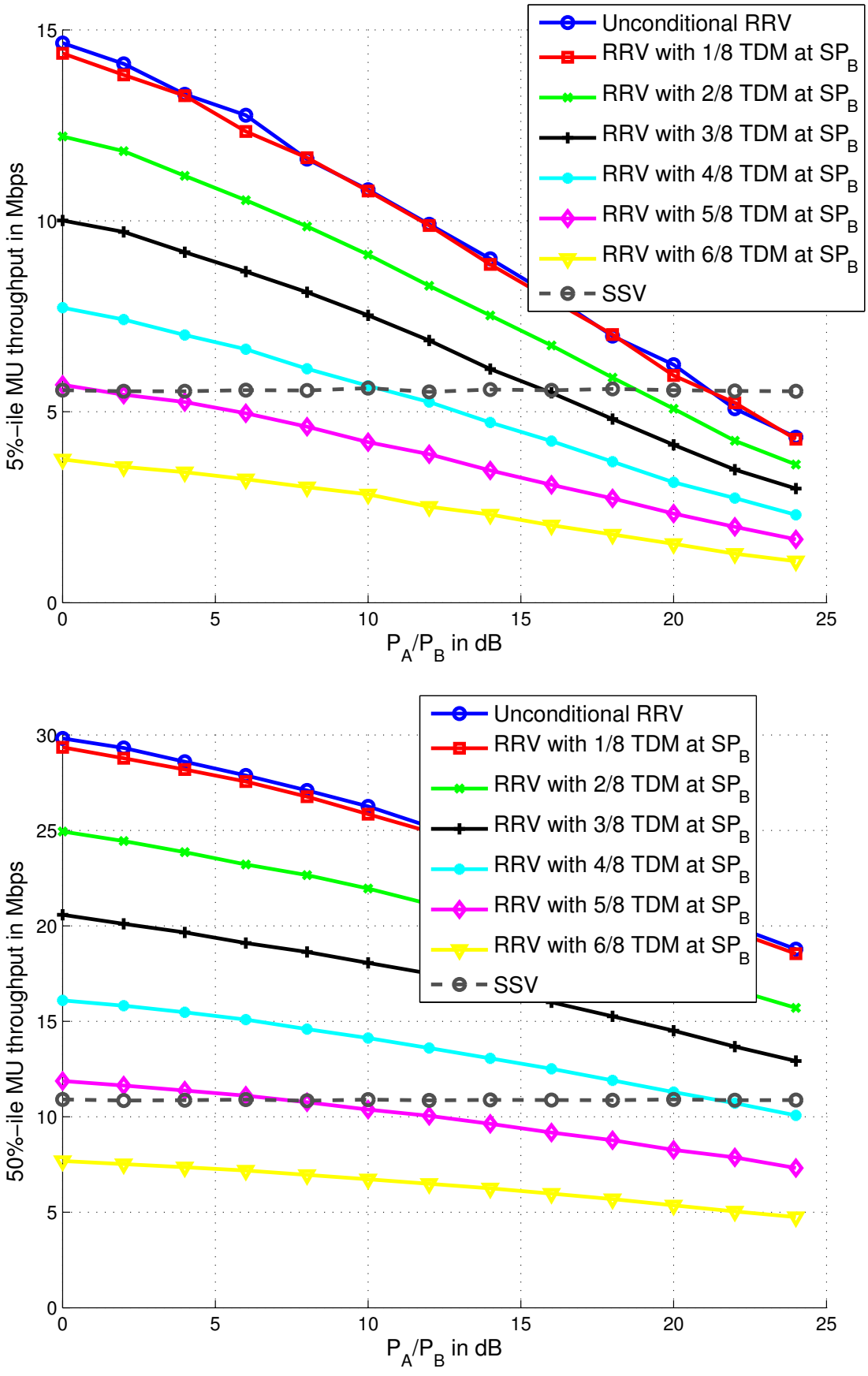

Figure 6.7: SP_B performance for Scenario 1 – top (5%-ile) and bottom (50%-ile)

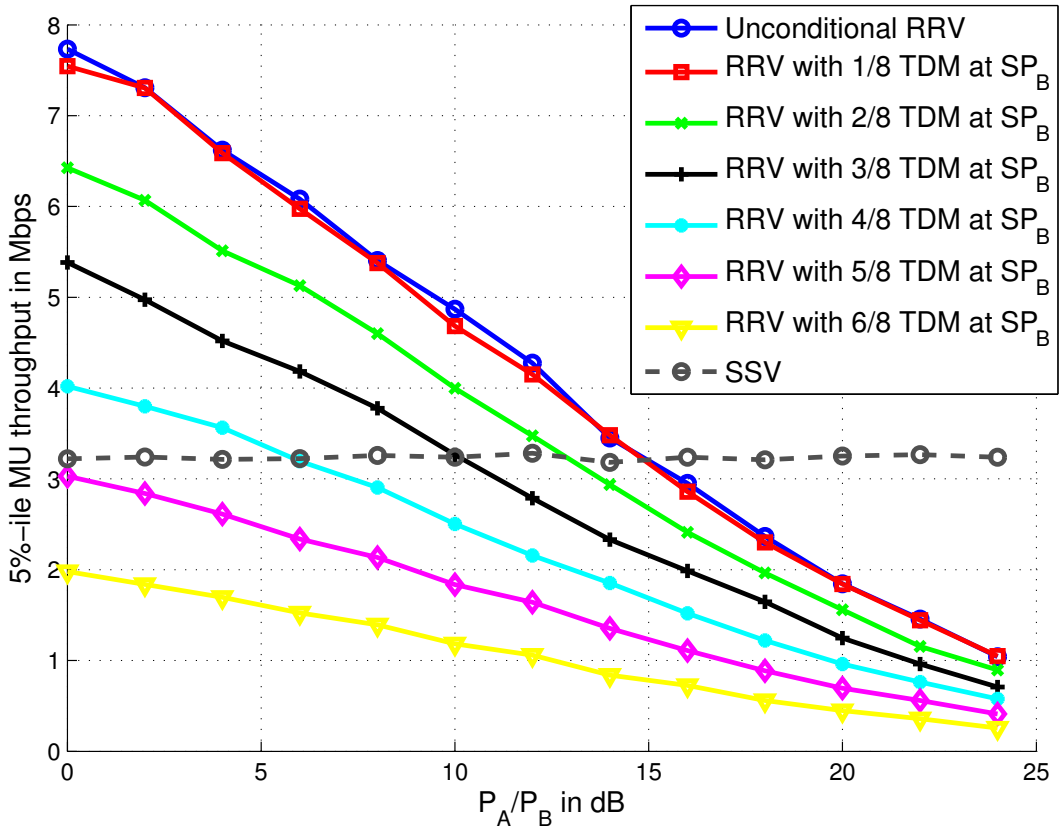

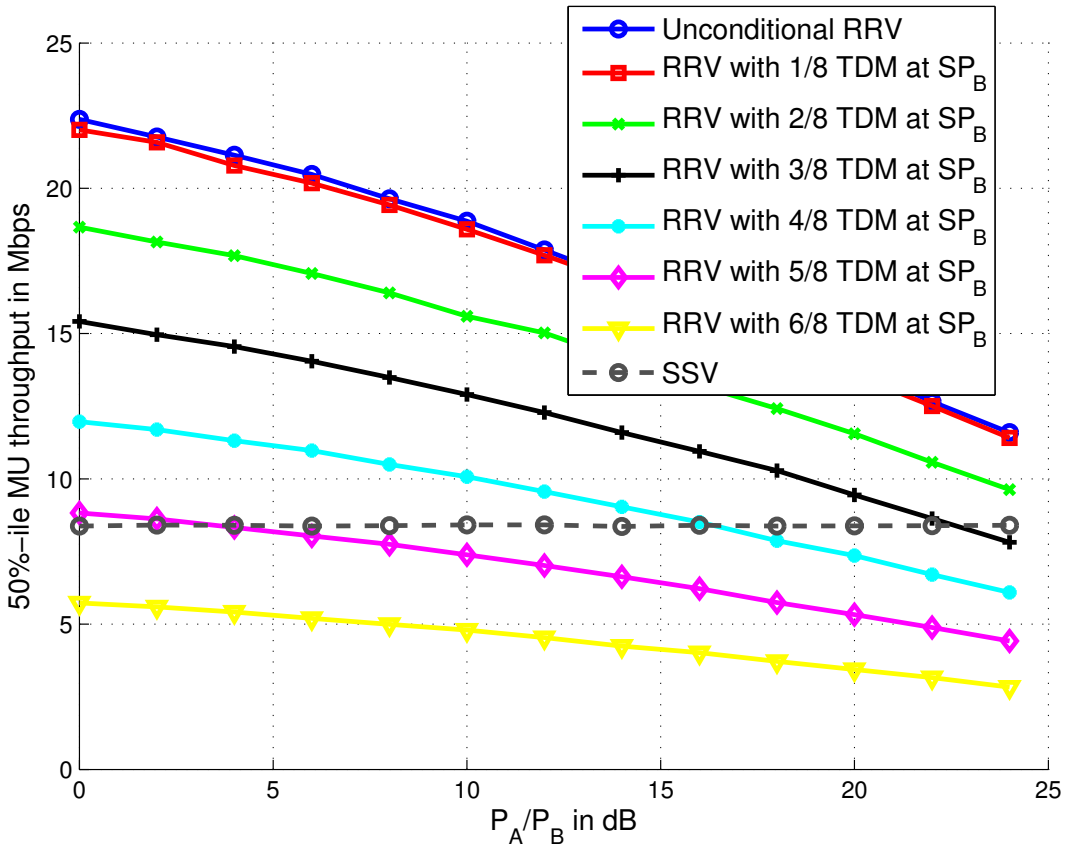

Figure 6.8: SP_B performance for Scenario 3 – top (5%-ile) and bottom (50%-ile)

and 95% of SP_B MUs get 4.8 Mbps when the transmit power ratio is 14 dB. A resource manager can possibly configure the virtual networks based on the QoS requirement of each SP and the networking layout. To this end, we extract results from 5%-ile and 50%-ile throughput from Figures 6.4 to Figure 6.8, then plot Figures 6.9 and 6.10 showing the throughput of MUs of SP_A Vs those of SP_B under the same conditions. We compute the absolute gains comparing RRV schemes to SSV schemes rather than absolute values of the actual throughput for these plots. We call these plots *"configuration maps"* as they provide guidelines for configurations that a resource manager can use to configure spectrum based on SPs' requirements and networking layouts. Here we only show the map corresponding to Network Layout 2 (using data from Figures 6.5 6.7) as an example. It is also easy to form the other two configuration maps using Figures 6.4 and 6.7, and Figures 6.6 and 6.8.

There are two parameters in each configuration – power ratio P_A/P_B (including values of 0 dB, 8 dB, 16 dB and 24 dB) and the TD Muting portion (ranges from 0 to 4/8). Therefore 20 configurations are shown in Figures 6.9 and 6.10. Every configuration indicates two gains, each of which refers to the RRV gain at SP_A and SP_B. Note that here "gain" means how much the increase in throughput is, compared to SSV, so it could be positive or negative. A positive gain means the corresponding RRV configuration is better than that of SSV while a negative gain indicates that SSV is better. We use the 5%-ile throughputs and 50%-ile throughputs of both SPs, but it is sometimes also useful to match 5%-ile throughput of one SP and 50%-ile throughput of the other SP together.

Creating appropriate configurations by resource managers depends on the agreements that SPs have made with the InPs. In Figure 6.9 and 6.10, three regions are represented – SP_A beneficial region, SP_B beneficial region and mutually beneficial region. Configurations in the SP_A beneficial region can obtain higher throughput compared to SSV, and the same situation in the SP_B beneficial region, but for one SP only. Further, both SPs are able to achieve better throughput at the same time using configurations in the mutual beneficial region. This makes configurations in the mutual beneficial region attractive and worth examining further. A guideline that a virtual resource manager could adopt to manage its virtual networks is described below: based on all possible networking scenarios over the same network infrastructure, a group of configuration maps are stored in the virtual

radio resource manager. In every TTI (or group of TTIs), the resource manager looks up the maps and locates the proper one according to the current network structure. All SPs reports information that may include CQI, QoS requirement, and abilities (e.g., MIMO) to the resource manager. Then the resource manager sends the configuration back to SPs by reading it from a configuration map. All SPs follow the instruction and configure their virtual networks accordingly. For example, if SP_A requires that 95% of its MUs need at least 50% gain while SP_B allows 10% capacity drop, from Figure 6.9, we can see that a configuration with power ratio 0 dB and 3/8 TD Muting is a proper one to be applied.

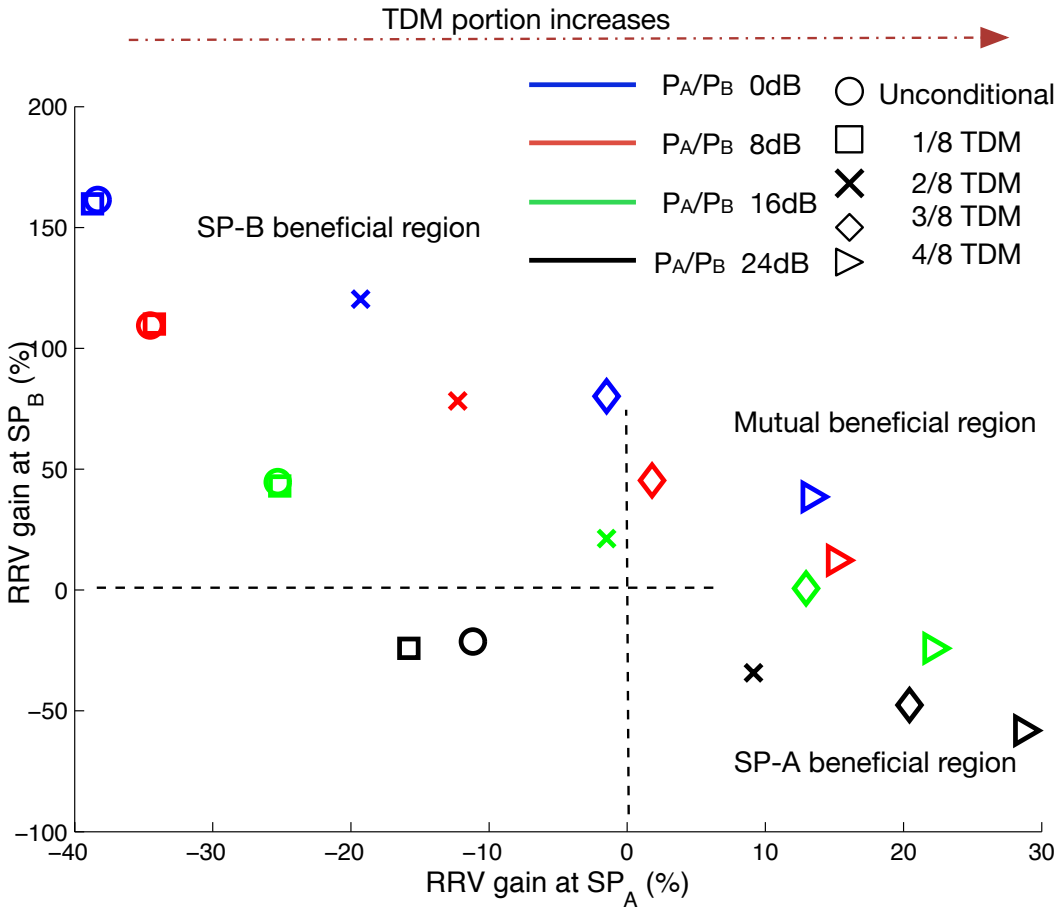

Figure 6.9: 5%-ile throughput based configuration map

Unfortunately, only a few configurations satisfy both SPs according to Figure 6.9 and 6.10. For instance, there are only 4 out of 20 configurations falling in the mutual beneficial

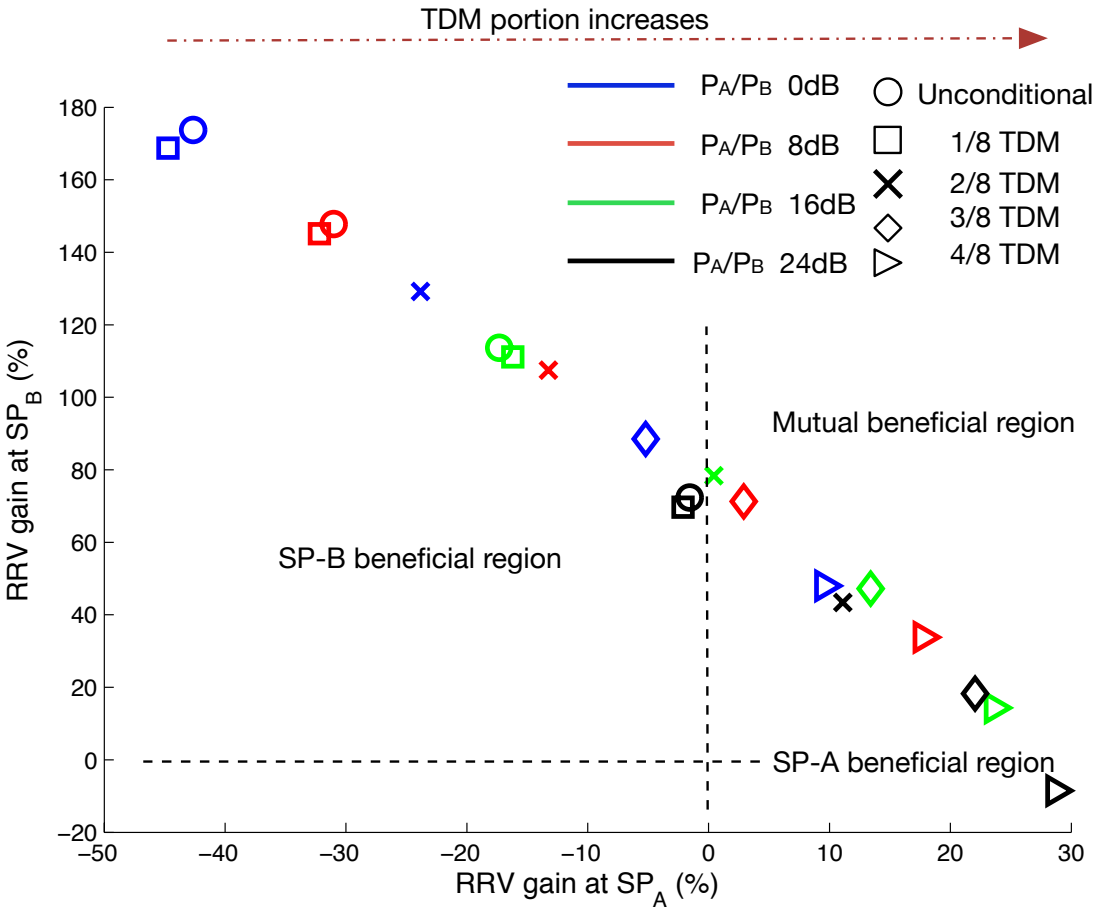

Figure 6.10: 50%-ile throughput based configuration map

region in Figure 6.9 – power ratio of 16 dB and 3/8 TD muting, power ratio of 8 dB and 3/8 TD muting, power ratio of 8 dB and 4/8 TD muting, and power ratio of 0 dB, 4/8 TD muting. More configurations can meet gains at both SPs when they just require throughput increase for 50% of their MUs. To exploit more configurations that benefit both SPs, we implement MI-TD muting RRV. The configuration maps including MI-TD muting RRV scheme are shown in Figure 6.11 and 6.12. MI-TD muting generates some configurations in the mutual beneficial region, which are emphasized in Figure 6.11 and 6.12. MI-TD muting with power ratio 16 dB increases 5%-ile MU throughput of both SPs. Moreover, MI-TD muting with power ratio 0, 8, 16 dB all significantly improves both SPs' performance.

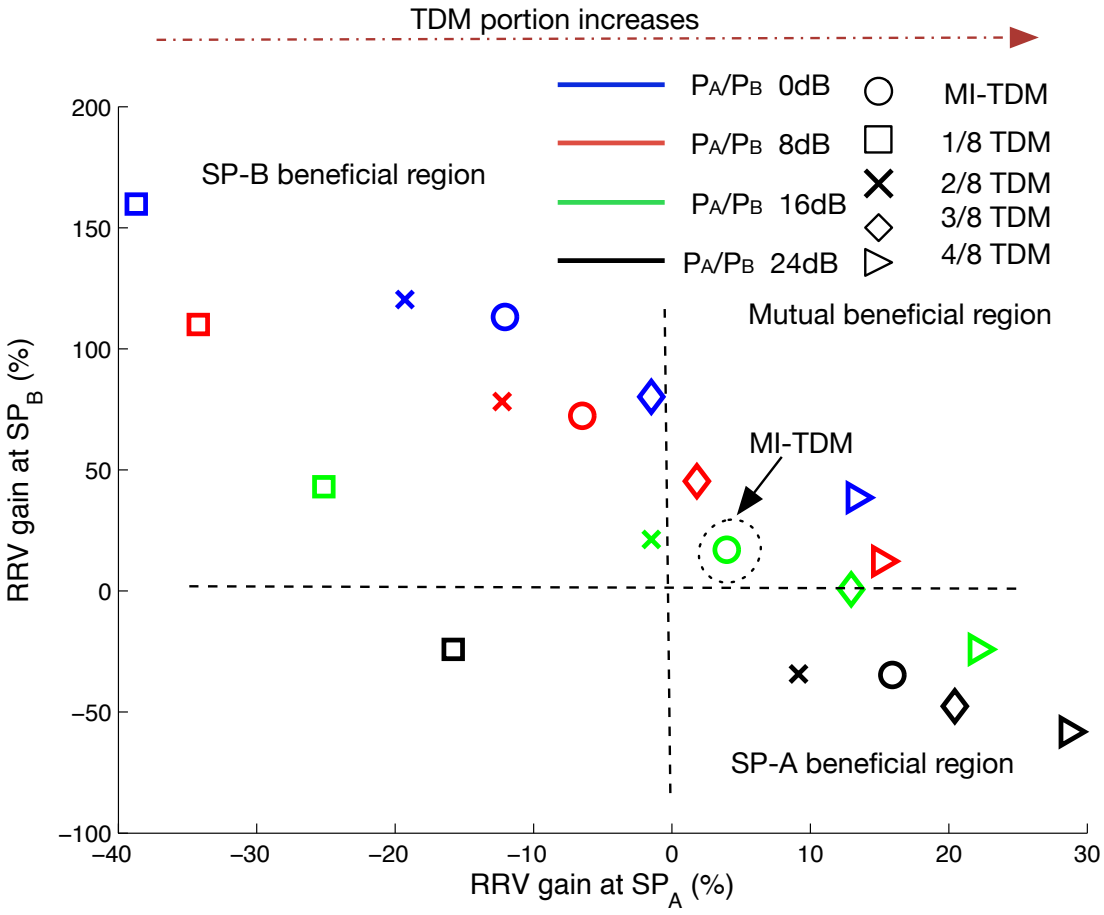

Figure 6.11: 5%-ile throughput of MI-TD muting RRV

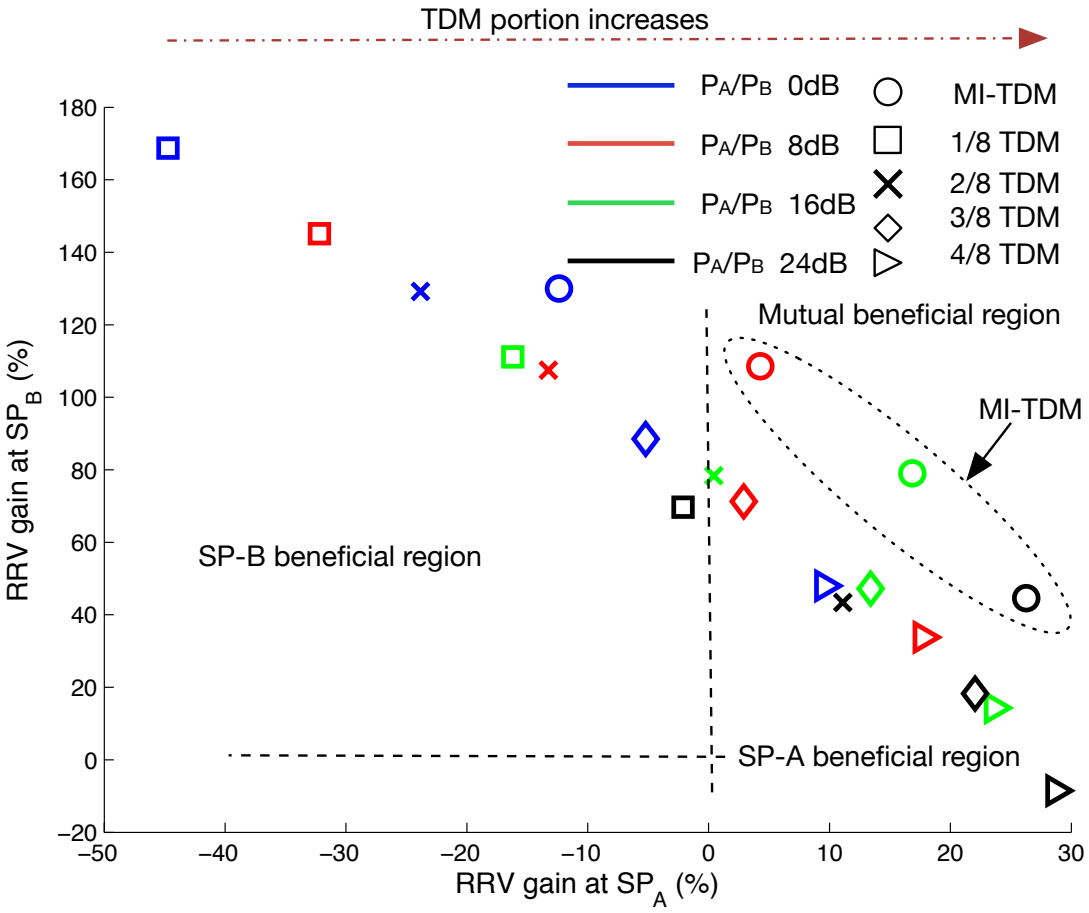

Figure 6.12: 50%-ile throughput of MI-TD muting RRV

6.5 LIMITATIONS AND DISCUSSION

Although a practical LTE system-level simulator is developed to test our proposed virtualization schemes, we built up simulations based on several specific assumptions and neglect effect of some functions of LTE MAC and upper layer that are involved in scheduling (like buffer state, frequency domain packet scheduler, etc.). In this section, we discuss the limitations of our work and possible outcome that would occur if some of our assumptions are relaxed. Also, other possible strategies that can be applied in virtualization are briefly mentioned.

In the system depicted in Figure 6.1, we consider the first wrap of co-channel cells of SP_A and assume the frequency reuse factor is 1 (used in LTE system). No inter-cell interference coordination (ICIC) is adopted. Therefore, when the radius of the large cell is 1000 m and transmit power is 30 dBm, the system performance of SP_A is very poor. We also test our schemes assuming some ICIC is applied hence the co-channel interference inter-SP_A is very low. In that case, interestingly, we find that RRV improves MU throughput significantly (36.7% and 32.1% respectively) even TD muting portion is 0 (unconditional RRV) (see Figure 6.13).

There are other ways to improve system performance like MI-TD muting RRV. One possible way is to deploy more antennas at SPs to improve throughput without interfere with each other much. The other way is to regulate the spectrum sharing to happen only if SPs' can meet their minimum requirements. However, this strategy is based on an estimation of throughput that one SP can achieve within certain time period, which may be related to many other issues in scheduling like buffer states.

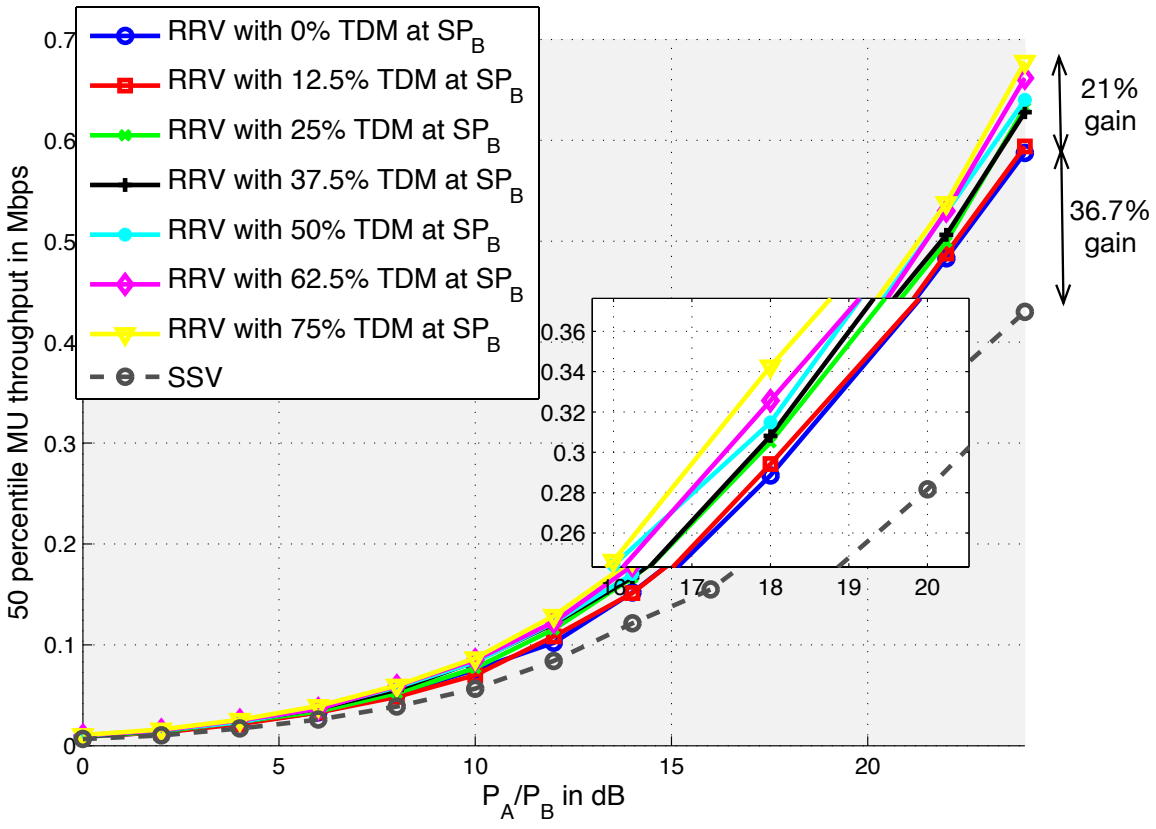

Figure 6.13: SP_A performance for Network Layout 1

7.0 CONCLUSION AND FUTURE DIRECTIONS

Spectrum virtualization in cellular networks is studied with a focus on reuse in time and space. Radio resource virtualization is a scheme proposed in this dissertation to facilitate service providers to access more spectrum from infrastructure providers by reusing some of the spectrum temporally and spatially. We investigate radio resource virtualization in the downlink and technologies like fractional frequency reuse, multiple-input multiple-output, and LTE radio resource management are considered in our system models. Based on the analysis of snapshots of networks as well as results from a system-level simulator, the advantage of radio resource virtualization is observed in certain scenarios. Strategies that could potentially enhance the advantage are also proposed and examined in the snapshots and the simulator.

We create a framework that includes parameters of influence to the virtual network capacity. The framework produces configuration maps showing tradeoffs between system performances of service provides. Through configuration maps, we expect a resource manager of a virtual network to properly configure spectrum according to each service provider's requirement and ability. Such configuration maps, in a way, guide virtualization evolving towards higher efficiencies, better isolation across service providers and easier customization of services.

As mentioned in our system model (see Chapter 3), we narrow down the big virtualization topic to specific simultaneous usage problems and place several assumptions to avoid complicated interdependent situations. There are other important issues in virtualization besides the specific one studied in this dissertation. First of all, the realization of virtualization is strongly related to policies and regulations. The ownership of resources and if it is entirely separated from service providers or not should be explicitly defined. Second, from

the perspective of a big picture of network, virtualization of radio access network (RAN) is required to be considered with core network. This may restrict how often a resource manager can reallocate spectrum and reconfigure the network. Third, we have not considered virtualization in many scenarios, for example, in the uplink or in a correlated MIMO channel. In Chapter 4 and 5, snapshots of networks are analyzed however the MUs' locations and requirements may vary over time. The LTE simulator in Chapter 6 only considers limited functions of the MAC layer and the physical layer. Future work should include such network scenarios, technologies and factors into the picture. Below we provide a brief list showing some possible future directions of our work.

- Beamforming enables MIMO to support multiple users at the same time within the same spectrum [68]. This could lead to higher efficiencies in virtualization. Combining the usage of multi-user beamforming with configuration maps for SPs needs to be examined carefully. Also, coordinated multiple point (COMP) enables multiple neighboring eNBs to support same group of MUs in one transmission [69]. Virtualization may affect the usage of COMP due to more complicated spectrum planning across multiple eNBs.
- In the LTE simulator, MIMO is used. However the number of antennas at either transmitter or receiver does not change. Varying the MIMO settings to investigate the effect on capacity is necessary. It is expected that changing MIMO settings based on SPs demands will provide better isolation of SPs from each other and help to further customize virtual networks.
- Transmissions in the uplink is more tricky than in the downlink. Power control and user grouping may be involved in transmissions of all users, and the scheduling procedure is different from the downlink. One potential approach is to examine the Pareto Optimal Power Control Scheduling [61] in the investigation of the uplink radio resource virtualization.

This dissertation examines wireless network virtualization from a technical perspective. Regulation and economic issues in virtualization are as important and they interact with technical issuers extensively. What we have worked on can be viewed as a bridge connecting the physical network performance and the regulation and economic issues, and what we have

completed is just a start of the virtualization journey.

APPENDIX

COMPARISON OF THE LTE SIMULATOR WITH OTHER'S WORK

As the system model we consider is similar to the one in performance analysis of eICIC [56], we compared outputs of our simulator with Figure 4 in [56]. Work in [56] studied eICIC for downlink co-channel deployment of a macro and several pico-eNBs. Traditional reference signal received power (RSRP)-based cell selection helps MUs pick the eNB with the highest RSRP as its serving eNB. But it often leads to only a few MUs being served by picocells. To prevent any imbalance in network load between macro and pico cells, a positive offset is added to pico-eNB RSRP values to force more MUs to select pico-eNBs. This offset is called cell range extension (CRE), i.e., CRE is used to offload more MUs to the pico cells. To protect MUs that face fierce interference from macro cell, TDM eICIC is required to be applied with CRE. [56] recommended moderate combination of CRE values and muting. We repeated simulations in [56] and Figure A.1 shows MU throughputs with various CRE offsets and macro muting ratios. The trends of our results are comparable to those of Figure 4 in [56] but throughput values are not exactly the same as we do not include as many functions of RRM in our simplified simulator.

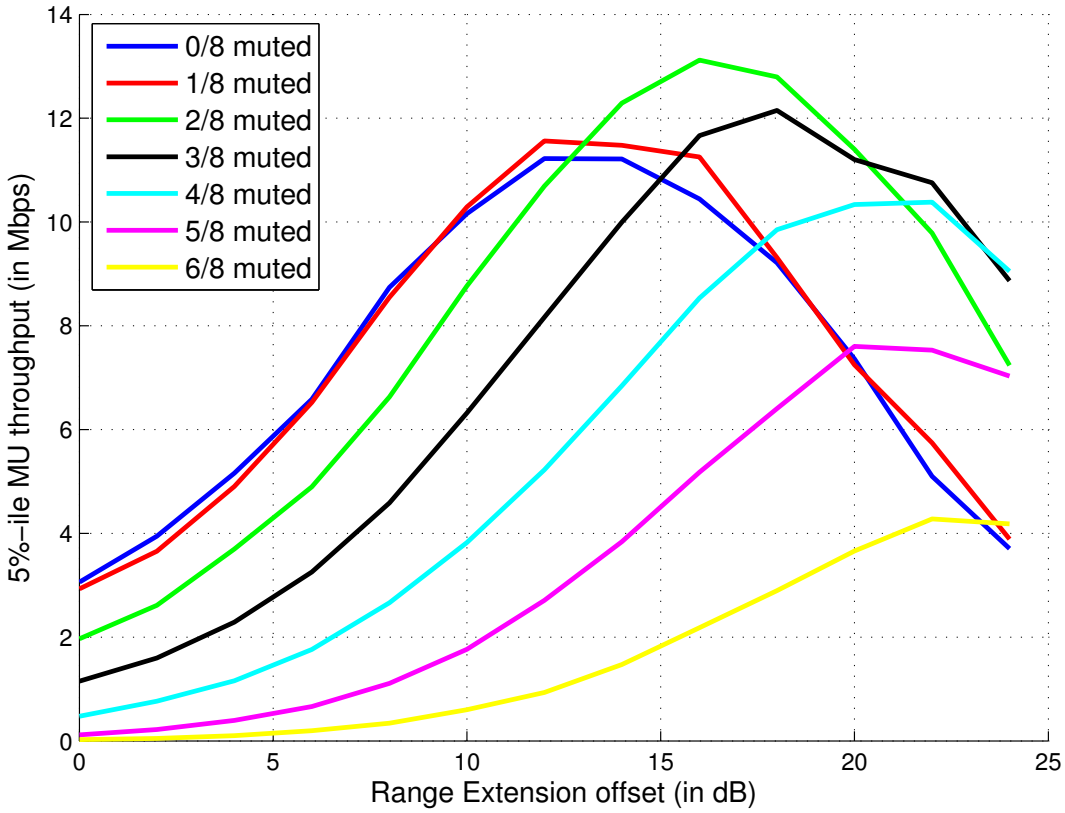

Figure A.1: Comparison with the work in [56]

BIBLIOGRAPHY

[1] X. Costa-Perez, J. Swetina, T. Guo, R. Mahindra, and S. Rangarajan, "Radio access network virtualization for future mobile carrier networks," *Communications Magazine, IEEE*, vol. 51, no. 7, 2013.

[2] Q. Zhao and B. M. Sadler, "A survey of dynamic spectrum access," *Signal Processing Magazine, IEEE*, vol. 24, no. 3, pp. 79–89, 2007.

[3] X. Wang, P. Krishnamurthy, and D. Tipper, "Wireless network virtualization," in *Computing, Networking and Communications (ICNC), 2013 International Conference on*, pp. 818–822, IEEE, 2013.

[4] N. M. Chowdhury and R. Boutaba, "A survey of network virtualization," *Computer Networks*, vol. 54, no. 5, pp. 862– 876, 2010.

[5] N. Egi, A. Greenhalgh, M. Handley, M. Hoerdt, F. Huici, L. Mathy, and P. Papadimitriou, "A platform for high performance and flexible virtual routers on commodity hardware," *ACM SIGCOMM Computer Communication Review*, vol. 40, no. 1, pp. 127–128, 2010.

[6] Y. Wang, E. Keller, B. Biskeborn, J. van der Merwe, and J. Rexford, "Virtual routers on the move: live router migration as a network-management primitive," in *ACM SIGCOMM Computer Communication Review*, vol. 38, pp. 231–242, ACM, 2008.

[7] D. E. Williams, *Virtualization with Xen (tm): Including XenEnterprise, XenServer, and XenExpress: Including XenEnterprise, XenServer, and XenExpress.* Syngress, 2007.

[8] M. M. Buddhikot and K. Ryan, "Spectrum management in coordinated dynamic spectrum access based cellular networks," in *New Frontiers in Dynamic Spectrum Access Networks, 2005. DySPAN 2005. 2005 First IEEE International Symposium on*, pp. 299–307, IEEE, 2005.

[9] K. Huang, V. K. Lau, and Y. Chen, "Spectrum sharing between cellular and mobile ad hoc networks: transmission-capacity trade-off," *Selected Areas in Communications, IEEE Journal on*, vol. 27, no. 7, pp. 1256–1267, 2009.

[10] Y. Zaki, L. Zhao, C. Goerg, and A. Timm-Giel, "LTE mobile network virtualization," *Mobile Networks and Applications*, vol. 16, no. 4, pp. 424–432, 2011.

[11] M. L. Y. Z. A. T.-G. L., Zhao and G. C., "LTE virtualization: from theoretical gain to practical solution.," in *the 23rd International Teletraffic Congress (ITC)*, 2011.

[12] H. Lee, S. Vahid, and K. Moessner, "A survey of radio resource management for spectrum aggregation in lte-advanced," 2013.

[13] P. Vieira, P. Queluz, and A. Rodrigues, "Lte spectral efficiency using spatial multiplexing mimo for macro-cells," in *Signal Processing and Communication Systems, 2008. ICSPCS 2008. 2nd International Conference on*, pp. 1–6, IEEE, 2008.

[14] T. Anderson, L. Peterson, S. Shenker, and J. Turner, "Overcoming the internet impasse through virtualization," *Computer*, vol. 38, no. 4, pp. 34–41, 2005.

[15] J. S. Turner and D. E. Taylor, "Diversifying the internet," in *Global Telecommunications Conference, 2005. GLOBECOM'05. IEEE*, vol. 2, pp. 6–pp, IEEE, 2005.

[16] C. Ersoy and S. S. Panwar, "Topological design of interconnected lan/man networks," *Selected Areas in Communications, IEEE Journal on*, vol. 11, no. 8, pp. 1172–1182, 1993.

[17] P. Ferguson and G. Huston, "What is a vpn?," 1998.

[18] N. Chowdhury and R. Boutaba, "A survey of network virtualization," *Computer Networks*, vol. 54, no. 5, pp. 862–876, 2010.

[19] L. Subramanian, I. Stoica, H. Balakrishnan, and R. H. Katz, "Overqos: An overlay based architecture for enhancing internet qos.," in *NSDI*, vol. 4, p. 6, 2004.

[20] W. Zhang *et al.*, "Linux virtual server for scalable network services," in *Ottawa Linux Symposium*, vol. 2000, 2000.

[21] J. J. D. K. Gifford, K. L. Johnson, M. F. Kaashoek, and J. W. O'Toole Jr, "Overcast: Reliable multicasting with an overlay network," in *Proceedings of USENIX Symposium on OSDI*, 2000.

[22] T. Maseng and T. Ulversoy, "Dynamic frequency broker and cognitive radio," in *Cognitive Radio and Software Defined Radios: Technologies and Techniques, 2008 IET Seminar on*, pp. 1–5, IET, 2008.

[23] G. Isiklar and A. B. Bener, "Brokering and pricing architecture over cognitive radio wireless networks," in *Consumer Communications and Networking Conference, 2008. CCNC 2008. 5th IEEE*, pp. 1004–1008, IEEE, 2008.

[24] M. M. Buddhikot, P. Kolodzy, S. Miller, K. Ryan, and J. Evans, "Dimsumnet: new directions in wireless networking using coordinated dynamic spectrum," in *World of*

Wireless Mobile and Multimedia Networks, 2005. WoWMoM 2005. Sixth IEEE International Symposium on a, pp. 78–85, Ieee, 2005.

[25] M. A. Khan and Y. Zaki, "Dynamic spectrum trade and game-theory based network selection in lte virtualization using uniform auctioning," in *Wired/Wireless Internet Communications*, pp. 39–55, Springer, 2011.

[26] T. K. Forde, I. Macaluso, and L. E. Doyle, "Exclusive sharing & virtualization of the cellular network," in *New Frontiers in Dynamic Spectrum Access Networks (DySPAN), 2011 IEEE Symposium on*, pp. 337–348, IEEE, 2011.

[27] V. Rodriguez, K. Moessner, and R. Tafazolli, "Market-driven dynamic spectrum allocation: Optimal end-user pricing and admission control for cdma," *Proc. 14th European information society technologies (IST) mobile and wireless communications summit. Dresden*, 2005.

[28] V. Rodriguez, K. Moessner, and R. Tafazolli, "Auction driven dynamic spectrum allocation: optimal bidding, pricing and service priorities for multi-rate, multi-class cdma," in *Personal, Indoor and Mobile Radio Communications, 2005. PIMRC 2005. IEEE 16th International Symposium on*, vol. 3, pp. 1850–1854, IEEE, 2005.

[29] K. Ryan, E. Aravantinos, and M. M. Buddhikot, "A new pricing model for next generation spectrum access," in *Proceedings of the first international workshop on Technology and policy for accessing spectrum*, p. 11, ACM, 2006.

[30] M. B. Weiss, M. Altamimi, and L. Cui, "Spatio-temporal spectrum modeling: Taxonomy and economic evaluation of context acquisition," *Telecommunications Policy*, vol. 36, no. 4, pp. 335–348, 2012.

[31] G. Bhanage, I. Seskar, R. Mahindra, and D. Raychaudhuri, "Virtual basestation: architecture for an open shared wimax framework," in *Proceedings of the second ACM SIGCOMM workshop on Virtualized infrastructure systems and architectures*, pp. 1–8, ACM, 2010.

[32] Y. He, J. Fang, J. Zhang, H. Shen, K. Tan, and Y. Zhang, "Mpap: virtualization architecture for heterogenous wireless aps," in *ACM SIGCOMM Computer Communication Review*, vol. 40, pp. 475–476, ACM, 2010.

[33] F. Fu and U. C. Kozat, "Wireless network virtualization as a sequential auction game," in *INFOCOM, 2010 Proceedings IEEE*, pp. 1–9, IEEE, 2010.

[34] Y. Zaki, L. Zhao, C. Goerg, and A. Timm-Giel, "A novel lte wireless virtualization framework," in *Mobile Networks and Management*, pp. 245–257, Springer, 2011.

[35] H. Anouar, C. Bonnet, D. Câmara, F. Filali, and R. Knopp, "An overview of openair-interface wireless network emulation methodology," *ACM SIGMETRICS Performance Evaluation Review*, vol. 36, no. 2, pp. 90–94, 2008.

[36] R. Kokku, R. Mahindra, H. Zhang, and S. Rangarajan, "Nvs: a virtualization substrate for wimax networks," in *Proceedings of the sixteenth annual international conference on Mobile computing and networking*, pp. 233–244, ACM, 2010.

[37] R. Kokku, R. Mahindra, H. Zhang, and S. Rangarajan, "Nvs: a substrate for virtualizing wireless resources in cellular networks," *Networking, IEEE/ACM Transactions on*, vol. 20, no. 5, pp. 1333–1346, 2012.

[38] A. T.-G. Y. Zaki, L. Zhao and C.Gorg, "A novel LTE wireless virtualization framework," *Second International ICST Conference on Mobile Networks And Management*, 2010.

[39] A. T.-G. Y. Zaki, L. Zhao and C.Gorg, "LTE wireless virtualization and spectrum management," *Third Joint IFIP Wireless and Mobile Networking Conference (WMNC)*, 2010.

[40] P. P. A. Banchs, P. Serrano and M. Natkaniec, "Providing throughput and fairness guarantees in virtualized WLANs through control theory," *Springer Mobile Networks and Applications*, 2012.

[41] I. S. G. Bhanage, D. Vete and D. Raychaudhuri., "Splitap: leveraging wireless network virtualization for flexible sharing of wlans.," in *IEEE Global Telecommunications Conference (GLOBECOM 2010)*, 2010.

[42] I. S. G. Bhanage and D. Raychaudhuri, "a virtualization architecture for mobile WiMAX networks," *ACM MC2R*, 2012.

[43] J. T. J. Lu, "Efficient mapping of virtual networks onto a shared substrate," *Tech. Rep. WUCSE-2006-35, Washington University*.

[44] Y. I. W. Szeto and R. Boutaba, "A multi-commodity flow based approach to virtual network resource allocation," in *Global Telecommunications Conference, GLOBECOM'03. IEEE.*, pp. 3004–3008, 2003.

[45] Y. Zhu and M. Ammar, "Algorithms for assigning substrate network resources to virtual network components," in *IEEE INFOCOM'06*, 2006.

[46] e. a. Zhang, Xu, "Efficient resource allocation for wireless virtualization using time-space division," in *Wireless Communications and Mobile Computing Conference (IWCMC)*, 2012.

[47] R. Madan, J. Borran, A. Sampath, N. Bhushan, A. Khandekar, and T. Ji, "Cell association and interference coordination in heterogeneous LTE-A cellular networks," *Selected Areas in Communications, IEEE Journal on*, vol. 28, no. 9, pp. 1479–1489, 2010.

[48] Y. Bai, J. Zhou, and L. Chen, "Hybrid spectrum usage for overlaying LTE macrocell and femtocell," in *Global Telecommunications Conference, 2009. GLOBECOM 2009. IEEE*, pp. 1–6, IEEE, 2009.

[49] S. W. Halpern, "Reuse partitioning in cellular systems," in *Vehicular Technology Conference, 1983. 33rd IEEE*, vol. 33, pp. 322–327, IEEE, 1983.

[50] C. G. Gerlach, I. Karla, A. Weber, L. Ewe, H. Bakker, E. Kuehn, and A. Rao, "ICIC in DL and UL with network distributed and self-organized resource assignment algorithms in LTE," *Bell Labs Technical Journal*, vol. 15, no. 3, pp. 43–62, 2010.

[51] A. Ghosh, N. Mangalvedhe, R. Ratasuk, B. Mondal, M. Cudak, E. Visotsky, T. A. Thomas, J. G. Andrews, P. Xia, H. S. Jo, *et al.*, "Heterogeneous cellular networks: From theory to practice," *Communications Magazine, IEEE*, vol. 50, no. 6, pp. 54–64, 2012.

[52] R. S. Blum, J. H. Winters, and N. R. Sollenberger, "On the capacity of cellular systems with MIMO," *IEEE Communications Letters*, vol. 6, no. 6, pp. 242–244, 2002.

[53] H. Dai, A. F. Molisch, and H. V. Poor, "Downlink capacity of interference-limited MIMO systems with joint detection," *Wireless Communications, IEEE Transactions on*, vol. 3, no. 2, pp. 442–453, 2004.

[54] Y. Song and S. D. Blostein, "MIMO channel capacity in co-channel interference," in *Proc. 21st Biennial Symposium on Communications*, vol. 2, pp. 220–224, 2002.

[55] D.-s. Shiu, *Wireless communication using dual antenna arrays*. Springer, 2000.

[56] Y. Wang and K. I. Pedersen, "Performance analysis of enhanced inter-cell interference coordination in lte-advanced heterogeneous networks," in *Vehicular Technology Conference (VTC Spring), 2012 IEEE 75th*, pp. 1–5, IEEE, 2012.

[57] 3GPP, "TR 36.931 version 9.0.0 Release 9," May 2011.

[58] X. Wang, P. Krishnamurthy, and D. Tipper, "On radio resource sharing in multi-antenna virtualized wireless networks," *ACM MSWiM*, November 2013.

[59] D. Bilios, C. Bouras, V. Kokkinos, A. Papazois, and G. Tseliou, "Optimization of fractional frequency reuse in long term evolution networks," in *Wireless Communications and Networking Conference (WCNC), 2012 IEEE*, pp. 1853–1857, IEEE, 2012.

[60] R. B. Marks *et al.*, "Ieee standard 802.16: a technical overview of the WirelessMAN™ air interface for broadband wireless access," *IEEE communications magazine*, p. 98, 2002.

[61] S. S. G. A. Burchardt, Harald and H. Haas., "Pareto optimal power control scheduling for ofdma networks.," in *In Vehicular Technology Conference (VTC Fall), 2012 IEEE*, pp. 1–5, 2012.

[62] 3GPP, "TS group radio access network - physical channel and modulation Release 8," tech. rep., May.

[63] S. Sesia and et al, eds., *LTE: The UMTS Long Term Evolution*. John Wiley and Sons, 2011.

[64] E. Dahlman, S. Parkvall, J. Skold, and P. Beming, *3G evolution: HSPA and LTE for mobile broadband*. Academic press, 2010.

[65] S. Stefania, T. Issam, and B. Matthew, "Lte-the umts long term evolution: from theory to practice," *A John Wiley and Sons, Ltd*, vol. 6, pp. 136–144, 2009.

[66] C. Johnson, "Lte in bullets," 2010.

[67] T. S. G. RAN, "E-utra; physical layer procedures,," Tech. Rep. TS 36.213, 3rd Generation Partnership Project (3GPP), Mar. 2009.

[68] Q. H. Spencer, C. B. Peel, A. L. Swindlehurst, and M. Haardt, "An introduction to the multi-user mimo downlink," *Communications Magazine, IEEE*, vol. 42, no. 10, pp. 60–67, 2004.

[69] Q. Wang, D. Jiang, G. Liu, and Z. Yan, "Coordinated multiple points transmission for lte-advanced systems," in *Wireless Communications, Networking and Mobile Computing, 2009. WiCom'09. 5th International Conference on*, pp. 1–4, IEEE, 2009.